

An examination of the design of mathematical models incorporating both  
microstructural and surface effects in anti-plane deformations

by

Taisiya Sigaeva

A thesis submitted in partial fulfillment of the requirements for the degree of

Doctor of Philosophy

Department of Mechanical Engineering  
University of Alberta

© Taisiya Sigaeva, 2015

## ABSTRACT

Micropolar theory and surface mechanics are rapidly becoming key tools in the development of more advanced models which can precisely describe the behavior of deformable elastic solids. Renewed interest in these areas has arisen due to the desire of researchers to generalize continuum-based models for applications in a wider class of materials, such as the micro-featured materials, and at smaller scales, such as the nano-scale. The analysis of such classes of materials, in which the effects of both the surface and microstructure are known to be significant, can be greatly benefited from micropolar theory and surface mechanics. However, the multidisciplinary study aimed to develop mathematically and physically adequate models based on both of these theories remains largely absent from the literature due to a number of difficulties.

To fill this void in the literature, in this work we employ the theory of linear micropolar elasticity in conjunction with a new representation of micropolar surface mechanics to develop a comprehensive model for the deformations of a linearly micropolar elastic solid subjected to anti-plane shear loading. The proposed model represents the surface effect as a thin micropolar film of separate elasticity, perfectly bonded to the bulk. Hence, this model captures not only the micro-mechanical behavior of the bulk, which is known to be considerable in many real materials, but also the contribution of the surface effect which has been experimentally well-observed for bodies with significant size-dependency and large surface area to volume ratios.

Our emphasis in this research is the rigorous mathematical treatment of this model, particularly its well-posedness analysis in the Hadamard's sense. Although challenging, the well-posedness analysis is vital in the development of brand-new models, since it can give a sufficient confidence to find numerically a uniquely existing solution to the problem. To perform this analysis, we apply boundary integral equation methods generalizing and utilizing them as necessary to account for strict requirements of the proposed model.

The coupling of surface mechanics to bulk models gives rise to a highly non-standard boundary condition which has not been accommodated by classical studies in this area. Therefore, a portion of this work is devoted to the study of the surface effect in the classical linear elastic analogue of the proposed model. This supplementary model is thoroughly analyzed for well-posedness and an example demonstrating its efficiency is given. These investigations provided valuable insight on how to tackle the mathematical complexity of the general model, for which bulky micropolar governing equations are used in addition to the similar highly non-standard surface effect boundary condition.

Accordingly, we supply a rigorous mathematical treatment of the mixed boundary-value problems in finite and infinite domains for the proposed model combining both microstructural and surface effects. Boundary integral equation methods are employed to reduce these problems to systems of singular integro-differential equations using a

representation of solutions in the form of modified single-layer potentials. Analysis of these systems demonstrates that the classical Noether's theorems reduce to Fredholm's theorems from which results on well-posedness are deduced. Finally, we demonstrate the proposed model's contribution to fracture mechanics and argue that more sophisticated models produce higher accuracy in predicting material behavior.

## Preface

Five journal papers were combined to compose the main body of the current manuscript.

Chapters 3 and 4 of this thesis has been published as T. Sigaeva and P. Schiavone, Solvability of the Laplace equation in a solid with boundary reinforcement, *The Journal of Applied Mathematics and Physics (ZAMP)*, 2014 (65), 809–815; Chapter 5 – as T. Sigaeva and P. Schiavone, Solvability of a theory of anti-plane shear with partially coated boundaries, *Archives of Mechanics*, 2014 (66), 113–125; Chapters 7 and 8 – as T. Sigaeva and P. Schiavone, Surface effects in anti-plane deformations of a micropolar elastic solid: Integral equation methods, *Continuum Mechanics and Thermodynamics*, 2014 (available online, DOI:10.1007/s00161-014-0404-3). I was responsible for the development of the models, their well-posedness analysis and writing the papers. P. Schiavone was the supervisory author who has suggested the problems, checked the analysis and corresponding results, and revised the manuscripts.

Chapter 6 of this thesis has been published as T. Sigaeva and P. Schiavone , *The Effect of Surface Stress on an Interface Crack in Linearly Elastic Materials*. *Mathematics and Mechanics of Solids*, 2014 (available online, DOI:10.1177/1081286514534871); Chapter 9 – as T. Sigaeva and P. Schiavone , *Influence of Boundary Elasticity on a Couple Stress Elastic Solid*, *The Quarterly Journal of Mechanics and Applied Mathematics*, 2015 (accepted). I have suggested the problem for the second paper, while idea

of the problem for the first paper came from Dr. Schiavone. I was responsible for the derivation of the asymptotic solutions and summarizing results for further publication. P. Schiavone is the supervisory author who has checked all results and written both papers on the basis of my summaries. Also, I have revised the final manuscripts.

*To my family*

---

# Acknowledgments

I would like to express my deepest appreciation to my supervisor Dr. Schiavone. Without his guidance and persistent help this thesis would not have been possible.

Great help in this research has come from advice and comments given by Dr. Ru. Prof. Zubov also gave insightful comments and suggestions on this work. I owe my sincere gratitude to them and to the members of my Supervisory and Examination Committees.

I am indebted to Prof. Karyakin, Prof. Yudin, Prof. Zubov, Prof. Ustinov, Prof. Vatulyan and Prof. Kadomtsev for the inspiration they instilled in me to pursue graduate studies in the field of Mechanical Engineering.

Besides, I wish to thank many of my colleagues and friends who have supported me. Finally, I would like to acknowledge my family for their continuous patience, care, encouragement and faith in me.

---

# Table of Contents

<b>1</b>	<b>Introduction</b>	<b>1</b>
<b>2</b>	<b>Preliminaries</b>	<b>16</b>
2.1	Function spaces and integral equations	17
2.2	Basic equations of classical linear elasticity	21
2.3	Basic equations of micropolar linear elasticity	24
2.3.1	Basic equations of couple stress theory	26
<b>I</b>	<b>Coupling of surface mechanics with a bulk material in the framework of classical linear, homogeneous and isotropic elasticity</b>	<b>29</b>
<b>3</b>	<b>Mathematical modeling: incorporation of surface effects</b>	<b>30</b>
3.1	Governing equations	32
3.2	Boundary conditions describing surface effect	33
<b>4</b>	<b>Well-posedness analysis of the model incorporating surface effects</b>	<b>36</b>
4.1	Boundary value problems (BVPs) for the proposed model	38

4.1.1	Bounded domain . . . . .	38
4.1.2	Unbounded domain . . . . .	41
4.2	Boundary integral equation method (BIEM) and potentials . . . . .	43
4.3	Application of BIEM to the analysis of well-posedness for the proposed model . . . . .	44
4.3.1	Bounded domain . . . . .	45
4.3.2	Unbounded domain . . . . .	48
4.4	Analysis of the singular integro-differential equations arising from the proposed model . . . . .	51
<b>5</b>	<b>Extension of the model to the open case reinforcement when surface effect is considered on a part of the boundary . . . . .</b>	<b>55</b>
5.1	Boundary conditions describing surface effect with end-point conditions taken into account . . . . .	57
5.2	BVPs and BIEM for the proposed model . . . . .	61
5.2.1	Bounded domain . . . . .	64
5.2.2	Unbounded domain . . . . .	68
<b>6</b>	<b>The contribution of surface effect to linear elastic fracture mechanics</b>	<b>71</b>
6.1	Interface crack with surface effect . . . . .	72
6.2	Some discussion and preliminary conclusions . . . . .	78
<b>II</b>	<b>Coupling of surface mechanics with a bulk material in</b>	

<b>the framework of micropolar linear, homogeneous and isotropic elasticity</b>	<b>81</b>
<b>7 Mathematical modeling: incorporation of microstructural effects . .</b>	<b>82</b>
7.1 Governing equations . . . . .	83
7.2 Boundary conditions describing microstructural effects . . . . .	86
<b>8 Well-posedness analysis of the model incorporating both surface and microstructural effects . . . . .</b>	<b>90</b>
8.1 BVPs for the proposed model . . . . .	91
8.1.1 Bounded domain . . . . .	91
8.1.2 Unbounded domain . . . . .	94
8.2 Application of BIEM to the analysis of well-posedness for the proposed model . . . . .	96
8.2.1 Bounded domain . . . . .	97
8.2.2 Unbounded domain . . . . .	100
8.3 Analysis of the resulting systems of singular integro-differential equations arising from the proposed model . . . . .	103
<b>9 The contribution of micropolar surface effect to fracture mechanics</b>	<b>109</b>
9.1 Governing equations and reinforcement boundary conditions . . . . .	110
9.2 The contribution of the microstructure to the crack with the surface effect on its tips . . . . .	113

<b>10 Conclusions and future works . . . . .</b>	<b>119</b>
<b>Bibliography . . . . .</b>	<b>123</b>

---

# List of Figures

4.1	Classical linear, homogeneous and isotropic elastic domain: bounded (a) and unbounded (b) cases . . . . .	39
6.1	Interface crack in a classical linear, homogeneous and isotropic elastic solid without (a) and with surface effect (b) on its tips . . . . .	74
8.1	Micropolar linear, homogeneous and isotropic elastic domain: bounded (a) and unbounded (b) cases . . . . .	92
9.1	Crack in a couple-stress linear, homogeneous and isotropic elastic solid without (a) and with surface effect (b) on its tips . . . . .	112

---

# CHAPTER 1

## Introduction

Because modern scientific society has a great need for models which are able to predict many behavioral properties for a wide range of materials, the development of novel mathematically and physically adequate models, although challenging, is a rewarding area of research.

Centuries of research aiming to describe the behavior of fluids, solids and complex structures were unified in the area of study called mechanics that provide engineers with a necessary background to develop new models. Suitable models, based on laws of physics and assumptions on the considered systems' behavior, should be functional as well as cost-efficient. Even though it is well-established that a body consists of discrete molecules and atoms, a quite common and convenient research methodology is to accept the concept that the substance comprising the body is distributed continuously throughout its volume and that it completely fills the space it occupies. This assumption forms the basis of Continuum Mechanics, a very important discipline, providing a useful and reliable apparatus to design real world application models.

However, having been developed, mechanical models are often not thoroughly analyzed on their adequacy. Unfortunately, their numerical implementation can result

in a completely misleading outcome, thus, causing loss of time and resources. In fact, solving the problem without a solid mathematical conclusion on its well-posedness is like looking for a needle in a haystack. How can we even be confident that there is a needle there? Can we be sure that a barely found needle is the right one? Ultimately, maybe it is even not the right haystack. Beryl Markham, the first woman-aviator who solely crossed the Atlantic ocean on the plane, has said: ‘The way to find a needle in a haystack is to sit down’. In the current research we add: ‘to sit down and perform well-posedness analysis first’. The reason for that is that the well-posedness analysis gives us the sufficient confidence that there is a uniquely existing solution to the brand-new proposed model, which continuously depends on the given data, so that chances to find the right needle in the haystack and, therefore, develop stable algorithm to solve the problem are quite high. That is why this research is intended not only to suggest interesting physically correct models discovering new horizons of real materials behavior, but also to confirm their mathematical adequacy through the available methods of examination analysis.

To this end, let us first to discuss two pronounced theories, i.e. micropolar and surface mechanics, which will be employed to design a new comprehensive model of deformations for a particular class of materials. It will be interesting to compare these theories with classical linear elasticity and underline their merits. After that, let us focus on the methodologies and techniques of the well-posedness analysis, particularly on boundary integral equations methods.

Classical linear elasticity, the most well-studied branch of continuum mechanics, has proven to be a reliable tool to describe elastic solid behavior undergoing relatively small deformations. An ultimate assumption of this theory is that two parts of the

body interact with each other over an infinitesimal surface element via a single force vector. Also, any rotational interaction is neglected in this theory. Linear elasticity, therefore, suggests strain and stress tensors to be symmetric. Although being simple and reasonable for many engineering design scenarios, theoretical and experimental observations for this theory agree well for only a limited class of materials (dense materials, e.g. concrete steel and aluminum) excluding, in particular, those in which the microstructure is known to play a significant role (e.g. polymeric composites, granular and fibrous materials). In fact, an intrinsic length scale for micro-featured materials is comparable to the average grain or molecule size. That is why it is common to say that these materials are also characterized by high size-dependency, so that the size affects their behavior. Due to the vast number of existing applications this class of materials offers to industry, science and engineering, in recent years much attention has been devoted to capturing the contribution of material microstructure in an appropriate theory which allows for a much wider range of deformations. Hence, the question remains how the effect of microstructure and size can be incorporated into the mathematical model.

Voigt [1] made the first attempt to overcome the limitations of the classical theory with the idea that the interaction between two parts of a body through an area element is carried out not only by a force vector, but also by a moment vector. This assumption results in a more realistic picture of the stress distribution in a body, emergence of couple stresses and asymmetry of the stress tensor. Subsequently, the Cosserat brothers [2] suggested that the motion of a material point could be represented by three displacement components as well as three additional independent microrotations; this idea formed the basis of a fully generalized continuum-based theory to consistently

incorporate the effects of microstructure and size-dependency.

Unfortunately, this work was mainly ignored for decades by researchers due to a number of reasons including an unclear formulation, lack of simplicity, consideration of non-linear theory only, difficulties in experimental verification and limited applications. However, in the middle of the 20th century the Cosserat theory was reconsidered because of significant achievements in solid mechanics. In fact, this time period was characterized by attempts to remedy shortcomings of classical elasticity, which failed to explain numerous phenomena occurring in newly invented materials as well as in the existing micro-featured ones [3].

Most of the studies were concentrated on couple stress theory, also referred to as Cosserat pseudo-continuum or Cosserat continuum with constrained rotations. As the latter name indicates, this theory is characterized by microrotations, which are not independent of displacements, although stresses and couple stresses are still taken into account. A number of influential papers have been published to address this particular case of Cosserat theory. These include works by Truesdell and Toupin [4], Rajagopal [5], Toupin [6], Mindlin and Tiersten [7], Koiter [8]. It should be noted that even though a particle has less degrees of freedom there, the couple stress theory should not be treated just as a simplification of the Cosserat continuum, but as an independent theory, which has proven reliable and even preferable for some particular types of problems [9].

At the same time, Eringen [10, 11] and Nowacki [12] have elaborated the general theory of the Cosserat continuum with independent displacements and microrotations. Nowadays, this theory is referred to as micropolar mechanics (as Eringen proposed) and continues to form the basis of ongoing research.

Despite the tremendous progress in micropolar theories during this Cosserat ‘renaissance’ period, there still was an evident gap between theoretical and experimental investigations. Regarding this situation, experimentalists have faced challenges in their attempts to determine parameters of a micropolar solid or just observe the effect of microstructure [13, 14]. In fact, there are too many parameters to look for; if a classical linear, homogeneous and isotropic elastic solid has just two material parameters, namely Lamé’s constants, a similar Cosserat material is estimated by six, while a couple stress solid by four. Another difficulty was to manufacture material displaying rotational effects captured by technologies of its time. As a result, many experiments were not successful; researchers were employing dense materials and/or oversized specimens that were not able to give evidence of micro-effects. In addition, they failed to control microstructure while estimating Cosserat parameters independently in several experiments. Nevertheless, this period was followed by Robert Lakes’ outstanding success in the 1980s. He could capture the effect of microstructure and estimate micropolar constants in numerous experiments with bones that led to a considerable growth of interest to micropolar mechanics [15]-[22]. It should be mentioned that the couple stress theory has always been regarded as a more promising theory than the general Cosserat theory for experimental verification [9].

Since that time, much progress was done in the experimental study of the Cosserat theory. Recent advances in finite element methods allowed for computational modeling of micropolar solids behavior [23]-[28]. The micropolar theory has proven reliable and efficient for a range of media with complicated structure such as bones and other biological matters; composites, particularly fibres, reinforced structures, layers and laminates; porous or cellular solids including concrete, polymeric and plastic foams; granular and

powder-like materials, polycrystalline materials, soils, rock and rock masses; nanostructures; chiral solids; electromagnetic and ferromagnetic materials (see, for example, [29, 30] and references therein). Although the couple stress theory was especially well-suited for materials consisting of rigid fibres or elongated grains [11], it showed many inconsistencies for regular granular bodies [31], accommodated more appropriately by the general micropolar theory.

Some of the major advantages of micropolar theories over classical elasticity are as follows. Firstly, a material, for which the intrinsic length scale is comparable to the average grain or molecule size, requires some additional degrees of freedom for its components. Micropolar mechanics, which assumes media to be made of constituents that can rotate independently, ensures this. It is especially important for granular materials [32, 33]; various investigations on this particular type of problems can be found, for example, in [34]. Also, size effects such as effective mechanical properties including stiffness are influenced by the ratio between constituent and specimen sizes that is neglected by the classical elasticity. For example, in a recent work Liu [35] showed an increase of the bending stiffness in multilayered beams, while in other investigations it was further illustrated by the evidence that the shear stiffness increases with a decrease in sample size [36].

Next, micropolar theories give a more adequate description of the material behavior near such defects as cracks, holes, inclusions, etc. For instance, in some problems, even though the classical elasticity would predict infinite singular stresses, the Cosserat theory gave either finite stresses or weaker singularities [37, 38]. Moreover, micropolar mechanics, in contrast to the classical theory of elasticity, takes into account the size of these defects. Indeed, this theory predicts lower stress concentrations near small inho-

mogeneities, while predictions for large size defects will be similar to those obtained by the classical methods. Lakes [19, 20] has demonstrated that bones as natural composites are able to distribute stress around defects; consequently the micropolar approach predicting the reduction of stress concentrations near drilled holes seems reasonable [39]. In addition to this, Fatemi [40] has showed that stress concentrations derived by means of the Cosserat theory at the bone-prosthesis interface are significantly smaller when compared to the stress concentrations predicted by the classical theory. Furthermore, similar effects were also observed in the analysis of porous or cellular media composed of holes or inclusions [17, 18]. For holes with a relatively large radius (larger in size than three neighboring cells) stresses and strains were largely unaffected by the microstructure added into the model via the Cosserat theory, while for smaller holes the situation changed dramatically [41]. All these illustrate the scientific opinion that more sophisticated models produce higher accuracy in predicting material behavior.

Needless to say, the Cosserat theory was also exploited for the development of new non-classical models of rods, plates and shells [42, 43]. In addition to these solid mechanics applications, there are a number of studies which apply the Cosserat theory to fluid mechanics [44]. Because of all of these advantages of the micropolar mechanics over the classical mechanics, the theory is worth being implemented into a mathematical model. Such a model demonstrates some microstructural features and size effects not predicted by the classical theory of elasticity.

Although the micropolar mechanics captures microstructural effects of solids, another interesting phenomenon observed for real materials, related to size and not captured by the classical theory of elasticity is the surface effect.

It is well-known that physical, chemical and mechanical properties of materials

near the surface differ significantly from those observed in the bulk. One can notice that atoms located near the boundary have a specific local environment, in which they are subjected to a fewer bonding connections and constraints. Also, distances between neighboring atoms are different from the regular spacing associated with atoms inside the body. These changes in the atomistic structure result in an excess of free energy near the boundary, which is referred to as surface energy.

The surface energy, stresses and tension as continuum quantities were firstly introduced by Gibbs in his works on thermodynamics [45]. He has pointed out that these quantities are characteristics of a mathematical surface of zero thickness, which is attached to the boundary. It means that surface energy and surface stresses are significant in a few atomic layers only. Therefore, they do not really affect the overall behavior of a solid at the macro-scale where their contribution can be considered negligible. However, they play a crucial role in the description of deformation for solids, in which the characteristic grain size is such that the surface area to volume ratio is large. Examples of these solids are nanostructured materials (e.g. nanocomposites, nanocrystalline and nanoporous materials) and nanosized structural elements (e.g. nanolayers, nanorods, nanoshells, nanomembranes, nanowires, nanotubes, nanocoatings and nanoplates), for which the microstructural characteristic length and one of the dimensions of structural element are in the nano-range, respectively [46].

Interestingly, the surface effect in liquids was extensively studied for a long period of time starting from the works of Newton on capillarity and followed up later by Young, Laplace (see, for example, the review [47]). In contrast, the study of the surface effect in solids remained untouched until, as far as the author is aware, the work of Lennard-Jones et al. [48], where it was investigated how the closeness to the boundary can

affect the atomic structure of crystalline materials. Nowadays, tremendous progress in theoretical, experimental and computational techniques makes it possible to observe the surface effect and demonstrate its influence on material properties [49]-[54].

Nanostructured materials have demonstrated unusual mechanical, electrical, optical, thermo-mechanical and magnetic properties, that have opened new horizons for application in engineering and biology. At the same time, nano-sized elements have proven to be irreplaceable in nanodevices such as micro-electromechanical systems (MEMS) [46]. Achievements in nanomechanics have all reflected the need to generalize continuum-based models for utilization at smaller scales. Classical elastic theories failed to recognize the critical effect of the grain size on the overall deformation of the bulk material. Gurtin, Murdoch and co-workers first proposed a continuum-based theory (the so-called ‘Gurtin-Murdoch model’) to account for surface energies, stresses and tension in an elastic solid [55, 56]. A comprehensive discussion of the various versions of the Gurtin-Murdoch model was presented recently by Ru [57]. Generally, the Gurtin-Murdoch model is mathematically equivalent to the assumption of a surface coated by or reinforced with a thin solid film of separate elasticity. Steigmann and Ogden have suggested a generalization of Gurtin-Murdoch theory, taking into account bending rigidity of the reinforcing film attached to the boundary [58]. Numerous successful applications of these models can be found in [59] and references contained therein. Moreover, atomistic simulations have shown good agreement with these theories [60]. Comprehensive discussion on these topics can also be found in the work [61].

An extremely relevant area of research into the contribution of the surface is related to nano-structured materials, such as nanocomposites and nanoporous solids [62]-[64].

It was observed that the surface effect significantly affects material properties and cannot be ignored. Analogous results hold for studies devoted to the role of the surface on such defects as holes, inclusions [65]-[70] and cracks [71]-[73]. The findings suggest that stress concentrations are reduced significantly if the contribution of surface mechanics is taken into account, so that mathematical models can become more accurate to describe behavior closer to reality. In addition, surface mechanics found its application in the development of powerful and efficient models of thin films, plates and rods [61, 74, 75].

To conclude, both theories of micropolar and surface mechanics, applied simultaneously, can contribute significantly to the development of adequate models describing the behavior of real materials, since they have clearly demonstrated advantages over classical linear elasticity. The following question arises: why not develop a model that captures not only the micro-mechanical behavior of the bulk, which is known to be considerable in many real materials, but also the contribution of the surface effect which has been well-observed for bodies with significant size-dependency and large surface area to volume ratios. Such a model can be of great value for particular classes of materials, in which the effects of both surface and microstructure are known to be significant.

Even though a limited number of studies have been conducted on this type of model [76]-[80], their importance was demonstrated numerically as well as experimentally [81]. As stated before, having been developed, such a comprehensive model requires a rigorous mathematical formulation and a thorough analysis of the related boundary value problems. Otherwise, any attempt to implement this model in numerical analysis will likely lead to ineffective, physically incorrect or time-consuming simulations. To the

author's knowledge, the question of well-posedness for the problems involving both microstructural and surface effect has never been considered. The lack of sufficient studies may be due to the mathematical complexity of the micropolar bulk governing equations and boundary conditions which are further complicated if micropolar surface mechanics is taken into account. Indeed, the addition of the surface effect results in the rise of extremely non-standard boundary conditions. Therefore, classical methods for the well-posedness analysis of the corresponding boundary value problems (BVPs), particularly boundary integral equation methods (BIEM), break down and it is necessary to modify these methods to face the challenging requirements of such a comprehensive model.

Kupradze [82] gives one of the best sources of information on uniqueness and existence analysis for a variety of BVPs arising in different areas of elasticity, thermodynamics and even couple stress theory. Common methodologies of the BIEM analysis includes a representation of a solution in the form of potentials and a reduction of BVPs to singular integral equations. Treatment of diverse types of singular integral equations can be found in works of Vekua [83], Ishanov [84], Gakhov [85], Muskhelishvili [86] and Mikhlin [87].

Prior studies have implemented these methodologies, but focused on BVPs of the classical linear elasticity with the surface effect [59, 71, 88] or micropolar linear elasticity [89]-[92] separately. The combination of both effects in a single boundary value problem was never considered due to the mentioned complexity; and, therefore, it represents a challenging and elegant mathematical study, which is of great theoretical interest. To this end, *the research presented in this work focuses on the rigorous mathematical treatment of the model combining both the surface and microstructural effects in the*

*deformation of a solid.*

To account for the non-standard boundary conditions expressing the surface effect as well as the highly complicated governing equations of a micropolar bulk, a multidisciplinary step-by-step approach should be proposed. As a first step, it is worth incorporating only the surface effect. For example, the classical linear elastic model with surface effect under the simplest type of deformation, e.g. an anti-plane shear, will give insight into how to tackle the more complicated general micropolar case.

The anti-plane shear deformation has attracted a number of researchers because of its physical, as well as mathematical, simplicity allowing it to serve as a pilot problem for introducing new effects into more complicated types of deformations [93]. In the case of linear elasticity and couple stress theory, this deformation is characterized by an axial displacement only, while for the micropolar theory it is necessary to deal with two additional in-plane microrotations. The governing equation of the anti-plane shear of a classical linear elastic solid in the absence of body forces is given by the Laplace equation; questions of uniqueness and existence have been thoroughly studied [94]. However, the well-posedness analysis of anti-plane problems with surface effect remains absent from the literature. That is why it is important to investigate the uniqueness and existence of a solution to the supplementary problem of anti-plane linear elastic solid with surface effect first. Moreover, only after this analysis will there be sufficient understanding of the mathematical model as a basis to further develop more generalized versions of micropolar elasticity with surface effects.

That is why Part I of this paper-based thesis is devoted to the study of the coupling of surface mechanics with a bulk material in the framework of classical linear elasticity. In Chapter 3, the first chapter of Part I, we proceed with the development of a model for

anti-plane deformations of a classical linear elastic bulk with a reinforcing film perfectly bonded to its boundaries. This coating introduces the surface effect into the model and is given by a set of closed curves in a cross-section of the body. Chapter 4 provides the reader with a detailed well-posedness analysis of the BVPs corresponding to the developed model. The author's publication [97] summarizes the contents of Chapters 3 and 4. In Chapter 5, we extend the results of the preceding analysis to a more general case when the surface effect is considered on a part of the boundary (a set of open curves in a cross-section). This allows for the modeling of a wider class of problems and can be found in the following paper of the author [98]. All these investigations show that the suggested model is of great interest and can be further enhanced with the introduction of microstructure in Part II.

Part II starts with Chapter 7 which suggests a model for anti-plane deformations of a micropolar linear elastic bulk with reinforced boundaries. In the following Chapter 8, we proceed with the examination of the corresponding BVPs on the well-posedness. These investigations are summarized in the paper [99] of the author.

After the models have been developed and analyzed on the mathematical well-posedness, we can proceed further and demonstrate their merits. Classical solutions to some problems in fracture mechanics, for example, are characterized with an unbounded and, therefore, unphysical behavior. How can we implement our models there and check if they will improve this behavior? Asymptotic analysis can provide us with a tool for quick testing of the proposed models and their contribution to fracture mechanics. As an illustration, let us take the case when the material contains cracks or regions which give rise to discontinuities, singularities and inconsistencies in the mathematical model, and then examine the role of surface and/or microstructure in this model. The

expectation would be that the contribution of these effects would in some way lessen or possibly completely eliminate the deficiencies of the classical models.

For example, Kim et al. [72], whose research is in the framework of classical linear elasticity, showed that the surface effect represented by a reinforcement effectively eliminated the oscillatory behavior of the stress field in the vicinity of a crack tip. Therefore, it is crucial to investigate how the supplementary model of anti-plane deformations in a classical linearly elastic solid with the surface effect influences the singularity at the crack tip. Available classical results on the cracks in a linear elastic solid without reinforcement will allow for a comparative study. This study is presented in the last chapter of Part I, Chapter 6, where we demonstrate the effectiveness of the developed model on the example of an interface crack with reinforced tips. The analysis can be also found in the author's publication [100].

As for the general case of a micropolar solid with the surface effect, a similar demonstration of the effectiveness on the example of a crack in the micro-featured solid with the surface effect is difficult but can be adequately done using the couple stress theory. As mentioned, this theory is preferable for many applications since it is less complicated, easier to be verified experimentally and also reflects micro-features of real materials as well as the Cosserat continuum theory. Furthermore, there are some studies available for the asymptotic analysis of anti-plane shear cracks in a couple stress solid [95, 96] so that a proper judgment of the surface effect contribution can be made. Unfortunately, to the best of the author's knowledge, similar investigations for the micropolar case are absent from the literature. Therefore, the couple stress theory, a particular case of micropolar mechanics, is able to serve as a testing theory for the demonstration of the proposed model's effectiveness. To this end, in Chapter

9, the content of which can be found in the author's publication [101], we examine a crack with coated tips in the framework of couple stress theory, a particular case of micropolar elasticity.

---

## CHAPTER 2

# Preliminaries

This chapter sets up notation and terminology which will be used throughout the thesis. It also provides a brief discussion of function spaces and integral equations necessary for well-posedness analysis. In addition, this chapter summarizes the basic equations of the classical and micropolar linear theories of elasticity as well as the couple stress theory. These sections will demonstrate how all these three theories are distinguished in terms of: number of material parameters and boundary conditions describing a solid, particle's degrees of freedom and types of stress tensor.

In what follows Greek and Latin indices take the values 1, 2 and 1, 2, 3, respectively, the convention of summation over repeated indices is understood and  $(\dots)_{,\alpha} \equiv \partial(\dots)/\partial x_\alpha$ . Also,  $|\cdot|$  denotes the Euclidean norm, while  $\langle \cdot, \cdot \rangle$  - the standard inner product.

When using Cartesian coordinates  $(x_1, x_2, x_3)$  to describe the deformation in the solid we regard  $x$  as a planar coordinate so that  $x = (x_1, x_2)$ .

When using normal-tangential coordinates  $(n, \tau)$  to obtain the conditions on the boundary we parametrize any curve by arclength  $s(x)$  and we denote by  $n(s)$  the unit outward normal to this curve at  $s$  and by  $\tau(s)$  the unit tangent at  $s$ . The direction of

$\tau(s)$  is governed by an angle  $\theta(s)$  and its orientation, in which  $s$  increases, is chosen so that  $(n(s), \tau(s))$  is right-handed. Transformation from the Cartesian to the normal-tangential coordinate system is performed with the help of a standard transformation matrix:

$$I(x) = \begin{pmatrix} \sin \theta(x) & \cos \theta(x) & 0 \\ -\cos \theta(x) & \sin \theta(x) & 0 \\ 0 & 0 & 1 \end{pmatrix}.$$

When using polar coordinates  $(\tilde{r}, \tilde{\theta})$  to describe the behavior of solutions in the far-field and crack tip vicinity we assume that  $\tilde{r}(x) = |x|$  and  $\tilde{\theta}(x) = \arctan(x_2/x_1)$ .

Next,  $\mathcal{M}_{m \times n}$  is the space of  $(m \times n)$ -matrices and when  $n = 1$ , for convenience, we call any element of this space ‘a vector’; a superscript ‘T’ indicates matrix or vector transposition. We employ the matrix space  $\mathcal{M}_{m \times n}$  together with the standard-ordered bases  $\{E_{ij}\}$  and  $\{e_{ij}\}$  to express components of stress tensors, traction vectors and other related mechanical quantities.  $\delta_{ij}$  and  $\epsilon_{ijk}$  are the Kronecker’s delta and alternator tensor components, respectively.

## 2.1 Function spaces and integral equations

We specify here the space of functions in which solution to the boundary value problems is to be sought as well as the requirements to the boundary curves. Throughout the paper, we are particularly interested in the class of Holder continuous functions with index  $\alpha \in (0, 1]$ , for which the following can be stated [102]: for all  $x$  and  $y$  in  $\overline{X}$  we can write the inequality  $|f(x) - f(y)| \leq c|x - y|^\alpha$ , where  $c$  is a constant, a bar denotes the closure of a set, i.e.  $\overline{X} = X \cup \partial X$ , and  $|x - y|$  represents the distance

between two points  $x$  and  $y$ . Then we say that  $f$  belongs to the real vector space of Holder continuous functions  $C^{0,\alpha}(\overline{X})$  in  $\overline{X}$ . Furthermore, we denote  $C(\overline{X})$  and  $C^1(\overline{X})$ , respectively, the spaces of real continuous and continuously differentiable functions in  $\overline{X}$ .  $C^{1,\alpha}(\overline{X})$  is used to indicate the subspace of  $C^1(\overline{X})$  of all functions whose derivatives are functions of  $C^{0,\alpha}(\overline{X})$ .

In addition, we specify the type of the curve which is sufficiently smooth to represent a boundary in our analysis [102]. A curve  $\partial X$  of length  $|\partial X|$  in a bi-dimensional domain can be specified with the function of its arc coordinate  $x = \psi(s)$ ,  $s \in [0, |\partial X|]$ ,  $\psi(0) = \psi(|\partial X|)$  with the inverse relationship  $s = s(x)$ ,  $x \in \partial X$ . We call  $\partial X$   $C^2$ -curve if  $\psi \in C^2[0, |\partial X|]$  and regard it suitable for our analysis. If  $\partial X$  is a closed curve, then the additional requirement should be held:  $\frac{d^\alpha \psi}{ds^\alpha}(0^+) = \frac{d^\alpha \psi}{ds^\alpha}(|\partial X|^-)$ .

The boundary integral equation method (BIEM) allows to reduce boundary value problems (BVPs) to integral equations. The advantage of using integral equations instead of working directly with the BVPs lies in the fact that there is a number of theories available for the solvability proof, so that well-posedness of the model can be established [82]. That is why it is necessary to address some properties of integral equations in the current section. First of all, an integral equation is an equation, in which the unknown function appears under the integral sign. The simplest examples of such integral equations are Fredholm's linear integral equations of the first and second kind, respectively [94]:

$$\int_{\partial X} K(x, y)\phi(y)dy = f(x), \quad \phi(x) - \int_{\partial X} K(x, y)\phi(y)dy = f(x), \quad \in \partial X,$$

where  $\phi$  is an unknown function, while functions  $K(x, y)$  and  $f(x)$  are called, respec-

tively, the kernel and forcing term. Existence and uniqueness of a solution to the integral equations can be equivalently expressed for the so-called adjoint equations, obtained from the above ones by switching the variables  $x$  and  $y$  in the kernel  $K$ . If any derivatives of the function  $\phi$  appears in the integral equations, we call these integro-differential equations.

Based on the nature of kernel  $K(x, y)$ , particularly on its unboundness, integral equations can be weakly singular, strongly singular and hypersingular. Each type of equations requires its own special theory to analyze the existence of any solutions [103].

We say that the kernel  $K(x, y)$  is weakly singular if it is defined  $\forall(x, y) \in \partial X$  excluding  $x = y$ , continuous there and  $\exists M, \alpha \in \mathbb{R}$  so that:  $|K(x, y)| \leq M|x - y|^{-\alpha}$   $\forall(x, y) \in X$  with  $x \neq y$  and  $0 \leq \alpha < 2$ .

For integral equations with continuous or weakly singular kernel  $K(x, y)$  we can employ Fredholm's theorems to settle the existence of solutions.

**Theorem 2.1.** *If the homogeneous integral equations*

$$\phi(x) + \int_{\partial X} K(x, y)\phi(y)dy = 0, \quad \psi(x) + \int K(y, x)\psi(y)dy = 0, \quad x \in \partial X$$

*only have the trivial solutions  $\phi = 0$  and  $\psi = 0$ , respectively, then the inhomogeneous integral equations*

$$\phi(x) + \int_{\partial X} K(x, y)\phi(y)dy = f(x), \quad \psi(x) + \int K(y, x)\psi(y)dy = g(x), \quad x \in \partial X$$

*have a unique continuous solutions  $\phi$  and  $\psi$  for each continuous forcing function  $f$  and  $g$ , respectively.*

Here integral equations with the unknown function  $\psi(x)$  are called adjoint equations; they represent counterparts of original equations obtained when the variables  $x$  and  $y$  are switched.

Next, let the kernel be of the form

$$K(x, y) = \frac{L(x, y)}{(x - y)^\alpha}, \quad x \in \partial X \quad (2.1)$$

If  $\alpha = 1$ , then the kernel  $K(x, y)$  has a strong singularity at  $x = y$ ; so that the improper integral containing this kernel exists only in the case when certain conditions are satisfied and is to be understood in the sense of Cauchy principal value. The corresponding integral equation is called singular integral equation with Cauchy type kernel or strongly singular integral equation. For such an integral equation, a special theory is required to prove the existence result. An example of singular integral equation with a Cauchy kernel

$$A(x)\phi(x) + \frac{1}{\pi i} \int_{\partial X} \frac{B(x, y)\phi(y)}{y - x} dy + \int K(x, y)\phi(y) dy = f(x) \quad x \in \partial X, \quad (2.2)$$

where  $A(x)$  and  $B(x, y)$  are known functions. Left hand side of this equation can be represented with the help of a singular operator  $\mathcal{K} = A(x)I + B(x)S + V$ , where  $B(x) = B(x, x)$ ,  $I$  is the identity operator,  $S$  is the singular integral operator with Cauchy kernel and  $V$  is the weakly singular integral operator. For a singular operator  $\mathcal{K}$  we can calculate an important value called index of the singular integral operator:

$$\kappa = \frac{1}{2\pi} \arg \left[ \frac{A(x) - B(x)}{A(x) + B(x)} \right], \quad (2.3)$$

where  $\arg[\ ]$  denotes the increment of the argument of the function in brackets along the contour in a positive direction and  $(A^2 - B^2)(x)$  is assumed to vanish nowhere on this contour. The index  $\kappa$  does not depend on the weakly singular part of the equation. In case (2.2) represents the system of singular integral equations the index can be found in the following manner assuming non-vanishing determinants

$$\kappa = \frac{1}{2\pi} \arg \left[ \frac{\det(A + B)}{\det(A - B)} \right]. \quad (2.4)$$

In fact, Fredholm's theorems do not hold for singular integral equations. However, under special circumstances we can still use Fredholm's theorems for equations of this type. Noether's theorem states that if a singular integral operator of an equation has a zero index then Fredholm's theorems can be used to prove the existence of a solution to this equation. Hence, as soon as boundary value problems will be reduced to integral equations (with the help of BIEM), we can use Noether's and Fredholm's theorems to prove that the proposed model is well-posed.

**Remark.** *If  $\alpha = 2$  in (2.1), then we deal with the hypersingular kernel and corresponding hypersingular equation, analysis of which is extremely challenging and out of the scope of the current research.*

## 2.2 Basic equations of classical linear elasticity

Classical linear elasticity theory is the most well-studied branch of continuum mechanics with the research dating back to the works of such prominent scientists as Cauchy and Navier. This theory contains stress equilibrium equations, kinematic equations,

constitutive equations, boundary equations and so on. These basic equations are derived with the help of the following fundamental assumptions on the properties of the body.

Let a solid to exist as a static continuum, so that the matter in the body is continuously distributed and fills the entire region of space it occupies. Hence, the continuum consists of an infinite number of particles connected together in a configuration which changes when deformation is applied. Assume that these changes in the configuration are relatively small compared with the body's original dimensions; and, as a result, all basic equations will be in the linearized form. Assume further we have an elastic solid meaning that the body recovers its original shape when loadings causing deformations are removed. Next, let us say that this solid is also homogeneous and isotropic, so that the properties of the body are the same at all locations and in all directions.

In classical linear elasticity [82] the change in the configuration can be tracked with the help of displacement vector  $u$  with components  $u_i$ . The interaction between two parts of the body is uniquely determined by the principal force vector. The equilibrium equations yield

$$\sigma_{ji,j} + F_i = 0,$$

where  $F_i$  are the components of the body force vector,  $\sigma_{ij} = \sigma_{ji}$  are the components of the symmetric stress tensor.

The kinematic relations

$$\varepsilon_{ij} = \frac{1}{2}(u_{i,j} + u_{j,i})$$

help to express the strains  $\varepsilon_{ij} = \varepsilon_{ji}$  through the displacements  $u_i$ .

The constitutive equations relating deformations with material properties are given

by

$$\sigma_{ij} = \lambda \varepsilon_{kk} \delta_{ij} + 2\mu \varepsilon_{ij}.$$

It can be seen that a classical linear, homogeneous and isotropic elastic material is determined with two material parameters only, namely the Lamé's constants  $\lambda$  and  $\mu$ .

The internal energy per unit volume can be expressed as

$$E = \frac{\lambda}{2} (\varepsilon_{kk})^2 + \mu \varepsilon_{ij} \varepsilon_{ij}.$$

Finally, boundary conditions of two types can be established:

- three displacements are imposed on the portion of the surface of the body:  $u_i = u_i^0$  (displacement Dirichlet boundary conditions);
- three tractions are prescribed on the portion of the surface of the body:  $n_i \sigma_{ij} = t_j^0$  (stress Neumann boundary conditions).

Other possible boundary conditions are given by a combination of these two conditions and referred to as mixed boundary conditions.

In brief, for a classical linear elastic solid we can state the following most relevant properties: the motion of a material point could be represented by three displacement components; the interaction between two parts of the body is uniquely determined by the force vector; the stress tensor is symmetric; a linear isotropic material is determined with two constants; and, finally, three conditions should be prescribed on every point of the boundary.

## 2.3 Basic equations of micropolar linear elasticity

Now, let us discuss in the similar manner the general micropolar linear elasticity [12], a more profound theory than a classical linear elasticity since it takes into account the microstructure of the body. In micropolar linear, isotropic and homogeneous elastic solid the deformation of a material point could be represented by three displacement components  $u_i$  as well as three additional independent microrotations  $\varphi_i$ . It is assumed that the interaction between two parts of the body is carried out not only by a force vector, but also by a moment vector. The equilibrium equations yield

$$\begin{aligned}\sigma_{ji,j} + F_i &= 0, \\ \mu_{ji,j} + \epsilon_{ijk}\sigma_{jk} + C_i &= 0.\end{aligned}$$

Here  $F_i$  and  $C_i$  are, respectively, the components of the body force and couple vectors, while  $\sigma_{ij} \neq \sigma_{ji}$  are the components of the asymmetric stress tensor.

Components of the asymmetric strain and micro-strain tensors are, respectively,

$$\gamma_{ij} = u_{j,i} - \epsilon_{kij}\varphi_k, \quad \kappa_{ij} = \varphi_{j,i}$$

The constitutive equations can be expressed as

$$\begin{aligned}\sigma_{ij} &= (\mu + \alpha)\gamma_{ij} + (\mu - \alpha)\gamma_{ji} + \lambda\gamma_{kk}\delta_{ij}, \\ \mu_{ij} &= (\gamma + \epsilon)\kappa_{ij} + (\gamma - \epsilon)\kappa_{ji} + \beta\kappa_{kk}\delta_{ij}.\end{aligned}$$

Clearly, a homogeneous and isotropic micropolar solid is fully determined with six

material parameters  $\lambda$ ,  $\mu$ ,  $\alpha$ ,  $\beta$ ,  $\gamma$  and  $\epsilon$ .

The internal energy per unit volume is given by

$$E = \frac{\mu + \alpha}{2} \gamma_{ji} \gamma_{ji} + \frac{\mu - \alpha}{2} \gamma_{ij} \gamma_{ji} + \frac{\lambda}{2} \gamma_{kk} \gamma_{nn} + \frac{\gamma + \epsilon}{2} \kappa_{ji} \kappa_{ji} + \frac{\gamma - \epsilon}{2} \kappa_{ji} \kappa_{ij} + \frac{\beta}{2} \kappa_{kk} \kappa_{nn}.$$

Boundary conditions of two types can be established:

- three displacements and three microrotations are imposed on the portion of the surface of the body:  $u_i = u_i^0$ ,  $\varphi_i = \varphi_i^0$  (displacement and microrotations boundary conditions);
- three tractions and three couples are prescribed on the portion of the surface of the body:  $n_i \sigma_{ij} = t_j^0$ ,  $n_i \mu_{ij} = \mu_j^0$  (stress and couple stress boundary conditions).

In short, for a micropolar linear elastic solid we can state the following most important properties: the motion of a material point could be represented by six independent components; the interaction between two parts of the body is uniquely determined by the force and couple vectors; the stress tensor is asymmetric; a linear isotropic material is determined with six constants; and, finally, six conditions should be prescribed on every point of the boundary.

Certainly, the consideration of microstructure implies considerable difficulties, in contrast to classical studies. However, there is a particular case of micropolar mechanics, the couple stress theory, in which simplified basic equations and assumptions will still reflect microstructural effects.

### 2.3.1 Basic equations of couple stress theory

In the couple stress theory, the microrotation  $\varphi$  is no longer independent of the displacement field but, in fact, is aligned with the usual continuum mechanics macrorotation of the body (one half of the curl of the displacement field). It should be noted that even though a particle has less degrees of freedom there, the couple stress theory should not be treated just as a simplification of the micropolar theory, but as an independent theory, which has proven reliable and even preferable for some particular types of problems [9]. Moreover, as in the general micropolar theory, in the couple stress theory two parts of the body still interact with each other over an infinitesimal surface element via both force and couple vectors, but this time some of the components of these vectors will be related.

As has been noted, in the couple stress theory the rotation vector is fully specified by the displacement vector through the following relations

$$\varphi_i = \frac{1}{2} \epsilon_{ijk} u_{k,j}.$$

The equilibrium equations for a linear, homogeneous and isotropic couple stress elastic solid under anti-plane deformations look as follows

$$\begin{aligned} \sigma_{ji,j} + F_i &= 0, \\ \mu_{ji,j} + \epsilon_{ijk} \sigma_{jk} + C_i &= 0. \end{aligned}$$

The components of the symmetric strain and micro-strain tensors are, respectively,

$$\varepsilon_{ij} = \frac{1}{2}(u_{i,j} + u_{j,i}), \quad \kappa_{ij} = \varphi_{j,i}$$

The constitutive equations can be expressed as

$$\begin{aligned} \sigma_{ij} &= \lambda \varepsilon_{kk} \delta_{ij} + 2\mu \varepsilon_{ij} - \frac{1}{2} \epsilon_{ijk} \mu_{lk,l}, \\ \mu_{ji} &= 4\alpha \kappa_{ij} + 4\beta \kappa_{ji}, \end{aligned}$$

so that a couple stress solid is determined by four material parameters  $\lambda$ ,  $\mu$ ,  $\alpha$  and  $\beta$ .

The strain energy per unit volume is expressed as

$$E = \frac{\lambda}{2} \varepsilon_{ll} \varepsilon_{kk} + \mu \varepsilon_{ij} \varepsilon_{ij} + 2\alpha \kappa_{ij} \kappa_{ij} + 2\beta \kappa_{ji} \kappa_{ij}.$$

Boundary conditions of two types can be established:

- three displacements and two microrotations are imposed on the portion of the surface of the body:  $u_i = u_i^0$ ,  $\varphi_\alpha = \varphi_\alpha^0$  (displacement and microrotations boundary conditions);
- three tractions and two couples are prescribed on the portion of the surface of the body:

$$n_j \sigma_{ji} - \frac{1}{2} \epsilon_{ijk} n_j (n_p \mu_{pq} n_q)_{,k} = t_i, \quad n_j \mu_{j\alpha} - (n_j \mu_{jk} n_k) n_\alpha = \mu_\alpha^0$$

(stress and couple stress boundary conditions).

It can be seen that in the couple stress theory we have a reduced number of boundary conditions since we are dealing with constrained microrotations [9].

On the whole, for a couple stress linear elastic solid we can state the following most important properties: the motion of a material point could be represented by three independent displacements and three dependent microrotations; the interaction between two parts of the body is uniquely determined by the force and couple vectors; the stress tensor is asymmetric; a linear isotropic material is determined with four constants; and, finally, five conditions should be prescribed on every point of the boundary. Indeed, the consideration of microstructure in the framework of couple stress theory implies less difficulties compared to general micropolar case. Moreover, it is generally accepted that the couple stress theory is a more promising theory than the general micropolar theory for experimental verification and numerical implementation [9].

## Part I

Coupling of surface mechanics with  
a bulk material in the framework of  
classical linear, homogeneous and  
isotropic elasticity

---

## CHAPTER 3

# Mathematical modeling: incorporation of surface effects

As noted, real physical materials naturally incorporate both surface and microstructural effects. The elimination of one of these effects in a model can be a convenient way to test the boundary integral equation method (BIEM) on a simplified yet interesting mathematical problem. After this, it will be easier to proceed to the model incorporating both effects. Clearly, in our particular case, the most reasonable decision is, at first, to consider the surface effect only because it will arise in boundary conditions only, while the governing equations can be easily obtained from the classical linear elasticity theory. Moreover, there are some types of deformation in the classical linear elasticity which are attractive because of their physical and mathematical simplicity. To this end, it will be convenient to use them as a pilot problem to test our BIEM. Among these simple deformations, anti-plane shear is especially attractive since its governing equation is given by the Laplace equation (in the absence of body forces) [93], for which questions of uniqueness and existence have been thoroughly studied [94]. At the same time, well-posedness analysis for the Laplace equation with extremely non-standard

boundary condition representing the surface effect has been never studied.

As indicated in the introduction, the properties of the material on the surface and in the bulk are quite different. This difference is especially significant for nano-sized objects or material with micro-features. One way to reflect this critical effect and account for surface energies, stresses and tension in an elastic solid is the Gurtin-Murdoch model. This model is based on the consideration of energy functions and is mathematically equivalent to the assumption of a surface coated by or reinforced with a thin solid film of separate elasticity. However, in our work we follow Steigmann and Ogden's generalization of this theory, which takes into account bending rigidity of the reinforcing film attached to the boundary [58] and is based on the equilibrium of the thin film.

To this end, in the beginning of Part I, we develop the model of anti-plane deformations of a linearly, elastic, homogeneous and isotropic solid in which the bounding surface of the solid is endowed with a separate elasticity which affects the overall deformation of the solid. The boundary elasticity consists of a distinct thin linearly, elastic, homogeneous and isotropic coating bonded to a part of the boundary of the solid.

We consider the equilibrium of a deformable solid occupying a cylindrical region whose generators are parallel to the  $x_3$ -axis of a rectangular Cartesian coordinate system. The cylinder is assumed to be sufficiently long so that end effects in the axial direction are negligible. We assume that the cross-section  $S$  of the cylinder is occupied by a homogeneous and isotropic elastic material with shear modulus  $\mu > 0$ . The boundary  $\partial S$  of  $S$  is described by the union of a finite number of sufficiently smooth closed curves. We regard a subset  $\Gamma$  (consisting of a finite number of sufficiently smooth closed curves) of  $\partial S$  as being coated with a thin, homogeneous and isotropic elastic

film with separate shear modulus  $\bar{\mu} > 0$ . Since the coating covers all surfaces of the particular cylindrical holes and is given by closed curves in the cross section, such a model can prove especially useful in the description of the behavior of porous materials or fibre-reinforced composites.

It should be noted that some passages in this and the next chapter have been quoted verbatim from the author's publication [97].

### 3.1 Governing equations

A state of anti-plane shear is characterized by a displacement field  $u = (u_1, u_2, u_3)$  of the form

$$u_1(x_1, x_2, x_3) = u_2(x_1, x_2, x_3) = 0; \quad u_3(x_1, x_2, x_3) = w(x),$$

where the out-of-plane displacement  $u_3$  is a function  $w$  of  $x$  on the cross-section  $S$  of the cylinder. It is well-known [93] that, in the absence of body forces, the governing equations for the anti-plane displacement  $w$  is given by the Laplace equation

$$Lw = \Delta w = 0, \tag{3.1}$$

where  $\Delta \equiv \frac{\partial^2}{\partial x_1^2} + \frac{\partial^2}{\partial x_2^2}$  is the Laplace operator in  $\mathbb{R}^2$ .

The boundary stress operator is given by  $T(\partial x) = \mu \frac{\partial w}{\partial n_x}$ , where  $\frac{\partial(\ )}{\partial n(x)} = \frac{\partial(\ )}{\partial n_x}$  represents the normal derivative at  $x$ .

The internal energy density given by

$$E(w, w) = \frac{\mu}{2}(w_{,1}^2 + w_{,2}^2) \quad (3.2)$$

is a positive quadratic form. Further,  $E(w, w) = 0$  if and only if  $w = c$ , where  $c$  is an arbitrary constant.

Finally, we recall the well-known fundamental solution [94] for the Laplace operator:

$$D(x, y) = -\frac{1}{2\pi} \ln |x - y|,$$

where  $x, y$  are generic points in  $\mathbb{R}^2$  and  $D(x, y)$  satisfies (3.1) at all  $x \neq y$ . This fundamental solution will help to analyze the boundary value problems formulated for the model with the help of integral equations.

## 3.2 Boundary conditions describing surface effect

To reflect the specific behavior of a material near the surface, i.e. the surface effect, we assume that this behavior arises because of the contact with the thin reinforcing film of thickness  $h$  perfectly bonded to the surface of the cylindrical holes. Indeed, this coating has different material properties described by the parameter  $\bar{\mu}$ ; and as a part of the bulk boundary it deforms only in the axial direction under the anti-plane shear loading. These result in the transmission of stresses from the film to the boundary of the bulk.

Thus, the conditions on the (reinforced) subset  $\Gamma$  of the boundary  $\partial S$  couple the response of the solid to that of the coating on  $\Gamma$ . To describe this response in terms

of a boundary condition on  $\Gamma$ , we propose to use the normal-tangential coordinates  $(n(s), \tau(s), x_3)$ , where  $s(x)$  is the arclength coordinate. The coated subset of the cylinder's boundary is composed of a thin plate, whose displacement field at any cross-section is characterized by

$$u_n = u_\tau = 0; \quad u_3(\tau).$$

Therefore, the equilibrium equations for the plate read

$$\bar{\mu} d_x^2 w + F_3 = 0$$

with  $d_x = \frac{d(\cdot)}{ds(x)} = \frac{d(\cdot)}{ds_x}$  denoting the directional derivative with respect to  $s(x)$  along  $\Gamma$  (tangential) and  $F_3$  representing the force per unit volume in the reinforcement and  $\bar{\mu}$  represents elastic material properties of the reinforcing film. Our reinforcement is thin and all quantities are independent of the thickness  $h$  in the normal direction, so we can write

$$\int_0^h (\bar{\mu} d_x^2 w + F_3) ds = 0, \quad h[\bar{\mu} d_x^2 w + F_3] = 0.$$

Since nothing depends on the axial direction, we assume that all cross sections behave in the same way. Subsequently, on each cross section the reinforcement transmits the stress  $-h\bar{\mu} d_x^2 w$  to the boundary at the hole. Therefore, the stress boundary condition on  $\Gamma$  is

$$\frac{1}{\mu} \sigma_{3n} = \frac{\partial w}{\partial n} = -h \frac{\bar{\mu}}{\mu} \frac{d^2 w}{ds^2}.$$

If we assume the existence of the prescribed stress  $Q(x) = \mu g(x)$  on the boundary

$\partial S$ , then the condition on the reinforced boundary reads

$$\frac{\partial w}{\partial n} = -h \frac{\bar{\mu}}{\mu} \frac{d^2 w}{ds^2} + g. \quad (3.3)$$

Thus, the modeling of the reinforcement gives rise to the boundary condition involving the second derivative of the unknown on the boundary which, in turn, leads to a most unusual yet extremely interesting boundary value problems for the Laplace equation. The next chapter will provide us with the rigorous mathematical analysis of these boundary value problems.

To conclude, it should be mentioned that we have assumed that surface effect spreads on the whole boundary of the cylindrical holes, so that the reinforced boundary  $\Gamma$  in the cross-section of the body was given by a set of closed curves. Later in the thesis we will discuss the more practical yet more mathematically sophisticated generalized case when only part of the boundary incorporates the surface effect, so that the reinforcement is given by arcs in the cross-section of the body.

---

## CHAPTER 4

# Well-posedness analysis of the model incorporating surface effects

Centuries of research in the field of mechanics have given an amazing tool for modern researchers to develop new mathematical models predicting the systems' response to applied deformations. As a result, today we are dealing with a number of models and choices. When choosing the model or judging the adequacy of the new one, one important aspect to consider is if it is well-posed or not. According to Hadamard, for a model of a physical phenomenon to be adequate, its solution should have the following properties:

- It exists.
- It is unique.
- Its behavior continuously depends on the initial data.

Mathematically ill-posed problems can lead to physically incorrect solutions. Attempts to perform numerical simulations on a model which has not been analyzed on well-posedness can waste time and resources. For example, sometimes it is hard to determine

whether there is a sufficient number of boundary and initial conditions for the particular model at hand or not. If a model is subjected to an excessive number of conditions, then there are high chances that no solution can be found. Thus, it is the same as using of a small fishing net to get a big fish. If a model has insufficient number of conditions, there is a chance that an infinite number of solutions satisfies the problem conditions. Therefore, the fisherman will end up with a large number of fishes, one of which is supposed to be the golden fish that grants him with three wishes. The last requirement for the problem to be well-posed can be adequately illustrated by recalling that all initial data for real physical phenomena are based on experimental measurements, which can be perfect only in impossible idealized conditions. Consequently, small changes in the initial data should not cause significant changes in the solution, Analogously, change of the color or material of the fishing net should not supply the fisherman with exotic fishes. Nevertheless, in many numerical problems the role of well-posedness analysis is ignored while uniqueness and existence of solution can be mistakenly assumed.

Of course, if a problem is ill-posed, it should not be immediately excluded. Many physical phenomena are modeled with the help of ill-posed models. For example, almost all inverse problems are ill-posed. Nevertheless, these models require a special treatment, reformulation, and usage of regularization methods.

An important role in well-posedness analysis is played by a proper choice of function space in which a solution is to be sought. This decision affects the methods for the well-posedness proof. A good source on this material can be found in the work of Kupradze [82]. In the current research to analyze boundary value problems (BVPs) and make a conclusion on their legitimacy we employ space of Holder-continuous functions and boundary integral equation method (BIEM). If the model is proved to be well-posed

there are good chances to develop a stable algorithm for it, which makes this model reliable and attractive to implement.

Thus, in the present chapter, we consider boundary value problems for the Laplace equation arising when the boundary of the (multiply-connected) domain is partly coated (reinforced) in such a way that the coated part of the boundary consists of only a finite number of sufficiently smooth closed curves. A combination of stress and displacement is prescribed on the remaining (non-reinforced) part of the boundary.

Using a generalization of the well-known boundary integral equation method [94, 104] to account for the non-standard boundary condition on the reinforced section of the boundary, we reduce the corresponding boundary value problems to singular integro-differential equations. Solvability results are derived for both the corresponding infinite domain (exterior) and finite domain (interior) boundary value problems.

## 4.1 Boundary value problems (BVPs) for the proposed model

### 4.1.1 Bounded domain

We consider the case when  $S$  is a bounded domain (interior problem) enclosed by a sufficiently smooth boundary  $\partial S$ . Write  $\partial S = \partial S_1 \cup \Gamma$  where the closed curve  $\partial S_1$  represents the non-reinforced section of  $\partial S$ . For simplicity, we divide  $\partial S_1$  into two open curves  $\partial S_u$  and  $\partial S_t$  with common endpoints  $a$  and  $b$  and let  $\Gamma$  represent a single closed reinforced curve (Figure 4.1). The case where  $\partial S_1$  is divided into more than two parts and where  $\Gamma$  consists of a finite number ( $> 1$ ) of closed curves is treated similarly

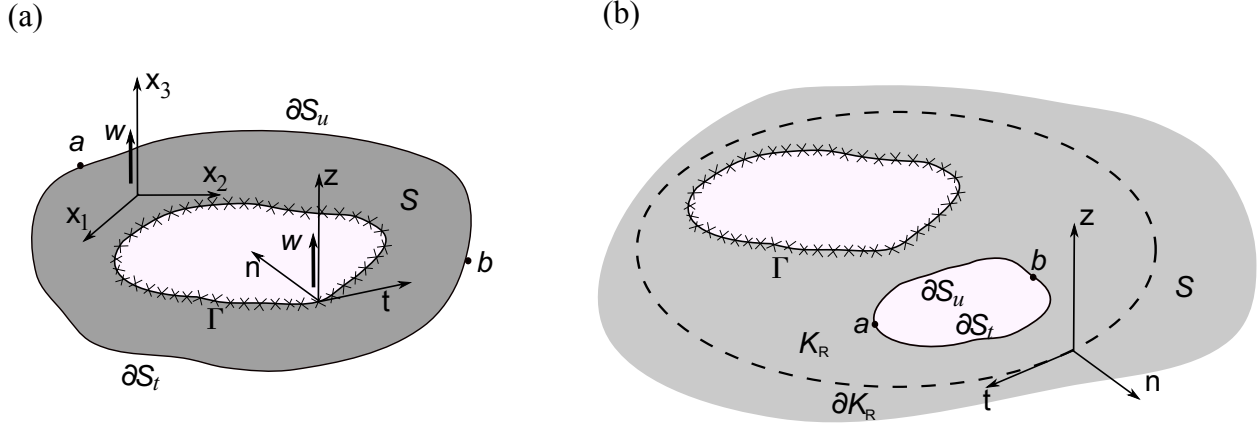


Fig. 4.1: Classical linear, homogeneous and isotropic elastic domain: bounded (a) and unbounded (b) cases

without any significant modifications to our method.

The interior mixed boundary value problem (problem in a finite domain) requires that we find  $w \in C^2(S \cup \Gamma) \cap C^1(\bar{S} \setminus \{a, b\})$  such that (3.1) is satisfied and

$$\begin{aligned}
 w(x) &= w^{(0)}(x), & x \in \partial S_u, \\
 \frac{\partial w(x)}{\partial n(x)} &= t^{(0)}(x), & x \in \partial S_t, \\
 \frac{\partial w(x)}{\partial n(x)} &= -h \frac{\bar{\mu}}{\mu} d_x^2 w(x) + g(x), & x \in \Gamma.
 \end{aligned} \tag{4.1}$$

Here  $w^{(0)}$  and  $t^{(0)}$  are, respectively, functions of prescribed displacement and stress on  $\partial S_u$  and  $\partial S_t$ .

In questions of uniqueness one usually has to consider the Betti formula. If  $w$  is a solution to the interior boundary value problem (4.1), then the following formula can be proved [102]

$$2 \int_S E(w, w) d\sigma = \int_{\partial S} w^T T w ds, \tag{4.2}$$

where  $Tw = \mu \partial w(x) / \partial n(x)$  is a boundary stress operator for a solid subjected to anti-plane deformations.

**Theorem 4.1.** *The interior boundary value problem (4.1) has at most one solution.*

*Proof.* Let  $\omega$  be the difference of two solutions  $w_1$  and  $w_2$ , then  $\omega = w_1 - w_2$  satisfies a homogeneous boundary value problem (4.1)<sup>0</sup> (with  $w^0(x) = 0$ ,  $t^0(x) = 0$ ,  $g(x) = 0$ ). The internal energy density is given by (3.2). From the Betti formula (4.2)

$$2 \int_S E(\omega, \omega) d\sigma = \int_{\partial S_u \cup \partial S_t} \omega^T T \omega ds - h \bar{\mu} \int_{\Gamma} \omega \frac{d^2 \omega}{ds^2} ds.$$

Notice, that we use positive orientation when  $S$  lies to the left as the boundaries are traversed. The first integral in the above expression is zero on the  $\partial S_u \cup \partial S_t$ , while the integral over  $\Gamma$  is taken clockwise to maintain positive orientation of the boundaries. For consistency, we should change the sign of this integral and make it counterclockwise:

$$2 \int_S E(\omega, \omega) d\sigma = h \frac{\bar{\mu}}{\mu} \int_{\Gamma} \omega \frac{d^2 \omega}{ds^2} ds.$$

Application of integration by parts to the remaining integral results in

$$h \frac{\bar{\mu}}{\mu} \int_{\Gamma} \omega \frac{\partial^2 \omega}{\partial s^2} ds = h \bar{\mu} \left[ \int_{\Gamma} \frac{d}{ds} \left( \omega \frac{d\omega}{ds} \right) ds - \int_{\Gamma} \left( \frac{d\omega}{ds} \right)^2 ds \right].$$

The first term in the right-hand side of this expression is the integral of an exact differential over a closed circuit and, therefore, equals zero. Finally, the Betti formula (4.2) is simplified to

$$2 \int_S E(\omega, \omega) d\sigma = -h \bar{\mu} \int_{\Gamma} \left( \frac{d\omega}{ds} \right)^2 ds.$$

The right-hand side of this expression is non-negative, while the left-hand side is non-positive. It means that both sides must be zero. Then  $E(\omega, \omega) = 0$  in  $S$  and  $\frac{d\omega}{ds} = 0$  or  $\omega$  is constant on  $\Gamma$ . Since  $\omega \in C^1(\overline{S})$  and  $\omega = 0$  on  $\partial S_u$ , it follows that  $\omega = 0$  in  $S$ . Therefore  $w_1 = w_2$  and the theorem is proved.  $\square$

### 4.1.2 Unbounded domain

If we will apply the well-known Saint-Venant's principle to our particular problem, then the presence of the reinforced holes in the cylindrical body should not affect the far-field behavior. It means that if we will consider an unbounded domain (exterior problem) and obtain results on the existence and uniqueness of a solution similar to those obtained for a bounded domain, then we can exclude the physical boundary and consider the regions of interest only. This is especially advantageous if the model will be employed for numerical analysis.

The exterior problem (problem of an infinite domain) is posed similarly to the interior problem except that  $S$  is now an unbounded domain and we need an additional condition as  $\tilde{r} = |x| \rightarrow \infty$  to apply the Betti formula (4.2). Let  $\mathcal{A}$  be a class of  $w$  admitting asymptotic expansion, so that  $w = O(\tilde{r}^{-1})$ . Consider also the set

$$\mathcal{A}^* = \{w := w_0 + c\}. \quad (4.3)$$

Here  $w_0 \in \mathcal{A}$  and  $c$  is an arbitrary constant.  $\mathcal{A}$  and  $\mathcal{A}^*$  are classes of finite energy functions (so that (3.2) is finite) and (4.3) represents the asymptotic condition.

The exterior mixed boundary value problem requires that we find  $w \in C^2(S \cup \Gamma) \cap$

$C^1(\bar{S} \setminus \{a, b\}) \cap \mathcal{A}^*$  such that (3.1) is satisfied and

$$\begin{aligned} w(x) &= w^{(0)}(x), & x \in \partial S_u, \\ \frac{\partial w(x)}{\partial n(x)} &= t^{(0)}(x), & x \in \partial S_t, \\ \frac{\partial w(x)}{\partial n(x)} &= -h \frac{\bar{\mu}}{\mu} d_x^2 w(x) + g(x), & x \in \Gamma. \end{aligned} \tag{4.4}$$

**Theorem 4.2.** *The exterior boundary value problem (4.4) has at most one solution.*

*Proof.* Let  $\omega = w_1 - w_2$  be the difference of any two solutions of (4.4) in  $S$ . Consider a disk  $K_R$  of radius  $R$  large enough to involve  $\partial S$  (see Figure 4.1). Applying the Betti formula in  $\bar{S} \cap \bar{K}_R$  and assuming that the boundary consists of  $\partial S$  and  $\partial K_R$  we have:

$$2 \int_{S \cap K_R} E(\omega, \omega) d\sigma = - \int_{\partial S} \omega^T T \omega ds + \int_{\partial K_R} \omega^T T \omega ds.$$

In terms of the polar coordinates with the pole at the center of  $K_R$  and using (4.3) for the second integral in the right-hand side of this expression we can state

$$\int_{\partial K_R} \omega^T T \omega ds = \int_0^{2\pi} \omega \frac{d^2 \omega}{d\tilde{r}^2} \tilde{r} d\tilde{\theta} = \int_0^{2\pi} O(\tilde{r}^{-3}) d\theta \rightarrow 0 \quad \text{as } \tilde{r} \rightarrow \infty.$$

Finally, the Betti formula (4.2) for the exterior case is given by

$$2 \int_S E(\omega, \omega) d\sigma = - \int_{\partial S} \omega^T T \omega ds = - \int_{\Gamma} \omega^T T \omega ds = h \bar{\mu} \int_{\Gamma} \omega \frac{d^2 \omega}{ds^2} ds.$$

The remaining part of the proof repeats the steps from Theorem 4.1 for the bounded domain  $S$  to conclude that again  $\omega = 0$  in  $S$ .  $\square$

## 4.2 Boundary integral equation method (BIEM) and potentials

In the previous section we have formulated BVPs and proved that they have unique solutions. To complete the well-posedness analysis we are to prove that these solutions exist. Boundary integral equation method (BIEM) is a well-known technique giving a rise to the numerical boundary element method (BEM) but also a convenient way to establish existence primarily because of the available theorems on existence of solutions to integral equations (Noether's and Fredholm's theorems) [107]. In BIEM we look for solution to boundary value problems in the form of potentials. Here we highlight some important properties of potentials which will prove useful throughout the thesis.

Single- and double-layer potential are, respectively, given by the following integrals with an unknown density  $\phi$ :

$$(V\phi)(x) = \int_{\partial S} D(x, y)\phi(y)ds_y, \quad (W\phi)(x) = \int_{\partial S} T(\partial y)D(x, y)\phi(y)ds_y, \quad x \in S.$$

Here  $T(\partial y) = \partial D(x, y)/\partial n_y$ .

**Theorem 4.3.** *Single- and double-layer potentials have the following properties [104]:*

1. *If  $\phi \in C(\partial S)$ , then single- and double-layer potentials are analytical functions of  $\mathcal{A}$ -class, class of finite energies (3.2), satisfying governing equations  $L(V\phi) = 0$  and  $L(W\phi) = 0$  in both  $S^+$  and  $S^-$  (the operator  $L = \Delta$  for the Laplace equation).*
2. *If  $\phi \in C^{0,\alpha}(\partial S)$ ,  $\alpha \in (0, 1)$ , then  $V\phi \in C^{1,\alpha}(\partial S)$ ,  $\alpha \in (0, 1)$  has extensions to*

$\overline{S^\pm}$ , i.e.  $(V\phi)^\pm$  and

$$T(V\phi)^\pm = \begin{cases} T(V\phi), & x \in S^\pm \\ \pm \frac{1}{2}I\phi + T(V_0\phi), & x \in \partial S \end{cases}$$

3. If  $\phi \in C^{1,\alpha}(\partial S)$ ,  $\alpha \in (0, 1)$ , then  $W\phi \in C^{1,\alpha}(\partial S)$ ,  $\alpha \in (0, 1)$  and

$$(W\phi)^\pm = \begin{cases} W\phi, & x \in S^\pm \\ \mp \frac{1}{2}I\phi + W_0\phi, & x \in \partial S. \end{cases}$$

4.  $T(W\phi)^+ = T(W\phi)^-$  on  $\partial S$ .

where  $V_0\phi$  and  $W_0\phi$  are direct values of  $V\phi$  and  $W\phi$  on  $\partial S$ , while ‘+’ and ‘-’ are used to denote bounded and unbounded domains, respectively.

### 4.3 Application of BIEM to the analysis of well-posedness for the proposed model

Now we know the properties of BIEM potentials and can proceed to the examination of solvability question for the corresponding BVPs.

It is well-known that, using results for the classical interior and exterior mixed boundary value problems for the Laplace equation [94], the inhomogeneous problem (4.1) and the corresponding exterior problem (4.4) can each be reduced to simpler problems with homogeneous conditions on  $\partial S_u$  and  $\partial S_t$ . Consequently, without loss of generality, we consider the following mixed reinforcement problem.

Find  $w \in C^2(S \cup \Gamma) \cap C^1(\bar{S} \setminus \{a, b\})$  such that (3.1) is satisfied and

$$\begin{aligned} w(x) &= 0, & x \in \partial S_u, \\ \frac{\partial w(x)}{\partial n(x)} &= 0, & x \in \partial S_t, \\ \frac{\partial w(x)}{\partial n(x)} &= -h \frac{\bar{\mu}}{\mu} d_x^2 w(x) + g(x), & x \in \Gamma. \end{aligned} \tag{4.5}$$

When  $S$  is bounded, (4.5) will describe the interior problem, henceforth denoted by  $(4.5)_I$ . When  $S$  is infinite, (4.5), with the added requirement (4.3), will describe the exterior problem, henceforth denoted by  $(4.5)_E$ .

The difficulty in applying the standard BIEM to the mixed boundary value problem (4.5) arises from the presence of the second derivative in the unknown  $w$  on the reinforced part  $\Gamma$  of the boundary. In fact, attempting to construct the solution in the form of either classical single- or double-layer potentials does not allow for the satisfaction of all conditions of the problem. Instead, we construct the solution in the form of a generalized single-layer potential whose integrand is adjusted to account for the non-standard boundary condition on  $\Gamma$ .

### 4.3.1 Bounded domain

Using the standard methods developed for mixed boundary value problems in bounded domain [82], we introduce the (in general) multiply-connected bounded domain  $\Omega_I$  with sufficiently smooth boundary  $\partial\Omega_I$  constructed so that  $S \in \Omega_I$ ,  $\Gamma \in \Omega_I$  and  $\partial S_u \cup \partial S_t \subseteq \partial\Omega_I$  and define the two-point function  $D_1(x, y)$ ,  $y = (y_1, y_2) \in \Gamma$  constructed specifically to satisfy the following classical mixed boundary value problem for the

Laplace equation:

$$\begin{aligned}\Delta D_1(x, y) &= 0, \quad x \in \Omega_I, \\ D_1(x, y) &= -\frac{1}{2\pi} \ln |x - y|, \quad x \in \partial\Omega_I \setminus \partial S_t \\ \frac{\partial D_1(x, y)}{\partial n(x)} &= -\frac{1}{2\pi} \frac{\partial \ln |x - y|}{\partial n(x)}, \quad x \in \partial S_t.\end{aligned}$$

In fact, the boundary values  $-\frac{1}{2\pi} \ln |x - y|$  and  $-\frac{1}{2\pi} \frac{\partial \ln |x - y|}{\partial n(x)}$  are smooth in this case since for  $x \in \partial\Omega_1$  and  $y \in \Gamma \subset \Omega_1$ ,  $x \neq y$ , ever. Consequently, from the existence result for the interior mixed problem for the Laplace equation (see [82]) it can be shown that that  $D_1(x, y)$  exists uniquely for each  $y \in \Gamma$  in the class  $C^2(\Omega_1) \cap C^1(\overline{\Omega_1} \setminus \{a, b\})$ .

We seek the solution of (4.5)<sub>I</sub> in the form of the generalized single-layer potential:

$$w(x) = (V\phi)_I(x) = \int_{\Gamma} [D(x, y) - D_1(x, y)]\phi(y)ds_y, \quad x \in S, \quad (4.6)$$

where  $\phi$  is an unknown density-function of the Holder class  $C^{1,\alpha}(\Gamma)$ ,  $\alpha \in (0, 1)$ , defined on  $\Gamma$ . We note that  $\phi \in C^{1,\alpha}(\Gamma)$  allows for the continuous extension of the second derivatives of  $(V\phi)_I(x)$  from  $S$  to  $\Gamma$  [102] as required by the boundary condition on  $\Gamma$ . Using results for harmonic potentials [94, 102], it is not difficult to show that  $(V\phi)_I(x)$  from (4.6) satisfies all conditions of the problem (4.5)<sub>I</sub> except the condition for reinforcement boundary:

$$\begin{aligned}\frac{1}{2}\phi(x) + h\frac{\bar{\mu}}{\mu}d_x^2 \int_{\Gamma} D(x, y)\phi(y)ds_y &= - \int_{\Gamma} \frac{\partial D(x, y)}{\partial n_x}\phi(y)ds_y + \\ + h\frac{\bar{\mu}}{\mu}d_x^2 \int_{\Gamma} D_1(x, y)\phi(y)ds_y &+ \int_{\Gamma} \frac{\partial D_1(x, y)}{\partial n_x}\phi(y)ds_y + g(x), \quad x \in \Gamma.\end{aligned} \quad (4.7)$$

The integral on the left-hand side of (4.7) will have strong singularities and we interpret them in the sense of principal value (see the following section for more details), while integrals on right-hand side are simply improper and do not affect the analysis. Now, let us establish the following result which will prove extremely useful in the next section.

**Theorem 4.4.** *The homogeneous equation (4.7)<sup>0</sup> (i.e. (4.7) with  $g \equiv 0$ ) has only the trivial solution.*

*Proof.* Let  $\phi_0 \in C^{1,\alpha}(\Gamma)$  be a solution of (4.7)<sup>0</sup>. Then,

$$(V\phi_0)_I(x) = \int_{\Gamma} [D(x, y) - D_1(x, y)]\phi_0(y)ds_y$$

solves the homogeneous interior problem (4.5)<sub>I</sub><sup>0</sup> (i.e. (4.5)<sub>I</sub> with  $g \equiv 0$ ). Theorem 4.1 now yields  $(V\phi_0)_I(x) = 0$ ,  $x \in S$ . The continuity of a single layer potential (see [94, 102]) now implies  $(V\phi_0)_I(x) = 0$ ,  $x \in \partial S$  so that, in particular,  $(V\phi_0)_I(x) = 0$ ,  $x \in \Gamma$ . Using the definition of the function  $D_1(x, y)$ , this means that

$$\begin{aligned} \Delta(V\phi_0)_I(x) &= 0, & x \in \Omega_I \setminus S, \\ (V\phi_0)_I(x) &= 0, & x \in \partial\Omega_I \setminus \partial S, \\ (V\phi_0)_I(x) &= 0, & x \in \Gamma. \end{aligned}$$

By the uniqueness result for the interior Dirichlet problem for the Laplace equation (see [94, 102]),  $(V\phi_0)(x) = 0$  in the bounded domain  $\Omega_1 \setminus S$ . Hence  $(V\phi_0)$  vanishes on both sides of the boundary  $\Gamma$ . The jump relations arising from the application of the

normal derivative operator to a single layer potential [94, 102] yields that on  $\Gamma$

$$\left(\frac{\partial V}{\partial n}\right)_I^+(\phi_0) - \left(\frac{\partial V}{\partial n}\right)_I^-(\phi_0) = \phi_0 = 0,$$

which completes the proof.  $\square$

### 4.3.2 Unbounded domain

The exterior problem  $(4.5)_E$  is treated similarly except that now since  $S$  is an unbounded domain, any solution must also satisfy the asymptotic condition given by (4.3).

Consider the far-field behavior of the fundamental solution. For  $y$  fixed and  $\tilde{r} = |x| \rightarrow \infty$  from [102] we have

$$\begin{aligned} \ln|x-y| &= \ln|x| - \langle x, y \rangle |x|^{-2} + \frac{1}{2}|y|^2|x|^{-2} - \langle x, y \rangle^2 |x|^{-4} + \langle x, y \rangle |y|^2|x|^{-4} - \\ &\quad - \frac{4}{3}\langle x, y \rangle^3 |x|^{-6} + O(|x|^{-4}). \end{aligned}$$

Then

$$\begin{aligned} \int_{\Gamma} D(x, y)\phi(y)ds_y &= -\frac{1}{2\pi} \ln|x| \int_{\Gamma} \left\{1 - \langle x, y \rangle |x|^{-2} + \frac{1}{2}|y|^2|x|^{-2} - \langle x, y \rangle^2 |x|^{-4} + \right. \\ &\quad \left. + \langle x, y \rangle |y|^2|x|^{-4} - \frac{4}{3}\langle x, y \rangle^3 |x|^{-6} + O(|x|^{-4})\right\} \phi(y)ds_y = -\frac{1}{2\pi} \ln|x| \int_{\Gamma} \phi(y)ds_y + w_0, \end{aligned}$$

where  $w_0$  admits asymptotic expansion, therefore it is of class  $\mathcal{A}$ . The remaining integral with coefficient  $-\frac{1}{2\pi} \ln|x|$  represents singular behavior at infinity.

Using the standard methods developed for mixed boundary value problems in un-

bounded domain [82], let introduce the (in general, multiply-connected) infinite domain  $\Omega_E$  with sufficiently smooth boundary  $\partial\Omega_E$  such that

$$(i) \quad S \subset \Omega_E; \quad (ii) \quad \Gamma \subset \Omega_E; \quad (iii) \quad (\partial S_u \cup \partial S_t) \subseteq \partial\Omega_E; \quad (iv) \quad \{0\} \notin \overline{\Omega}_E.$$

Taking into account the singular behavior of the fundamental solution at infinity we seek a solution in the form

$$w(x) = (V\phi)_E(x) = \int_{\Gamma} [D(x, y) + \frac{1}{2\pi} \ln |x| - D_2(x, y)] \phi(y) ds_y, \quad x \in S, \quad (4.8)$$

where the function  $D_2(x, y)$  (for each  $y \in \Gamma$ ) is the unique solution of the following mixed boundary value problem in  $C^2(\Omega_E) \cap C^1(\overline{\Omega}_E \setminus \{a, b\})$  satisfying (4.3) (see [82]):

$$\begin{aligned} \Delta D_2(x, y) &= 0, \quad x \in \Omega_E, \\ D_2(x, y) &= -\frac{1}{2\pi} \ln |x - y| + \frac{1}{2\pi} \ln |x|, \quad x \in \partial\Omega_E \setminus \partial S_t \\ \frac{\partial D_2(x, y)}{\partial n(x)} &= -\frac{1}{2\pi} \frac{\partial [\ln |x - y| - \ln |x|]}{\partial n(x)}, \quad x \in \partial S_t. \end{aligned}$$

Here  $\phi$  is again an unknown density-function of the Holder class  $C^{1,\alpha}(\Gamma)$ ,  $\alpha \in (0, 1)$ , defined on  $\Gamma$ . The fact that  $(V\phi)_E$  from (4.8) satisfies the asymptotic condition (4.3) follows from the asymptotic behavior of  $D(x, y)$  as  $|x| \rightarrow \infty$  and the definition of the function  $D_2$  which is chosen specifically to satisfy (4.3), i.e. as  $|x| \rightarrow \infty$ ,

$$\begin{aligned} \int_{\Gamma} [D(x, y) + \frac{1}{2\pi} \ln |x| \phi(y)] ds_y &= w_0 + \frac{1}{2\pi} \ln |x| \int_{\Gamma} \phi(y) ds_y - \frac{1}{2\pi} \ln |x| \int_{\Gamma} \phi(y) ds_y = \\ &= w_0, \end{aligned}$$

where  $w_0 \in \mathcal{A}$ . Additionally,

$$\int_{\Gamma} D_2(x, y)\phi(y)ds_y \in \mathcal{A}^*,$$

since  $D_2(x, y) \in \mathcal{A}^*$  and therefore  $(V\phi)_E(x) \in \mathcal{A}^*$  as required.

It is again can be shown that (4.8) satisfies all the conditions of problem (4.5)<sub>E</sub> provided  $\phi$  satisfies the following integral equation on the reinforced curve  $\Gamma$ :

$$\begin{aligned} \frac{1}{2}\varphi(x) + h\frac{\bar{\mu}}{\mu}d_x^2 \int_{\Gamma} D(x, y)\phi(y)ds_y = & - \int_{\Gamma} \frac{\partial D(x, y)}{\partial n_x} \phi(y)ds_y + h\frac{\bar{\mu}}{\mu}d_x^2 \int_{\Gamma} \left\{ D_2(x, y) - \right. \\ & \left. - \frac{1}{2\pi} \ln|x| \right\} \phi(y)ds_y + \int_{\Gamma} \frac{\partial [D_2(x, y) - \frac{1}{2\pi} \ln|x|]}{\partial n_x} \phi(y)ds_y + g(x), \quad x \in \Gamma. \end{aligned} \quad (4.9)$$

As before, the integral on the left-hand side of (4.9) will have strong singularities and we interpret them in the sense of principal value (see the following section for more details), while the integrals on the right-hand side are simply improper and do not affect the analysis.

**Theorem 4.5.** *The homogeneous equation (4.9)<sup>0</sup> (i.e. (4.9) with  $g \equiv 0$ ) has only the trivial solution.*

*Proof.* The proof proceeds as in the proof of Theorem 4.4 □

## 4.4 Analysis of the singular integro-differential equations arising from the proposed model

The boundary value problems  $(4.5)_I$  and  $(4.5)_E$  have each been reduced to an integral equation of the form

$$\frac{1}{2}\varphi(x) + h\frac{\bar{\mu}}{\mu}d_x^2 \int_{\Gamma} D(x, y)\phi(y)ds_y = \int_{\Gamma} \Lambda(x, y)\phi(y)ds_y + g(x), \quad x \in \Gamma. \quad (4.10)$$

For the interior boundary value problem and equation (4.7)

$$\Lambda(x, y) = -\frac{\partial D(x, y)}{\partial n_x} + h\frac{\bar{\mu}}{\mu}d_x^2 D_1(x, y) + \frac{\partial D_1(x, y)}{\partial n_x},$$

while for the exterior boundary value problem and equation (4.9)

$$\Lambda(x, y) = -\frac{\partial D(x, y)}{\partial n_x} + h\frac{\bar{\mu}}{\mu}d_x^2 \left\{ D_2(x, y) - \frac{1}{2\pi} \ln |x| \right\} + \frac{\partial [D_2(x, y) - \frac{1}{2\pi} \ln |x|]}{\partial n_x}.$$

From the definition of the matrices  $D_1(x, y)$ ,  $D_2(x, y)$  and the properties of the fundamental solutions  $D(x, y)$  (see [94]) it can be deduced that  $\Lambda(x, y)$  is a weakly singular kernel, so that the integral on the right-hand side of (4.10) is weakly singular and does not affect the index of the corresponding singular integral operator. Nevertheless, the same can not be stated for the integral on the left-hand side; and it will be shown further that this this integral contains a strong singularity. To this end, at this stage, Fredholm's alternative does not apply to (4.10) because of the presence of the Cauchy Principal value integral and, therefore, the absence of the weak singularity condition

for the kernel. Precise analysis of this integral-differential equation will lead to another more recognizable form of the integral equations in the sense of Vekua [83] and, thus, will allow us to use Fredholm's alternative.

In what follows the notations  $x$  and  $y$  will denote complex representations of the points  $x = (x_1, x_2)$  and  $y = (y_1, y_2)$ . In other words, we assume that  $x = x_1 + ix_2$ ,  $y = y_1 + iy_2$  and adopt the convention that for a function  $f$  on  $\Gamma$ , we write  $f(z) = f(x)$ , where  $z = x_1 + ix_2$ . Let  $\beta(x - y)$  represent the angle between axis  $x_1$  and the vector  $x - y$ . Then

$$\frac{x_1 - y_1}{|x - y|} = \cos \beta, \quad \frac{x_2 - y_2}{|x - y|} = \sin \beta.$$

Let us consider the integral on the left-hand side of (4.10)

$$I = h \frac{\bar{\mu}}{\mu} d_x^2 \int_{\Gamma} D(x, y) \varphi(y) ds_y = -\frac{h\bar{\mu}}{2\pi\mu} d_x \oint_{\Gamma} d_x \ln|x - y| \phi(y) ds_y.$$

Using the expressions

$$e^{i\theta(x)} ds_x = dx, \quad e^{i\theta(y)} ds_y = dy, \quad x - y = |x - y| e^{i\beta(x-y)},$$

$$\lim_{x \rightarrow y} \cos(\theta(x) - \beta(x - y)) e^{i(\beta(x-y) - \theta(y))} = 1,$$

and the result from [102]:

$$\begin{aligned} \frac{d \ln|x - y|}{ds_x} &= \frac{\langle \tau(x), x - y \rangle}{|x - y|^2} = \frac{(x_1 - y_1) \cos \theta(x) + (x_2 - y_2) \sin \theta(x)}{|x - y|(x - y) e^{-i\beta(x-y)}} = \\ &= \frac{\cos(\theta(x) - \beta(x - y))}{(x - y) e^{-i\beta(x-y)}}, \end{aligned}$$

the integral  $I$  can be expressed as:

$$I = -\frac{h\bar{\mu}}{2\pi\mu} d_x \int_{\Gamma} \frac{\cos(\theta(x) - \beta(x-y))}{x-y} e^{i\beta(x-y) - \theta(y)} \phi(y) dy = -\frac{h\bar{\mu}}{2\pi\mu} \frac{d}{ds_x} \int_{\Gamma} \frac{\phi(y)}{x-y} dy.$$

Following differentiation and application of integration by parts with respect to  $y$  for the closed contour  $\Gamma$  gives

$$\begin{aligned} I &= e^{i\theta(x)} \frac{h\bar{\mu}}{2\pi\mu} \int_{\Gamma} \frac{\phi(y)}{(x-y)^2} dy = e^{i\theta(x)} \frac{h\bar{\mu}}{2\pi\mu} \int_{\Gamma} \phi(y) \frac{d}{dy} \left( \frac{1}{x-y} \right) dy \\ &= \left( e^{i\theta(x)} \frac{h\bar{\mu}}{2\pi\mu} \frac{\phi(y)}{x-y} \right) \Big|_{\Gamma} - e^{i\theta(x)} \frac{h\bar{\mu}}{2\pi\mu} \int_{\Gamma} \frac{\phi'(y)}{x-y} dy = -e^{i\theta(x)} \frac{h\bar{\mu}}{2\pi\mu} \int_{\Gamma} \frac{\phi'(y)}{x-y} dy. \end{aligned}$$

Finally, the singular integro-differential equation can be written as

$$\frac{1}{2}\varphi(x) - e^{i\theta(x)} \frac{h\bar{\mu}}{2\pi\mu} \int_{\Gamma} \frac{\phi'(y)}{x-y} dy = \int_{\Gamma} \Lambda^*(x, y) \phi(y) ds_y + g(x), \quad x \in \Gamma, \quad (4.11)$$

where  $\Lambda^*(x, y)$  is a weakly singular kernel.

Comparing (4.11) with the class of singular integro-differential equation examined in [83], it can be found that the index of the singular operator from (4.11) is zero when  $h\bar{\mu} \neq 0$ . This value is derived similarly as for (2.3), but singular integral equations looks a bit different (see [83] for details). Consequently, Fredholm's theorems hold for (4.11) and its corresponding adjoint equation.

**Theorem 4.6.** *The interior problem (4.5)<sub>I</sub> with reinforced boundary  $\Gamma$  has a unique solution whenever  $g \in C^{1,\alpha}(\Gamma)$ ,  $0 < \alpha < 1$ . This solution is given by (4.6) with  $\phi \in C^{1,\alpha}(\Gamma)$ ,  $0 < \alpha < 1$ , the unique solution of (4.7) whenever  $g \in C^{1,\alpha}(\Gamma)$ .*

*Proof.* From what has been said above, Fredholm's theorems hold for (4.11) and its

associated (adjoint) system. The same result can be stated for (4.7). From Theorem 4.4, the homogeneous system (4.7)<sup>0</sup> has only the trivial solution. Hence, by Fredholm's theorems and results on smoothness of solution for equations of the type (4.7) (see [84]), we have that (4.7) always has a unique solution  $\phi \in C^{1,\alpha}(\Gamma)$  whenever  $g \in C^{1,\alpha}(\Gamma)$ . Finally, (4.6) is the unique solution of (4.5)<sub>I</sub> with  $\phi \in C^{1,\alpha}(\Gamma)$  delivered from (4.7).  $\square$

**Theorem 4.7.** *The exterior problem (4.5)<sub>E</sub> with reinforced boundary  $\Gamma$  has a unique solution whenever  $g \in C^{1,\alpha}(\Gamma)$ ,  $0 < \alpha < 1$ . This solution is given by (4.8) with  $\phi \in C^{1,\alpha}(\Gamma)$ ,  $0 < \alpha < 1$ , the unique solution of (4.9) whenever  $g \in C^{1,\alpha}(\Gamma)$ .*

*Proof.* The proof is analogous to the proof of Theorem 4.6  $\square$

To sum-up, the solvability and uniqueness result were deduced for the highly non-standard boundary value problems for the Laplace equation arising when separate boundary elasticity is incorporated in the description of anti-plane deformations of a linearly elastic solid. Therefore we have confirmed two out of three requirements for the model to be well-posed. In fact, the third postulate requires the study of continuous dependence of the solutions on the model's initial data, which follows Kupradze analysis [82] step-by-step, so it is out of the scope of the current work. Therefore, we can conclude that the proposed model is well-posed and can be implemented to analyze real world applications.

However, this model and its well-posedness analysis is limited to the case when  $\Gamma$  is given by a finite number of closed curves. It can be also beneficial to consider a more generalized case-scenario, in which  $\Gamma$  is represented by a finite number of open curves. In the following chapter we will proceed to this case and will highlight some examples of its applications.

---

## CHAPTER 5

# Extension of the model to the open case reinforcement when surface effect is considered on a part of the boundary

In the previous chapter, we have considered BVPs for the case when the reinforced part of the boundary was consisted of a finite number of sufficiently smooth closed curves. This was done to facilitate the mathematics since an examination of integrals over closed contours is much simpler; and, therefore, it is easier to derive well-posedness result. However, there is also a practical case to be considered when only part of the boundary has the surface effect represented by a coating. This more general case, in which the reinforced section of the boundary can be represented by a finite number of open curves, allows for the modeling of a wider class of problems [105]. Examples can include sputtering and shot peening techniques. Sputtering is the process of thin film deposition onto the surface of materials. It is present in many manufacturing processes,

for example, in the building industry, where it is used to coat skyscrapers' mirror-like windows and reflective layers. Shot peening, in turn, is the process of dimpling of metal surfaces, that causes compression stresses and prevent materials from corrosion, cracking, erosion and so on. And finally, the simplest illustration is cracks with the surface effect on their tips.

Hence, it is of great importance to develop a model of open case reinforcement and analyze it on the well-posedness. Unfortunately, this more general case of the model incorporating the surface effect is associated with reinforcement boundary conditions posed over a series of open arcs and the associated end-point conditions to be satisfied at the ends of each arc. This means that the standard boundary integral equation approach cannot be applied in this particular case without imposing solvability conditions which carry no clear physical meaning. Instead, we proceed by utilizing an alternative lower-order form of the reinforcement boundary condition which is designed to automatically incorporate the corresponding end-point conditions. This particular form of the reinforcement boundary condition allows for the application of the boundary integral equation method albeit in generalized form.

We assume that boundary  $\partial S$  of  $S$  is described by the union of a finite number of sufficiently smooth closed curves. We regard a subset  $\Gamma$  (consisting of a finite number  $m$  of sufficiently smooth open curves  $L_i$  with endpoints  $a_i$  and  $b_i$ , such that  $L_j$  and  $L_k$  have no point in common for  $j \neq k$ ;  $i, j, k = 1 \dots m$ ) of  $\partial S$  as being coated with a thin, homogeneous and isotropic elastic film with separate shear modulus  $\bar{\mu} > 0$ .

In the absence of body forces, the governing equation for the anti-plane displacement field  $w$  is given by Laplace equation (3.1).

It should be noted that some passages in this chapter have been quoted verbatim

from the author's publication [98].

## 5.1 Boundary conditions describing surface effect with end-point conditions taken into account

The boundary condition on the (reinforced) subset  $\Gamma$  of the boundary  $\partial S$  couples the response of the solid to that of the coating on  $\Gamma$  and is given by (3.3).

In addition to (3.3), we must impose conditions at the end-points of  $\Gamma$  [98]. Natural end-point conditions describe 'Free-Ends' at which the appropriate shearing force given by  $h\bar{\mu}\frac{dw}{ds}$  must vanish. Consequently, we impose the conditions of the form

$$\frac{dw}{ds}(a_i) = \frac{dw}{ds}(b_i) = 0, \quad i = 1 \dots m. \quad (5.1)$$

Alternatives to the end-point conditions (5.1) include, for example, the cases when one of the end-points of the coating is fixed

$$\frac{dw}{ds}(a_i) = 0, \quad w(b_i) = 0, \quad i = 1 \dots m \quad (5.2)$$

or both are fixed

$$w(a_i) = 0, \quad w(b_i) = 0, \quad i = 1 \dots m. \quad (5.3)$$

The reinforcement condition (3.3) is required over open arcs and when coupled with the end-point conditions (5.1), (5.2) or (5.3) leads to a nonstandard boundary value problem whose analysis is not accommodated by the methods used in the previous chapter. Instead, we proceed by integrating (3.3) along the reinforcement using

the accompanying end-point conditions (from (5.1), (5.2) or (5.3)) to evaluate the constants of integration. In this way, we incorporate the reinforcement condition (3.3) and the corresponding end-point conditions into an equivalent single lower-order boundary condition on the reinforcement.

We begin by writing (3.3) and (5.1) as

$$\begin{aligned}\frac{d^2w}{ds^2}(x) &= -\frac{1}{h\bar{\mu}}(\sigma_{3n}(x) - t(x)) = -\frac{1}{h\bar{\mu}}\mathcal{S}(x), \quad x \in \Gamma, \\ \frac{dw}{ds}(a_i) &= \frac{dw}{ds}(b_i) = 0, \quad i = 1\dots m,\end{aligned}\tag{5.4}$$

where  $t(x) = h\frac{\bar{\mu}}{\mu}g(x)$ . Integrate (5.4)<sub>1</sub> over the interval  $[a_i, x]$ ,  $x \in \Gamma$ :

$$\frac{dw}{ds}(x) - \frac{dw}{ds}(a_i) = -\frac{1}{h\bar{\mu}} \int_{a_i}^x \mathcal{S}(t) ds_t, \quad x \in L_i.$$

Using the end-point conditions (5.4)<sub>2</sub>, we obtain

$$\frac{dw}{ds}(x) = -\frac{1}{h\bar{\mu}} \int_{a_i}^x \mathcal{S}(t) ds_t, \quad x \in L_i.\tag{5.5}$$

To satisfy the remaining condition  $\frac{dw}{ds}(b_i) = 0$ ,  $i = 1\dots m$ , from (5.5) it is necessary and sufficient that

$$\int_{a_i}^{b_i} \mathcal{S}(t) ds_t = 0, \quad i = 1\dots m,\tag{5.6}$$

which expresses the requirement for  $\mathcal{S}$  to be a self-equilibrating system of tractions along the arcs  $L_i$ ,  $i = 1\dots m$ . Clearly, (5.5), (5.6) are equivalent to (5.4).

Integrating (5.5) again, we obtain

$$w(x) - w(a_i) = -\frac{1}{h\bar{\mu}} \int_{a_i}^x \int_{a_i}^{t_2} \mathcal{S}(t_1) ds_{t_1} ds_{t_2}, \quad x, t_2 \in L_i, \quad i = 1 \dots m. \quad (5.7)$$

Here  $w(a_i)$  are constrained by conditions (5.6) and must therefore be chosen accordingly. In fact, (5.6) requires that for  $i = 1 \dots m$

$$w(a_i) = \frac{1}{|L_i|} \int_{a_i}^{b_i} (w(x) + \frac{1}{h\bar{\mu}} \int_{a_i}^x \int_{a_i}^{t_2} \mathcal{S}(t_1) ds_{t_1} ds_{t_2} + \lambda \mathcal{S}(x)) ds_x, \quad x, t_2 \in L_i, \quad (5.8)$$

where  $\lambda$  is a suitably chosen parameter introduced to ensure that the term  $\lambda \mathcal{S}$  is dimensionally correct.

It is seen that the reinforcement conditions (5.4) are equivalent to the Dirichlet condition (5.7) in which  $w(a_i)$  are given by (5.8). For convenience, we write the specific values  $w(a_i)$  from (5.8) as  $\mathcal{C}^i$   $i = 1 \dots m$ . Then, from (5.7), we have the following Dirichlet boundary condition equivalent to (5.4):

$$w(x) = -\frac{1}{h\bar{\mu}} \int_{a_i}^x \int_{a_i}^{t_2} \mathcal{S}(t_1) ds_{t_1} ds_{t_2} + \mathcal{C}^i, \quad x, t_2 \in L_i, \quad i = 1 \dots m. \quad (5.9)$$

Now let us proceed to the cases of ‘Free-Fixed’ and ‘Fixed-Fixed’ end-point conditions given by (5.2) and (5.3). In the case of (5.2), we again arrive at (5.7) with the  $w(a_i)$  constrained by the requirement that  $w(b_i) = 0$ . Consequently, we choose

$$w(a_i) = \frac{1}{h\bar{\mu}} \int_{a_i}^{b_i} \int_{a_i}^{t_2} \mathcal{S}(t_1) ds_{t_1} ds_{t_2}, \quad i = 1 \dots m. \quad (5.10)$$

Using (5.10) in (5.7) we again obtain a Dirichlet condition of the form (5.9) with the constants  $\mathcal{C}^i$ ,  $i = 1 \dots m$  given by (5.10).

In the case of (5.3), an integration over the interval  $[a_i, x]$   $x \in L_i$ ,  $i = 1 \dots m$ , again brings us to

$$\frac{dw}{ds}(x) - \frac{dw}{ds}(a_i) = -\frac{1}{h\bar{\mu}} \int_{a_i}^x \mathcal{S}(t) ds_t, \quad x \in L_i, \quad i = 1 \dots m.$$

But now  $\frac{dw}{ds}(a_i) \neq 0$ , so we integrate again over the interval  $[a_i, x]$ ,  $i = 1 \dots m$ :

$$w(x) - w(a_i) - \frac{dw}{ds}(a_i)(x - a_i) = -\frac{1}{h\bar{\mu}} \int_{a_i}^x \int_{a_i}^{t_2} \mathcal{S}(t_1) ds_{t_1} ds_{t_2}, \quad x \in L_i.$$

Applying the condition  $w(a_i) = 0$ ,

$$w(x) = \frac{dw}{ds}(a_i)(x - a_i) - \frac{1}{h\bar{\mu}} \int_{a_i}^x \int_{a_i}^{t_2} \mathcal{S}(t_1) ds_{t_1} ds_{t_2}, \quad x \in L_i, \quad i = 1 \dots m. \quad (5.11)$$

We choose the value of  $\frac{dw}{ds}(a_i)$  to satisfy the condition  $w(b_i) = 0$ , i.e.:

$$w(b_i) = \frac{dw}{ds}(a_i)(b_i - a_i) - \frac{1}{h\bar{\mu}} \int_{a_i}^{b_i} \int_{a_i}^{t_2} \mathcal{S}(t_1) ds_{t_1} ds_{t_2} = 0, \quad i = 1 \dots m,$$

so that

$$\frac{dw}{ds}(a_i) = \frac{1}{h\bar{\mu}(b_i - a_i)} \int_{a_i}^{b_i} \int_{a_i}^{t_2} \mathcal{S}(t_1) ds_{t_1} ds_{t_2}, \quad i = 1 \dots m. \quad (5.12)$$

(5.11) with (5.12) now leads to the following Dirichlet condition on  $\Gamma$  for  $i = 1 \dots m$ :

$$w(x) = \frac{(x - a_i)}{h\bar{\mu}(b_i - a_i)} \int_{a_i}^{b_i} \int_{a_i}^{t_2} \mathcal{S}(t_1) ds_{t_1} ds_{t_2} - \frac{1}{h\bar{\mu}} \int_{a_i}^{t_2} \int_{a_i}^x \mathcal{S}(t_1) ds_{t_1} ds_{t_2}, \quad x \in L_i$$

or in the form of a Dirichlet condition similar to (5.9), we have

$$w(x) = C^i(x - a_i) - \frac{1}{h\bar{\mu}} \int_{a_i}^{t_2} \int_{a_i}^x \mathcal{S}(t_1) ds_{t_1} ds_{t_2}, \quad x \in L_i, \quad i = 1 \dots m, \quad (5.13)$$

where the constants  $C^i$ ,  $i = 1 \dots m$  are given by the values of  $\frac{dw}{ds}(a_i)$  from (5.12).

To sum-up, in this section we have derived lower-order reinforcement boundary conditions (5.9) and (5.13), equivalent to (5.4) or (3.3) with (5.2) and (3.3) with (5.3), respectively.

## 5.2 BVPs and BIEM for the proposed model

In the formulation of the corresponding boundary value problems, we first consider the case when  $S$  is a bounded domain enclosed by sufficiently smooth boundary  $\partial S$ . Write  $\partial S = \partial S_1 \cup \Gamma$  where the closed curve  $\partial S_1$  represents the non-reinforced section of  $\partial S$ . We divide  $\partial S_1$  into two open curves  $\partial S_u$ ,  $\partial S_t$  (with common point  $c$ ) and let  $\Gamma$  represent two open curves  $L_1$  and  $L_2$  with endpoints  $a_1$ ,  $b_1$  and  $a_2$ ,  $b_2$ , respectively, such that they have no point in common. The case where  $\partial S_1$  is divided into more than two parts and where  $\Gamma$  consists of a finite number ( $> 2$ ) of open curves is treated similarly without any significant modifications to our method.

The interior mixed boundary value problem requires that we find  $w \in C^2(S \cup \Gamma) \cap C^1(\bar{S} \setminus \{c\})$  such that (3.1) is satisfied and

$$\begin{aligned} w(x) &= w^{(0)}(x), & x \in \partial S_u, \\ \frac{\partial w(x)}{\partial n(x)} &= t^{(0)}(x), & x \in \partial S_t, \\ \frac{\partial w(x)}{\partial n(x)} &= -h \frac{\bar{\mu}}{\mu} d_x^2 w(x) + g(x), & x \in \Gamma. \end{aligned} \tag{5.14}$$

In addition, we require the end-point conditions (5.1), (5.2) or (5.3).

The exterior problem is posed similarly except that  $S$  is now an unbounded domain in which we require (4.3).

**Theorem 5.1.** *Both the interior and exterior problems have at most one solution.*

*Proof.* The proof repeats the steps of the proof of Theorems 4.1 and 4.2. The only difference is observed at the stage of integration by parts:

$$\begin{aligned} h\bar{\mu} \int_a^b \omega \frac{\partial^2 \omega}{\partial s^2} ds &= h\bar{\mu} \left[ \int_a^b \frac{d}{ds} \left( \omega \frac{\partial \omega}{\partial s} \right) ds - \int_a^b \left( \frac{\partial \omega}{\partial s} \right)^2 ds \right] = \\ &= h\bar{\mu} \left( \left[ \omega(b) \frac{\partial \omega}{\partial s}(b) - \omega(a) \frac{\partial \omega}{\partial s}(a) \right] - \int_a^b \left( \frac{\partial \omega}{\partial s} \right)^2 ds \right). \end{aligned}$$

Now the first term in the right-hand side of this expression does not represent the integral of an exact differential over a closed circuit as before, but still can be equal to zero with the help of the boundary conditions (5.1), (5.2) or (5.3). And it again will lead to the fact that the solution is unique.  $\square$

Without loss of generality, we consider the following mixed (interior) reinforcement

problem. Find  $w \in C^2(S \cup \Gamma) \cap C^1(\bar{S} \setminus \{c\})$  such that (3.1) is satisfied and

$$\begin{aligned}
w(x) &= 0, & x \in \partial S_u, \\
\frac{\partial w(x)}{\partial n(x)} &= 0, & x \in \partial S_t, \\
\frac{\partial w(x)}{\partial n(x)} &= -h \frac{\bar{\mu}}{\mu} d_x^2 w(x) + g(x), & x \in \Gamma, \\
\frac{dw}{ds}(a_i) &= \frac{dw}{ds}(b_i) = 0, & i = 1, 2.
\end{aligned} \tag{5.15}$$

If we apply the standard boundary integral equation method (BIEM) and seek the solution of the interior problem in the form of a single-layer potential, we obtain the following singular integro-differential equation (see the previous chapter for details):

$$\frac{1}{2} \phi(x) + \frac{h\bar{\mu}}{2\pi\mu} \int_{\Gamma} e^{i\theta(x)} \frac{\phi(y)}{(x-y)^2} dy = \int_{\Gamma} \Lambda(x,y) \phi(y) ds_y + g(x), \quad x \in \Gamma, \tag{5.16}$$

where,  $\Lambda(x,y)$  is a weakly singular kernel. Following standard procedures, we can show that the imposition of two supplementary conditions on any solution  $\phi$  of (5.16), namely

$$\phi(a_i) = \phi(b_i) = 0, \tag{5.17}$$

(see, for example, [106]), reveals that the singular operator associated with (5.16) has zero index. As was demonstrated in the previous chapter, this allows for the application of Fredholm's alternative and the establishment of solvability results for the corresponding BVPs.

However, the conditions (5.17) have no apparent physical meaning in the context of this theory of reinforcement and are thus inconvenient in any existence theory.

To address this issue, we will show that if the reinforcement condition (3.3) is replaced with the alternative lower-order form (5.9) or (5.13), we can establish the required solvability results without resorting to conditions similar to (5.17). Let us, for instance, choose the form (5.9).

Therefore, we consider the following mixed reinforcement problem equivalent to (5.15) and its corresponding exterior problem. Find  $w \in C^2(S \cup \Gamma) \cap C^1(\bar{S} \setminus \{c\})$  such that (3.1) is satisfied and

$$\begin{aligned} w(x) &= 0, & x \in \partial S_u, \\ \frac{\partial w(x)}{\partial n(x)} &= 0, & x \in \partial S_t, \end{aligned} \tag{5.18}$$

$$w(x) = -\frac{1}{h\bar{\mu}} \int_{a_i}^x \int_{a_i}^{t_2} \mathcal{S}(t_1) ds_{t_1} ds_{t_2} + \mathcal{C}^i, \quad x, t_2 \in \Gamma, \quad i = 1, 2.$$

When  $S$  is bounded, (5.18) will describe the interior problem, henceforth denoted by  $(5.18)_I$ . When  $S$  is infinite, (5.18), with the added requirement (4.3), will describe the exterior problem, henceforth denoted by  $(5.18)_E$ .

### 5.2.1 Bounded domain

To this end, we introduce the (in general, multiply-connected) domain  $\Omega_I$  with sufficiently smooth boundary  $\partial\Omega_I$  constructed so that

$$(i) \ S \in \Omega_I; \quad (ii) \ \Gamma \in \Omega_I, \quad \partial S_u \cup \partial S_t \subseteq \partial\Omega_I.$$

We write

$$\Omega_I = S + M_1 \cup M_2; \quad \partial\Omega_I = \partial S_u \cup \partial S_t \cup S_1 \cup S_2,$$

where the subregions  $M_1$  and  $M_2$  are enclosed by  $S_1, L_1$  and  $S_2, L_2$ , respectively. The domains  $S_i$  ( $i = 1, 2$ ) are divided, in turn, into two parts:  $S_{i1}$  and  $S_{i2}$  such that  $S_{i1} \cap L_i$  consists of the endpoints  $L_i$  and  $S_{i2} \cap L_i$  is the empty set.

Introduce the function  $P_1$  satisfying

$$\begin{aligned} \Delta P_1(x, y) &= 0, \quad x \in \Omega_I, \\ P_1(x, y) &= -\frac{1}{2\pi} \frac{\partial \ln |x - y|}{\partial n(y)}, \quad x \in \partial\Omega_I \setminus (\partial S_t + S_1 \cup S_2) \\ \frac{\partial P_1(x, y)}{\partial n(x)} &= -\frac{1}{2\pi} \frac{\partial^2 \ln |x - y|}{\partial n(x) \partial n(y)}, \quad x \in \partial S_t + S_1 \cup S_2. \end{aligned}$$

It is well-known [82] that  $P_1$  exists uniquely for each  $y \in \Gamma$  in the class  $C^2(\Omega_I) \cap C^1(\overline{\Omega_I} \setminus c)$ .

Now seek the solution of the interior mixed reinforcement problem in the form of a modified double layer potential

$$w(x) = (W\phi)_I(x) = \int_{\Gamma} \left[ \frac{\partial D(x, y)}{\partial n(y)} - P_1(x, y) \right] \phi(y) ds_y, \quad x \in S. \quad (5.19)$$

It is not difficult to show that all conditions of the interior problem are satisfied except for the reinforcement boundary condition (5.9) which leads to the following

integral equations ( $i = 1, 2$ ) for  $x, t_2 \in L_i$ :

$$\begin{aligned} \frac{1}{2}\phi(x) - \int_{a_i}^{b_i} \left[ \frac{\partial D(x, y)}{\partial n(y)} - P_1(x, y) \right] \phi(y) ds_y &= \frac{1}{h\mu_2} \int_{a_i}^x \int_{a_i}^{t_2} \mathcal{S}(t_1) ds_{t_1} ds_{t_2} - \\ &- \frac{1}{|L_i|} \int_{a_i}^{b_i} (w(x) + \frac{1}{h\mu_2} \int_{a_i}^x \int_{a_i}^{t_2} \mathcal{S}(t_1) ds_{t_1} ds_{t_2} + \lambda \mathcal{S}(x)) ds_x. \end{aligned} \quad (5.20)$$

Using the standard results from [104], we can write (5.20) in the equivalent form of a Fredholm equation of the second kind:

$$\frac{1}{2}\phi(x) + \int_{a_i}^{b_i} K(x, y)\phi(y) ds_y = T^*(x), \quad x \in L_i. \quad (5.21)$$

Here,  $K(x, y)$  is a Fredholm kernel and  $T^*(x)$  is determined by the data  $g(x)$  prescribed on  $\Gamma$ .

Consequently, Fredholm's theorems hold for (5.21) and its corresponding adjoint equation. According to the properties of a standard double-layer potential for the Laplace equation as well as those of the function  $P_1$ , it follows that if we can show that (5.21) has a unique solution in  $C^{1,\alpha}(\Gamma)$  whenever  $T^* \in C^{1,\alpha}(\Gamma)$ , then the modified potential (5.19) must be the unique solution of the interior reinforcement problem. To this end, we have the following theorem.

**Theorem 5.2.** *The homogeneous equation (5.21)<sup>0</sup> (i.e. (5.21) with  $T^*(x) \equiv 0$ ) has only the trivial solution.*

*Proof.* Let  $\phi_0 \in C^{1,\alpha}(\Gamma)$  be a solution of (5.21)<sup>0</sup>. Then,

$$w_0 = (W\phi_0)_I(x) = \int_{\Gamma} \left[ \frac{\partial D(x,y)}{\partial n(y)} - P_1(x,y) \right] \phi_0(y) ds_y \quad x \in S.$$

solves the homogeneous interior problem (5.18)<sub>I</sub><sup>0</sup> (i.e. (5.18)<sub>I</sub> with  $g \equiv 0$ ). Theorem 5.1 now yields  $w_0 = (W\phi_0)(x) = 0$ ,  $x \in S$ . Consequently,  $\frac{\partial w_0(x)}{\partial n(x)} = 0$ ,  $x \in S \rightarrow \Gamma$ . By the last property for the double-layer potential from the last chapter, we have that  $\frac{\partial w_0(x)}{\partial n(x)} = 0$ ,  $x \in \Omega_I \setminus S \rightarrow \Gamma$ . Using the definition of  $P_1(x,y)$  this means that

$$\begin{aligned} \Delta w_0(x) &= 0, & x \in \Omega_1 \setminus S, \\ w_0(x) &= 0, & x \in S_1 \cup S_2, \\ \frac{\partial w_0(x)}{\partial n(x)} &= 0, & x \in S_{11} \cup S_{21} \cup \Gamma. \end{aligned}$$

By the uniqueness result for the classical interior mixed problem for Laplace equation (see [82]),  $w_0(x) = 0$  in the bounded domain  $\Omega_I \setminus S$ . Hence  $(W\phi_0)_I$  vanishes on both sides of the boundary  $\Gamma$ . The jump relations arising from the double layer potential [104] now yield that necessarily on  $\Gamma$

$$W_I^+(\phi_0) - W_I^-(\phi_0) = \phi_0 = 0,$$

which completes the proof. □

This theorem now allows us to prove the main existence result for the boundary value problem (5.18)<sub>I</sub>.

**Theorem 5.3.** *The interior problem (5.18)<sub>I</sub> with reinforced boundary  $\Gamma$  has a unique*

solution whenever  $g \in C^{1,\alpha}(\Gamma)$ ,  $0 < \alpha < 1$ . This solution is given by (5.19) with  $\phi \in C^{1,\alpha}(\Gamma)$ ,  $0 < \alpha < 1$ , the unique solution of (5.21) whenever  $T^* \in C^{1,\alpha}(\Gamma)$ .

*Proof.* From what has been said above, Fredholm's theorems hold for (5.21) and its associated (adjoint) system. From Theorem 5.2, the homogeneous system (5.21)<sup>0</sup> has only the trivial solution. Hence, by Fredholm's theorems and results on smoothness of solution for equations of the type (5.21) [104], we have that (5.21) always has a unique solution  $\phi \in C^{1,\alpha}(\Gamma)$  whenever  $T^* \in C^{1,\alpha}(\Gamma)$ . Finally, (5.19) is the unique solution of (5.18)<sub>I</sub> with  $\phi \in C^{1,\alpha}(\Gamma)$  delivered from (5.21).  $\square$

## 5.2.2 Unbounded domain

The exterior problem from (5.18)<sub>E</sub> is treated similarly except that now since  $S$  is an unbounded domain, any solution must also satisfy the asymptotic condition given by (4.3). We proceed as for the interior problem and introduce the (in general, multiply-connected) infinite domain  $\Omega_E$  with sufficiently smooth boundary  $\partial\Omega_E$  such that

$$(i) \quad S \subset \Omega_E; \quad (ii) \quad \Gamma \subset \Omega_E; \quad (iii) \quad (\partial S_u \cup \partial S_t) \subseteq \partial\Omega_E; \quad (iv) \quad \{0\} \notin \bar{\Omega}_E.$$

We write

$$\Omega_E = S + M_1 \cup M_2; \quad \partial\Omega_E = \partial S_u \cup \partial S_t \cup S_1 \cup S_2,$$

where subregions  $M_1$  and  $M_2$  are enclosed by  $S_1, L_1$  and  $S_2, L_2$ , respectively.  $S_i$  ( $i = 1, 2$ ) are divided, in turn, into two parts:  $S_{i1}$  and  $S_{i2}$  such that  $S_{i1} \cap L_i$  consists of

the endpoints  $L_i$  and  $S_{i2} \cap L_i$  is empty set. We then seek a solution in the form

$$w(x) = (W\phi)_E(x) = \int_{\Gamma} \left[ \frac{\partial D(x, y)}{\partial n(y)} - P_2(x, y) \right] \phi(y) ds_y, \quad x \in S, \quad (5.22)$$

where the function  $P_2(x, y)$  (for each  $y \in \Gamma$ ) is the unique solution of the following mixed boundary value problem in  $C^2(\Omega_E) \cap C^1(\bar{\Omega}_E \setminus c)$  satisfying (see [82]):

$$\begin{aligned} \Delta P_2(x, y) &= 0, \quad x \in \Omega_E, \\ P_2(x, y) &= -\frac{1}{2\pi} \frac{\partial \ln |x - y|}{\partial n(y)}, \quad x \in \partial\Omega_E \setminus (\partial S_t + S_1 \cup S_2) \\ \frac{\partial P_2(x, y)}{\partial n(x)} &= -\frac{1}{2\pi} \frac{\partial^2 \ln |x - y|}{\partial n(x) \partial n(y)}, \quad x \in \partial S_t + S_1 \cup S_2. \end{aligned}$$

Here  $\phi$  is again an unknown density-function of the Holder class  $C^{1,\alpha}(\Gamma)$ ,  $\alpha \in (0, 1)$ , defined on  $\Gamma$ . The fact that  $(W\phi)_E$  from (5.22) satisfies the asymptotic condition (4.3) follows from the asymptotic behavior of  $\frac{\partial D(x, y)}{\partial n(y)}$  as  $|x| \rightarrow \infty$  and the definition of the function  $P_2$  which is chosen specifically to satisfy the boundary value problem above.

It is again possible to show that (5.22) satisfies all the conditions of the exterior problem from (5.18)<sub>E</sub> except the reinforcement boundary condition (5.9). Proceeding as above for the interior problem we again obtain Fredholm-type equations for  $\phi$  on  $\Gamma$ , almost identical to (5.21), for which the analogue of Theorem 5.2 can be established. Moreover, Theorem 5.3 also holds for the exterior problem, except that the unique solution is now given by (5.22).

**Remark.** *The ‘free-fixed’ and ‘fixed-fixed’ end-point conditions lead only to insignificant changes in detail in the ensuing integral equations of the form (5.21). Consequently, it is a relative simple matter to write down similar existence results for these*

*particular cases.*

To summarize, we have considered the anti-plane shear of an elastic solid whose boundary is partially reinforced by a thin solid film represented by the union of a finite number of open curves. The solvability of the resulting boundary value problems was complicated by the presence of end-point conditions which must be satisfied at the ends of each section of the reinforcing film. In order to avoid complicated solvability conditions which carry no clear physical meaning, we have modified the boundary integral equation method using an equivalent (lower-order) reinforcement condition which led to the desired solvability results for the corresponding boundary value problems.

As shown above, the classical linear elastic model of the coupling of surface mechanics with a bulk material has been developed and thoroughly analyzed on well-posedness for the anti-plane shear deformations. We have demonstrated that the corresponding boundary value problems have uniquely existing solutions. Moreover, the correctness of the model was proved not only for the case when the cross-section reinforcement is presented by a finite number of closed curves, but also for a more general case with the reinforcement given by arcs. Therefore, the current research validates the legitimacy of the proposed model.

Now we are in the position to support our investigations with a striking example which clearly demonstrates the model's effectiveness and surface effect contribution to the field of linear elastic fracture mechanics.

---

## CHAPTER 6

# The contribution of surface effect to linear elastic fracture mechanics

In the current chapter we are going to address the following questions: How can the proposed model incorporating surface effect be useful? Is there an example of the surface effect contribution? Why should we bother ourselves with the model that has such a complicated boundary condition while so many well-studied simple classical models exist?

Unfortunately, in classical linear mechanics there are many theories and models predicting unphysical behavior. For example, many uncertainties arise in linear elastic fracture mechanics, where classical models predict infinite singular stresses. However, there is a chance that an addition of new effects into the model can lead to either finite stresses or weaker singularities.

In [72], for example, the authors used the idea of a thin reinforcing film on the surface of a bulk substrate material to investigate the effect of surface mechanics on the classical mixed boundary value problem describing the plane-strain field near a point at the interface between free and fixed boundary segments in an elastic half-

plane. It is well-known that in the classical problem, both surface displacements along the free boundary and contact stress distributions exhibit oscillatory behavior in the vicinity of the point [86]. An asymptotic analysis [72] showed that the addition of a thin reinforcing film along the free boundary effectively eliminated the oscillatory behavior of the stress field in the vicinity of the point leading to a strong square-root singularity and a displacement field which was smooth locally and bounded at the point of interest.

In this chapter, we continue the study began in [72] by analyzing the classical problem of an interface crack in anti-plane elasticity. In the previous chapters we have developed a well-posed comprehensive model of a linear elastic solid with the surface effect represented by a coating. Our purpose here is to show that the addition of a thin reinforcing layer on the crack faces indeed improves the corresponding classical models from linear elastic fracture mechanics. At the end of this chapter we provide a preliminary conclusion for Part I and briefly discuss the benefits of the approach used to model the surface effect in our model.

It should be noted that some passages in this chapter have been quoted verbatim from the author's publication [100].

## **6.1 Interface crack with surface effect**

In the case of anti-plane elasticity, the reduced displacement field and the corresponding stress components can be described in terms of a single analytic function  $\psi(z)$  of the

complex variable  $z$  by

$$\begin{aligned} w(z) &= \operatorname{Re}(\psi(z)) = \frac{1}{2}(\psi(z) + \overline{\psi(z)}), \\ \sigma_{13}(z) &= \mu \operatorname{Re}(\psi'(z)) = \frac{\mu}{2}(\psi'(z) + \overline{\psi'(z)}), \\ \sigma_{23}(z) &= \mu \operatorname{Im}(\psi'(z)) = -\frac{i\mu}{2}(\psi'(z) - \overline{\psi'(z)}). \end{aligned}$$

Here  $\mu > 0$  is the shear modulus of the material.

We assume that two dissimilar elastic materials are bonded together so that the material interface lies along the  $x_1$ -axis of the Cartesian coordinate system. We further assume the presence of an interface crack extending along the negative  $x_1$ -axis (so that the crack tip is located at the origin) and that the materials are perfectly bonded along the positive  $x_1$ -axis. It is well-known that the stress field near the crack-tip exhibits singular behavior making the classical solution physically inadmissible there [109]. Our particular interest lies in the case when the crack faces (described here in the Cartesian coordinates by  $x_2 = 0^+$  and  $x_2 = 0^-$ ,  $x_1 < 0$  or in the polar coordinates by  $\tilde{\theta} = \pm\pi$ ,  $0 < \tilde{r} < \infty$ ) are reinforced with a thin solid film whose bending rigidity is taken to be negligible (see Figure 6.1). A similar scenario was mentioned in [110] using the Gurtin-Murdoch theory of the mechanics of surface-stressed solids [55].

For consistency, we assume that no initial tension is applied on the reinforced crack faces. For convenience, we represent  $w$  and  $\sigma_{13}$ ,  $\sigma_{23}$  by the same functions when referred to the polar coordinate system and we adopt the notation  $[ \cdot ]$  to represent the jump in the given quantity across the specified boundary.

Using the theory of a reinforced surface developed for anti-plane strain in previous chapters, the corresponding boundary conditions pertaining to this problem can be

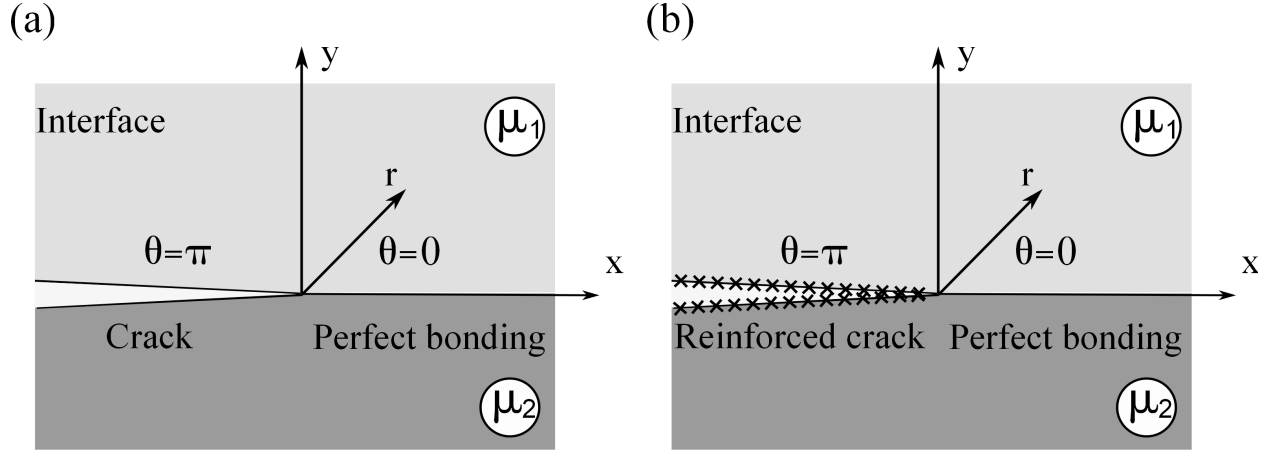


Fig. 6.1: Interface crack in a classical linear, homogeneous and isotropic elastic solid without (a) and with surface effect (b) on its tips

summarized as

$$\begin{aligned}
 [w(\tilde{r}, 0)] &= 0, \\
 [\sigma_{23}(\tilde{r}, 0)] &= 0, \\
 \sigma_{23}(\tilde{r}, \pm\pi) &= -h\mu_2 \frac{d^2 w}{dx_1^2}(\tilde{r}, \pm\pi).
 \end{aligned} \tag{6.1}$$

We are particularly interested in displacement solutions which admit the asymptotic representation

$$w = \tilde{r}^\rho f_1(\tilde{\theta}) + \tilde{r}^\rho \ln \tilde{r} f_2(\tilde{\theta}) + O(\tilde{r}^{\rho+1}), \text{ as } \tilde{r} \rightarrow 0 \tag{6.2}$$

uniformly for  $\tilde{\theta} \in [-\pi, \pi]$ , where  $\rho$  is a real constant in the range  $0 < \rho < 1$  and  $f_\alpha$  are smooth functions on  $[-\pi, \pi]$ . Solutions of the form (6.2), to leading order, take the form

$$w = \tilde{r}^\rho f_1(\tilde{\theta}) + \tilde{r}^\rho \ln \tilde{r} f_2(\tilde{\theta}), \text{ as } \tilde{r} \rightarrow 0 \tag{6.3}$$

It is clear from (6.1) that we can achieve the leading order solution (6.3) by assuming

that  $\psi$  for both materials takes the form

$$\begin{aligned}\psi^{(1)}(z) &= Az^\rho + Bz^\rho \ln z, \quad \text{Im } z > 0, \\ \psi^{(2)}(z) &= Cz^\rho + Dz^\rho \ln z, \quad \text{Im } z < 0,\end{aligned}\tag{6.4}$$

where  $0 < \rho < 1$  and  $A, B, C, D$  are complex constants to be determined.

From (6.1) and (6.4) it follows that the leading order solution (6.3) corresponds to the singular stress

$$\sigma_{23} = O_1(\tilde{r}^{\rho-1}) + O_2(\tilde{r}^{\rho-1} \ln \tilde{r}), \quad \text{as } \tilde{r} \rightarrow 0.\tag{6.5}$$

Moreover, it can be shown that

$$\frac{d^2 w}{dx_1^2} = \frac{1}{2}(\psi''(z) + \overline{\psi''(z)}).\tag{6.6}$$

Thus, the leading order solution (6.3) is such that

$$w_{,11} = O_1(\tilde{r}^{\rho-2}) + O_2(\tilde{r}^{\rho-2} \ln \tilde{r}), \quad \text{as } \tilde{r} \rightarrow 0.\tag{6.7}$$

From (6.5) and (6.7) the reinforcement boundary conditions on  $\tilde{\theta} = \pm\pi$  from (6.1) require that, to leading order,

$$\frac{d^2 w}{dx_1^2}(\tilde{r}, 0) = 0 \quad \text{as } \tilde{r} \rightarrow 0.\tag{6.8}$$

In summary, the leading order solution satisfies the boundary conditions

$$\begin{aligned}
[w(\tilde{r}, 0)] &= 0, \\
[\sigma_{23}(\tilde{r}, 0)] &= 0, \\
\frac{d^2 w}{dx_1^2}(\tilde{r}, \pm\pi) &= 0.
\end{aligned} \tag{6.9}$$

The first two boundary conditions in (6.9) (assuming (6.4)) yield

$$\begin{aligned}
\operatorname{Re} A &= \operatorname{Re} C, & \operatorname{Re} B &= \operatorname{Re} D; \\
\mu_1(\rho \operatorname{Im} A + \operatorname{Im} B) &= \mu_2(\rho \operatorname{Im} C + \operatorname{Im} D); \\
\mu_1 \rho \operatorname{Im} B &= \mu_2 \rho \operatorname{Im} D.
\end{aligned}$$

Here,  $\mu_1$  and  $\mu_2$  are the shear moduli in the respective regions  $\operatorname{Im} z > 0$  and  $\operatorname{Im} z < 0$ .

The third boundary condition from (6.9) requires that:

$$\begin{aligned}
\{A\rho(\rho - 1) + B(2\rho - 1 + i\pi\rho(\rho - 1))\}e^{i(\rho-2)\pi} &= \\
= -\{\bar{A}\rho(\rho - 1) + \bar{B}(2\rho - 1 - i\pi\rho(\rho - 1))\}e^{i(2-\rho)\pi}, \\
\{C\rho(\rho - 1) + D(2\rho - 1 + i\pi\rho(\rho - 1))\}e^{i(\rho-2)\pi} &= \\
= -\{\bar{C}\rho(\rho - 1) + \bar{D}(2\rho - 1 - i\pi\rho(\rho - 1))\}e^{i(2-\rho)\pi}, \\
\rho(\rho - 1)(Be^{i(\rho-2)\pi} + \bar{B}e^{i(2-\rho)\pi}) &= 0, \\
\rho(\rho - 1)(De^{i(\rho-2)\pi} + \bar{D}e^{i(2-\rho)\pi}) &= 0.
\end{aligned} \tag{6.10}$$

There are several cases of interest which arise from these equations. The eigenvalue  $\rho = 0$  leads to  $O(\frac{1}{\tilde{r}})$  singularity in stresses, while  $\rho = \frac{1}{2}$  gives the classical solution with

$O(\frac{1}{\sqrt{\tilde{r}}})$  stress singularity. However, we are more interested in the case when  $\rho = 1$  since it provides us with the solution which does not arise for cracks without reinforcement. Specifically, when  $\rho = 1$  we have

$$\begin{aligned}\operatorname{Re} B &= \operatorname{Re} D = 0, \\ \operatorname{Im} C &= \frac{\mu_1}{\mu_2} \operatorname{Im} A, \\ \operatorname{Im} D &= \frac{\mu_1}{\mu_2} \operatorname{Im} B.\end{aligned}$$

The corresponding displacement and stress distributions corresponding to the leading order solution are then given by

$$\begin{aligned}w^{(\alpha)} &= \tilde{r}[(\operatorname{Re} A - l_\alpha \tilde{\theta} \operatorname{Im} B) \cos \tilde{\theta} - l_\alpha \operatorname{Im} A \sin \tilde{\theta}] - l_\alpha (\operatorname{Im} B) \tilde{r} \ln \tilde{r} \sin \tilde{\theta}, \\ \sigma_{13}^{(\alpha)} &= \mu_\alpha (\operatorname{Re} A - l_\alpha \tilde{\theta} \operatorname{Im} B), \\ \sigma_{23}^{(\alpha)} &= \mu_\alpha \{\operatorname{Im} A + \operatorname{Im} B(1 + \ln \tilde{r})\}.\end{aligned}$$

Here, the superscript  $\alpha = 1, 2$ , denotes the corresponding quantity in the half-plane  $x_2 > 0$  and  $x_2 < 0$ , respectively,  $l_1 = 1$  and  $l_2 = \frac{\mu_1}{\mu_2}$ .

This solution demonstrates the possibility of a weakened singularity of the logarithmic type as opposed to the strong square-root singularity predicted by the classical theory [109] and the case when  $\rho = \frac{1}{2}$ . The fact that so many different solutions for  $\rho$  emerge is a consequence of the approximation (6.8) used to represent the effect of the reinforcement in the vicinity of the crack tip. This is sufficiently ‘weak’ (general) to accommodate several cases inducing the ones of interest. For instance, in Wang’s work [111] it was shown that for the anti-plane crack with the non-zero curvature and

surface energy both square-root and logarithmic singularities co-exist. The author also indicates there that, in the limit, as the crack becomes flat, only the logarithmic singularity survives, which agrees with several works including [72]. As such, the results derived here are in accordance with those presented in [72] albeit for a mode-III crack in a homogeneous material incorporating surface elasticity on the crack faces. Even though in our analysis we pick up both possibilities of singularity, further conditions such as remote loading or curved crack would rule out the inappropriate singularity of a square-root type. Thus, we found out that an addition of the surface effect to the crack tips allows for the solution with the weakened type of singularity.

**Remark.** *Similar analysis of the anti-plane shear field near a point at the interface between free and fixed boundary segments in an elastic half-plane (as well as for the case where this boundary is located between two materials) leads to a similar conclusion.*

To summarize, we have obtained an asymptotic solutions for an interface crack whose crack faces are coated with a thin reinforcing film of separate elastic material. In the case of anti-plane elasticity, the effect of the reinforcement is to discover a solution with the reduced order of the stress singularity at the crack tip. This clearly demonstrates the contribution of the proposed model to linear fracture mechanics.

## 6.2 Some discussion and preliminary conclusions

In Part I we have introduced the model of coupling of surface mechanics with a classical linear elastic bulk. Well-posedness of this model was established. An example demonstrating the contributions of this model to linear fracture mechanics was given. Clearly, the addition of microstructural effects into the model is promising. But before

proceeding to Part II, it is necessary to discuss the approach used to model the surface effect.

It is well-known that, in the Gurtin-Murdoch theory, the surface effect is modeled with a pre-stretched elastic thin film of zero thickness perfectly bonded to the surface. Therefore, it assumes the surface tension even in cases when a solid is not subjected to any loadings. In addition, traction-boundary condition is derived mathematically via direct consideration of the surface energy.

In contrast to this, our model has the following advantages. First of all, it does not include any residual stresses, so that the absence of any loadings applied to the body can be adequately modeled. Next, the thickness of the membrane is included into the model explicitly, so that it is possible to control how far the surface effect spreads into the bulk. Finally, the proposed model is much simpler for understanding since it is based on the equilibrium consideration of the thin reinforcing elastic film. Therefore, it does not need rigorous mathematical energy consideration and is intuitively clearer for mechanical engineers.

We note and emphasize here the fact that, in the particular case of anti-plane deformations, the reinforcing elastic film is modeled by a plate. Interestingly, in the case of plane deformations [59], this reinforcement is represented by a beam so that bending effects are taken into account. We suggest that for different types of applied deformation, different supplementary models of reinforcement (e.g. shell, beam, plate) can be employed to adequately represent the surface effect.

To summarize, we have introduced a number of arguments, proofs and an example that makes our approach attractive enough to be complicated with further introduction of the microstructural effect into the model. Hence, the remaining part of the thesis will

be devoted to the coupling of surface mechanics with a bulk material in the framework of micropolar linear elasticity.

## Part II

Coupling of surface mechanics with  
a bulk material in the framework of  
micropolar linear, homogeneous  
and isotropic elasticity

---

## CHAPTER 7

# Mathematical modeling: incorporation of microstructural effects

Real materials naturally incorporate both surface and microstructural effects. The elimination of either or both of these from classical models is a convenience designed to satisfy the strict mathematical requirements. In the previous chapters we have analyzed the model incorporating surface effect only and, thus, armed our further investigations with a solid supplementary model on which our modified boundary integral equation method (BIEM) was tested. Now we can do better and enhance the model developed in Part I by taking into account the effect of microstructure. In the following chapters we will develop the necessary mathematical well-posedness analysis to incorporate both microstructural and surface effects into the model of deformations, thereby increasing the accuracy and effectiveness of the material behavior prediction. It should be noted that some passages in this chapter have been quoted verbatim from the author's publication [99].

Let us consider anti-plane deformations of a micropolar linear, homogeneous and isotropic elastic solid in which the bounding surface of the solid is endowed with a separate elasticity which affects the overall deformation of the solid. The boundary elasticity consists of a distinct thin micropolar linear, homogeneous and isotropic elastic coating bonded to part of the boundary of the solid.

We consider the equilibrium of a deformable solid occupying a cylindrical region whose generators are parallel to the  $x_3$ -axis of a rectangular Cartesian coordinate system. The cylinder is assumed to be sufficiently long so that end effects in the axial direction are negligible. We assume that  $S$  is occupied by a homogeneous and isotropic linearly elastic micropolar material with elastic constants  $\lambda, \mu, \alpha, \beta, \gamma, \kappa$  [12]. The boundary  $\partial S$  of  $S$  is described by the union of a finite number of sufficiently smooth closed curves. Part of the boundary of the cylindrical body is coated with a thin, homogeneous and isotropic linearly elastic micropolar film with separate elastic constants  $\bar{\lambda}, \bar{\mu}, \bar{\alpha}, \bar{\beta}, \bar{\gamma}, \bar{\kappa}$  and we regard a subset  $\Gamma$  (consisting of a finite number of sufficiently smooth closed curves) of  $\partial S$  to represent this coating in the cross-section  $S$ .

## 7.1 Governing equations

For the micropolar bulk occupying domain  $S$  a state of anti-plane shear is characterized by a displacement field  $u = (u_1, u_2, u_3)^T$  and a microrotation field  $\varphi = (\varphi_1, \varphi_2, \varphi_3)^T$  of

the forms

$$\begin{aligned} u_1(x_1, x_2, x_3) = u_2(x_1, x_2, x_3) = 0, \quad u_3(x_1, x_2, x_3) = w(x), \\ \varphi_1(x_1, x_2, x_3) = \varphi_1(x), \quad \varphi_2(x_1, x_2, x_3) = \varphi_2(x), \quad \varphi_3(x_1, x_2, x_3) = 0, \end{aligned} \quad (7.1)$$

where the out-of-plane displacement  $w$  and in-plane microrotations  $\varphi_1, \varphi_2$  are functions of  $x$  on a cross-section  $S$  of the cylinder. For the sake of simplicity of derivations we neglect body forces and body couples and obtain the following equations of equilibrium [92]:

$$L(\partial x)u(x) = 0, \quad (7.2)$$

where  $u = (\varphi_1, \varphi_2, w)^T$ ,  $L(\partial x) = L(\partial/\partial x_1, \partial/\partial x_2)$  is the matrix partial-differential operator with  $\xi_\alpha = \partial/\partial x_\alpha$ , defined by  $L(\xi_1, \xi_2) =$

$$= \begin{pmatrix} (\gamma + \kappa)\Delta - 4\alpha + (\beta + \gamma - \kappa)\xi_1^2 & (\beta + \gamma - \kappa)\xi_1\xi_2 & 2\alpha\xi_2 \\ (\beta + \gamma - \kappa)\xi_1\xi_2 & (\gamma + \kappa)\Delta - 4\alpha + (\beta + \gamma - \kappa)\xi_2^2 & -2\alpha\xi_1 \\ -2\alpha\xi_2 & 2\alpha\xi_1 & (\mu + \alpha)\Delta \end{pmatrix}$$

with  $\Delta = \xi_1^2 + \xi_2^2$ . The boundary stress operator  $T(\partial x)$  with the unit outward normal  $n = (n_1, n_2)^T$  is given by [92]  $T(\xi_1, \xi_2) =$

$$= \begin{pmatrix} (2\gamma + \beta)\xi_1 n_1 + (\gamma + \kappa)\xi_2 n_2 & (\gamma - \kappa)\xi_2 n_1 + \beta\xi_1 n_2 & -2\alpha n_2 \\ (\gamma - \kappa)\xi_1 n_2 + \beta\xi_2 n_1 & (\gamma + \kappa)\xi_1 n_1 + (2\gamma + \beta)\xi_2 n_2 & \alpha n_1 \\ 0 & 0 & (\mu + \alpha)(\xi_1 n_1 + \xi_2 n_2) \end{pmatrix}.$$

Assuming  $2\gamma + \beta > 0$  and  $\kappa, \alpha, \gamma, \mu > 0$ , it can be seen that  $L$  is an elliptical operator, while the internal energy density [92]

$$\begin{aligned}
E(u, u) = & \frac{\gamma + \kappa}{2}(u_{1,2}^2 + u_{2,1}^2) + (\gamma - \kappa)u_{1,2}u_{2,1} + (\gamma + \frac{\beta}{2})(u_{1,1}^2 + u_{2,2}^2) + \beta u_{1,1}u_{2,2} + \\
& + \frac{\mu}{2}(u_{3,1}^2 + u_{3,2}^2) + \frac{\alpha}{2}((2u_2 + u_{3,1})^2 + (2u_1 - u_{3,2})^2) \quad (7.3)
\end{aligned}$$

is a positive quadratic form. Moreover,  $E(u, u) = 0$  if and only if

$$u(x) = (0, 0, c)^T, \quad (7.4)$$

where  $c$  is an arbitrary constant. Here (7.4) is the most general rigid displacement and microrotation vector associated with (7.2). Clearly, the space of such rigid displacements and microrotations is spanned by the single vector  $(0, 0, 1)^T$ . Consequently, if we write

$$F = \begin{pmatrix} 0 & 0 & 0 \\ 0 & 0 & 0 \\ 0 & 0 & 1 \end{pmatrix},$$

then  $LF = 0$  in  $\mathbb{R}^2$ ,  $TF = 0$  on  $\partial S$  and a generic vector of the form (7.4) can be written as  $Fk$ , where vector  $k \in \mathcal{M}_{3 \times 1}$  is constant and arbitrary.

The matrix of fundamental solutions for the operator  $L$  is given by [92]

$$D(x, y) = \tilde{D} \ln |x - y| + \Omega(x, y),$$

where  $\Omega(x, y)$  is the matrix with weak singularities in the sense of [102] and  $\tilde{D} \in \mathcal{M}_{3 \times 3}$

is the matrix of coefficients given by

$$\tilde{D} = -\frac{1}{2\pi} \left( bE_{\gamma\gamma} + \frac{1}{\mu + \alpha} E_{33} \right), \quad b = \frac{3\gamma + \beta + \kappa}{2(\gamma + \kappa)(2\gamma + \beta)}.$$

It is easily verified that the columns  $D^{(\alpha)}(x, y)$  satisfy (7.2) at all  $x \in \mathbb{R}^2$ ,  $x \neq y$ .

## 7.2 Boundary conditions describing microstructural effects

The conditions on the (reinforced) subset  $\Gamma$  of the boundary  $\partial S$  couple the response of the solid to that of the coating on  $\Gamma$ . To describe this response in terms of a boundary condition on  $\Gamma$ , we suggest to use the normal-tangential coordinates  $\{n, \tau, x_3\}$  and following assumptions:

1. The coated subset of the cylinder's boundary is considered to be a thin plate in the plane  $\tau - x_3$  with thickness  $h$  along normal  $n$ ;
2. The bulk together with the boundary and coating is subjected to the anti-plane shear deformations, so that relative to the thin plate we deal with a plane stress type of deformation;
3. Deformations along the thickness  $h$  of the thin film are uniform, so that all mechanical quantities in the reinforcement do not depend on the normal direction;
4. There is no microrotation  $\varphi_\tau$  along the tangent to the reinforced boundary;
5. The influence of the bulk on the thin film can be considered as body forces and

couples represented by a vector  $G(s)$ ;

6. The influence of the thin film on the bulk is significant not for the whole body but for the boundary only, so that this effect will arise in the boundary conditions as stresses transmitted  $\Sigma(s)$  by the reinforcement.

Under the above assumptions 1-4, the displacement and microrotation fields in the reinforcing film at any cross-section are characterized by

$$u_n = u_\tau = 0, \quad u_3 = w(\tau), \quad \varphi_\tau = \varphi_3 = 0, \quad \varphi = \varphi_n(\tau).$$

The system of equilibrium equations, where a body force and couple vector  $G(s) = (0, C_n(s), F_3(s))^T$  represents the influence of the bulk material (as stated in assumption 5), is

$$\begin{aligned} (\bar{\gamma} + \bar{\kappa})d_x^2\varphi_n - 2\bar{\alpha}d_x w - 4\bar{\alpha}\varphi_n + C_n &= 0, \\ (\bar{\mu} + \bar{\alpha})d_x^2 w + 2\bar{\alpha}d_x\varphi_n + F_3 &= 0, \end{aligned}$$

where  $F_3$  and  $C_n$  are, respectively, the force in the axial direction and the couple about the normal direction; or these equations can be written in more convenient form as

$$R(d_x)(\varphi_\tau, \varphi_n, w)^T + G(s) = 0$$

with  $d_x = d/ds_x$  denoting the directional derivative with respect to  $s(x)$  along  $\Gamma$ . Here  $R(d_x)$  is a tangential differential operator in the thin reinforcing film with material parameters  $\bar{\lambda}, \bar{\mu}, \bar{\alpha}, \bar{\beta}, \bar{\gamma}, \bar{\kappa}$ , defined by  $R(d_x) = R_0 + R_1 d_x + R_2 d_x^2 = R_0 + R^*(d_x)$  with

coefficient matrices

$$R_0 = \begin{pmatrix} 0 & 0 & 0 \\ 0 & -4\bar{\alpha} & 0 \\ 0 & 0 & 0 \end{pmatrix}, R_1 = \begin{pmatrix} 0 & 0 & 0 \\ 0 & 0 & -2\bar{\alpha} \\ 0 & 2\bar{\alpha} & 0 \end{pmatrix}, R_2 = \begin{pmatrix} 0 & 0 & 0 \\ 0 & (\bar{\gamma} + \bar{\kappa}) & 0 \\ 0 & 0 & (\bar{\mu} + \bar{\alpha}) \end{pmatrix}.$$

Next, as was indicated in assumption 6, the reinforcement transmits stresses  $\Sigma(s)$  to the bulk, which is to be reflected in the boundary conditions on  $\Gamma$ . These stresses  $\Sigma(s)$  can be derived from the body force and couple vector  $G(s)$  using the fact that all deformations are uniform along the thickness  $h$  of the thin film:

$$\Sigma(s) = \int_0^h G(s) ds = -hR(d_x)(\varphi_\tau, \varphi_n, w)^T,$$

guaranteed by assumption 3.

After transforming from the normal tangential coordinates  $(n, \tau)$  to the Cartesian coordinates  $(x_1, x_2)$  we obtain the following boundary conditions on the reinforcement  $\Gamma$ :

$$T(\partial x)u(x) = -hI(x)R(d_x)I^{-1}(x)u(x) + I(x)g(x), \quad x \in \Gamma. \quad (7.5)$$

Here  $T(\partial x)$  is the micropolar anti-plane boundary stress operator,  $I(x)$  is the transformation matrix, defined in Chapter 2, so that  $(\varphi_\tau, \varphi_n, w)^T = I^{-1}(x)u(x)$  and  $g(x) \in \mathcal{M}_{3 \times 1}$  is a vector of prescribed stresses on  $\Gamma$ .

Now, we wish to give an in-depth examination of the boundary condition (7.5), since it plays a crucial role in our model.

From the mathematical point of view, (7.5) represents a highly non-standard boundary condition. Firstly, on the left-hand side we see the boundary stress operator  $T(\partial x)$

corresponding to the anti-plane deformations in the micropolar bulk and given by a cumbersome matrix partial differential operator of the first order. Secondly, on the right-hand side of (7.5) we have to deal with, at least, equally complicated tangential differential operator of the second order  $R(d_x)$  describing the plane stress deformation occurring in the thin micropolar reinforcement, which subsequently transmits stresses to the boundary of the bulk. The natural difficulty arises due to the fact that the order of the derivatives on the right-hand side of the boundary condition (7.5) is higher than of those on the left-hand side. As a consequence, classical methods for well-posedness analysis for boundary value problems with the reinforcement condition break down and it is necessary to modify these methods for our purpose. Overall, any boundary value problem involving the reinforcement boundary condition (7.5) represents an elegant mathematical challenge, which is of great theoretical interest.

Next, from the physical point of view, the surface effect was introduced into the micropolar model, at the cost of some increase of complexity in the boundary value problems, by modeling this effect as an addition of the thin reinforcing film perfectly bonded to the boundary of the bulk causing transmission of stresses arising in the right-hand side of (7.5). It should be emphasized again, that both micropolar and surface effects form the basis of the comprehensive mathematical model developed. As a result, this model provides us with a more accurate description of the behavior for the wider range of materials at the smaller scales.

To sum-up the above, it is of practical and theoretical relevance to look more closely at the developed model from the point of view of well-posedness and, by doing that, check whether it is reliable or not.

---

## CHAPTER 8

# Well-posedness analysis of the model incorporating both surface and microstructural effects

We have incorporated both microstructural and surface effects into the model. Now it becomes necessary to develop the mathematics for demonstration of the fact that our model is well-posed. We again apply boundary integral equation methods (BIEM) generalizing and utilizing them as necessary to account for higher order derivatives on the boundary.

As was noted in the preceding chapter, the contribution of the surface mechanics to the ensuing boundary-value problem gives rise to a highly non-standard boundary condition that is not accommodated by classical methods in this area. We could overcome these difficulties for the case of coupling of surface mechanics with a bulk material in the framework of classical linear, homogeneous and isotropic elasticity. Analogously, in this chapter, the corresponding interior and exterior mixed boundary-value problems with appropriately formulated reinforcement conditions are analyzed for well-posedness

in classical function spaces, but this time in the framework of micropolar linear, homogeneous and isotropic elasticity. Specifically, we generalize the boundary integral equation method to account for the ensuing non-standard boundary conditions and reduce the corresponding boundary-value problems to systems of singular integro-differential equations to which Noether's theorems apply and subsequently reduce to the simpler Fredholm's theorems. Finally, we establish solvability results in appropriate classical function spaces.

## 8.1 BVPs for the proposed model

### 8.1.1 Bounded domain

We consider a multiply-connected bounded domain  $S$  with sufficiently smooth boundary  $\partial S$ . Let this boundary  $\partial S$  consist of two curves  $\partial S_1$  and  $\Gamma$  representing, respectively, non-reinforced and reinforced sections of the boundary. We assume for the sake of simplicity that  $\partial S_1$  is divided into two open curves  $\partial S_u$  and  $\partial S_t$  with common endpoints  $a$  and  $b$ .  $\partial S_u$  is a part of the boundary with prescribed displacements and microrotations  $u^{(0)} \in \mathcal{M}_{3 \times 1}$ , while on  $\partial S_t$  we have prescribed stresses and couple-stresses  $t^{(0)} \in \mathcal{M}_{3 \times 1}$ . Finally, we assume that  $\Gamma$  is a single closed curve with reinforcement conditions (7.5) on it (See Figure 8.1 for details).

Now, we wish to find a vector-solution  $u \in \mathcal{M}_{3 \times 1}$  of the system (7.2) in  $S$ , which belongs to an appropriate space of vector functions  $C^2(S \cup \Gamma) \cap C^1(\bar{S} \setminus \{a, b\})$  and

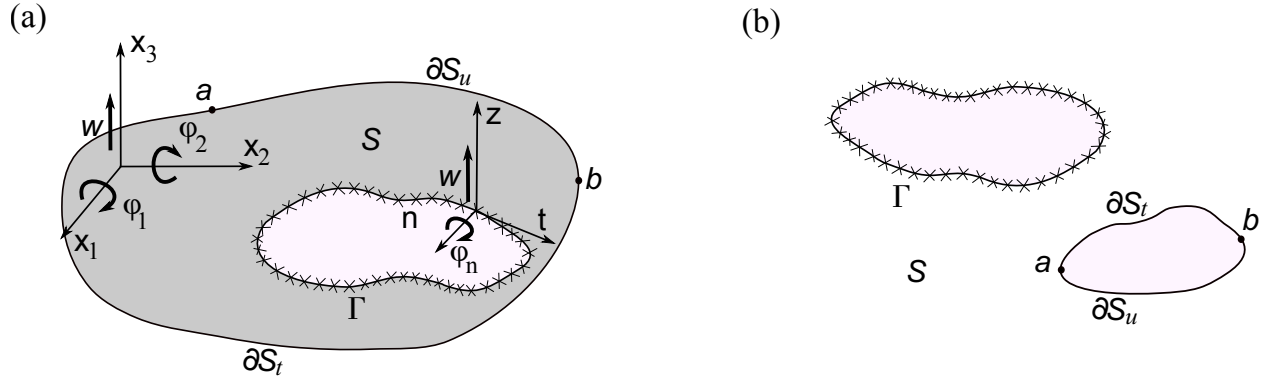


Fig. 8.1: Micropolar linear, homogeneous and isotropic elastic domain: bounded (a) and unbounded (b) cases

satisfies the boundary conditions

$$\begin{aligned}
 u(x) &= u^{(0)}(x), \quad x \in \partial S_u, \\
 T(\partial x)u(x) &= t^{(0)}(x), \quad x \in \partial S_t, \\
 T(\partial x)u(x) &= -hI(x)R(d_x)I^{-1}(x)u(x) + I(x)g(x), \quad x \in \Gamma.
 \end{aligned} \tag{8.1}$$

Let us recall the Betti formula:

$$2 \int_S E(u, u) d\sigma = \int_{\partial S} u^T T u ds. \tag{8.2}$$

**Theorem 8.1.** *The interior boundary value problem (8.1) has at most one solution.*

*Proof.* Let  $\omega$  be the difference of any two solutions to the interior boundary value problem (8.1). Applying (8.2) to  $\omega$  and, noting that  $\omega = 0$  on  $\partial S_u$  and  $T\omega = 0$  on  $\partial S_t$  we obtain:

$$2 \int_S E(\omega, \omega) d\sigma = - \int_{\Gamma} \omega^T T \omega ds.$$

Next, noting that  $T(\partial x)\omega(x) = -hI(x)R(d_x)I^{-1}(x)\omega(x)$ ,  $x \in \Gamma$  so that, expressed in the  $(n, \tau)$  coordinate system:

$$\omega^T T \omega = -h(\varphi_\tau, \varphi_n, w)[R(d_x)(\varphi_\tau, \varphi_n, w)]^T$$

on  $\Gamma$ . Consequently, using integration by parts, the integral on the right-hand side of (8.2) can be rewritten as

$$2 \int_S E(\omega, \omega) d\sigma = -h \int_\Gamma \left( 4\bar{\alpha}\varphi_n^2 + (\bar{\gamma} + \bar{\kappa}) \left( \frac{d\varphi_n}{ds} \right)^2 + (\bar{\mu} + \bar{\alpha}) \left( \frac{dw}{ds} \right)^2 + 4\bar{\alpha}\varphi_n \frac{dw}{ds} \right) ds = -h \int_\Gamma N(s) ds.$$

If we denote  $q_1 = \varphi_n$ ,  $q_2 = d\varphi_n/ds$ ,  $q_3 = dw/ds$  then it can be shown that

$$N(s) = 4\bar{\alpha}q_1^2 + (\bar{\gamma} + \bar{\kappa})q_2^2 + (\bar{\mu} + \bar{\alpha})q_3^2 + 4\bar{\alpha}q_1q_3 = (q_1, q_2, q_3)K(q_1, q_2, q_3)^T$$

is a positive definite quadratic form as main minors of the coefficient matrix

$$K = \begin{pmatrix} 4\bar{\alpha} & 0 & 2\bar{\alpha} \\ 0 & \bar{\gamma} + \bar{\kappa} & 0 \\ 2\bar{\alpha} & 0 & \bar{\mu} + \bar{\alpha} \end{pmatrix}$$

are positive assuming  $\bar{\alpha} > 0$ ,  $\bar{\mu} > 0$ ,  $\bar{\gamma} + \bar{\kappa} > 0$ . This assumption is valid here since it is applicable for the general case of plane-stress deformations in micropolar elasticity [90].

From the Betti formula and the fact that  $E(\omega, \omega)$  is positive definite, we conclude

that vector  $\omega$  is constant. Standard arguments now lead to the fact that  $\omega = 0$  in  $S$ , so the solution to the interior boundary value problem is unique.  $\square$

### 8.1.2 Unbounded domain

In fact, the exterior boundary value problem is posed similarly to the interior one except that  $S$  is now an unbounded domain with boundary  $\partial S = \partial S_1 \cup \Gamma$ , where  $\partial S_1$  and  $\Gamma$  represent single closed curves (as shown on Fig. 1b).

For the Betti formula to be used for the case of an unbounded domain  $S$  we have to impose some restrictions on the behavior of the solution at infinity. To do this, let consider two classes of vector-functions  $\mathcal{A}$  and  $\mathcal{A}^*$ , the elements of which will have finite energies (7.3). The class  $\mathcal{A}$  contains vectors  $u \in \mathcal{M}_{3 \times 1}$ , whose components in terms of the polar coordinates  $(\tilde{r}, \tilde{\theta})$ , as  $\tilde{r} \rightarrow \infty$ , admits an asymptotic expansion of the form [92]

$$\begin{aligned}\varphi_1(\tilde{r}, \tilde{\theta}) &= \tilde{r}^{-2}[m_0 \sin 2\tilde{\theta} + m_1(1 - \cos 2\tilde{\theta}) + m_2] + O(\tilde{r}^{-3}), \\ \varphi_2(\tilde{r}, \tilde{\theta}) &= \tilde{r}^{-2}[-m_0 \sin 2\tilde{\theta} - m_1(1 - \cos 2\tilde{\theta}) + m_3] + O(\tilde{r}^{-3}), \\ w(\tilde{r}, \tilde{\theta}) &= \tilde{r}^{-1}[(m_3 - m_0) \cos \tilde{\theta} - (m_2 - m_1) \sin \tilde{\theta}] + O(\tilde{r}^{-2}),\end{aligned}$$

where  $m_0, \dots, m_3$  are arbitrary constants.

Let set  $\mathcal{A}^*$  consist of vectors  $u = Fk + u_0 \in \mathcal{M}_{3 \times 1}$ , where  $k \in \mathcal{M}_{3 \times 1}$  is an arbitrary constant vector, while  $u_0 \in \mathcal{M}_{3 \times 1} \cap \mathcal{A}$ .

Now we can proceed to the formulation of the exterior boundary value problem containing this additional requirement on the behavior at the infinity: we wish to find

a vector-solution  $u \in \mathcal{M}_{3 \times 1}$  of the system (7.2) in an unbounded domain  $S$ , which belongs to an appropriate vector space  $C^2(S \cup \Gamma) \cap C^1(\bar{S} \setminus \{a, b\}) \cap \mathcal{A}^*$  and satisfies the following boundary conditions:

$$\begin{aligned} u(x) &= u^{(0)}(x), & x \in \partial S_u, \\ T(\partial x)u(x) &= t^{(0)}(x), & x \in \partial S_t, \\ T(\partial x)u(x) &= -hI(x)R(d_x)I^{-1}(x)u(x) + I(x)g(x), & x \in \Gamma. \end{aligned} \tag{8.3}$$

**Theorem 8.2.** *The exterior boundary value problem (8.3) has at most one solution.*

*Proof.* We describe a circle  $K_R$  of sufficiently large radius  $\tilde{r} = R$  on the unbounded domain  $S$  so that it contains both single curves  $\partial S_1$ ,  $\Gamma$  and let  $\omega$  be the difference of any two solutions of the exterior boundary value problem (8.3). Applying (8.2) to  $\omega$  and, noting that  $\omega = 0$  on  $\partial S_u$  and  $T\omega = 0$  on  $\partial S_t$  we obtain:

$$2 \int_S E(\omega, \omega) d\sigma = \int_{K_R} \omega^T T \omega ds - \int_{\Gamma} \omega^T T \omega ds.$$

However, it can be easily shown that

$$\lim_{R \rightarrow \infty} \int_{K_R} \omega^T T \omega ds = \lim_{R \rightarrow \infty} R \int_0^{2\pi} \omega^T T \omega d\tilde{\theta} = 0,$$

so that the remaining part of the proof repeats the steps from Theorem 8.1 for the bounded domain  $S$ . □

**Remark.** *The interior and exterior boundary value problems can be generalized for the cases when  $\partial S_1$  and  $\Gamma$  consist of union of a finite number of closed curves or  $\partial S_1$  is*

*divided into more than two open curves. Nevertheless, these modifications will not lead to any significant changes in the procedure of the derivation of existence and uniqueness result.*

## 8.2 Application of BIEM to the analysis of well-posedness for the proposed model

For simplicity and without loss of generality, using the results from [91] we reduce both inhomogeneous interior problem (8.1) and the corresponding exterior problem (8.3) to the simpler problems with homogeneous conditions on  $\partial S_u$  and  $\partial S_t$ . Hence, neglecting the prescribed vectors  $u_0$  and  $t_0$  on  $\partial S_u$  and  $\partial S_t$ , respectively, we arrive at the formulation of our mixed boundary value problem: we seek a vector-function  $u \in C^2(S \cup \Gamma) \cap C^1(\overline{S} \setminus \{a, b\})$ , which solves (7.2) in  $S$  and satisfies the boundary conditions

$$\begin{aligned} u(x) &= 0, & x \in \partial S_u, \\ T(\partial x)u(x) &= 0, & x \in \partial S_t, \\ T(\partial x)u(x) &= -hI(x)R(d_x)I^{-1}(x)u(x) + I(x)g(x), & x \in \Gamma. \end{aligned} \tag{8.4}$$

When  $S$  is bounded, the notation  $(8.4)_I$  will be employed for the interior boundary value problem associated with (8.4). For the case of the unbounded domain  $S$ , the notation  $(8.4)_E$  will indicate the exterior problem boundary value problem (8.4), with the added requirement  $u \in \mathcal{A}^*$ .

Now, with the help of boundary integral equation methods, we are going to trans-

form the boundary value problems  $(8.4)_I$  and  $(8.4)_E$  into entirely different kind of problems which are amenable to an existence theory. To do this we need to construct the solution to the problems  $(8.4)_I$  and  $(8.4)_E$  in the form of so-called single-layer potentials [102]. However, the standard method of boundary integral equation methods can not be applied to our problems due to the complexity of the reinforcement conditions on  $\Gamma$ . To this end, the solutions we suggest are given by generalized single-layer potentials whose integrands are adjusted to account for the non-standard boundary condition on  $\Gamma$ .

### 8.2.1 Bounded domain

We wish to find the solution of the boundary value problem  $(8.4)_I$  which is of the form of the generalized single layer potential:

$$u(x) = (V\phi)_I(x) = \int_{\Gamma} [D(x, y) - D_1(x, y)] I(y) \phi(y) ds_y, \quad x \in S. \quad (8.5)$$

Here  $\phi \in \mathcal{M}_{3 \times 1}$  is an unknown vector density of the Holder class  $C^{1, \alpha}(\Gamma)$ ,  $\alpha \in (0, 1)$  (Holder continuously differentiable vector functions on  $\Gamma$ ), defined on  $\Gamma$ , and columns  $D_1^{(\alpha)}$  of matrix  $D_1(x, y) \in \mathcal{M}_{3 \times 3}$ ,  $y = (y_1, y_2) \in \Gamma$  are constructed to satisfy the following classical mixed boundary value problem. Let  $\Omega_I$  be the multiply-connected bounded domain with sufficiently smooth boundary  $\partial\Omega_I$  so that  $S \in \Omega_I$ ,  $\Gamma \in \Omega_I$  and

$\partial S_u \cup \partial S_t \subseteq \partial \Omega_I$ . Then

$$\begin{aligned} L(\partial x)D_1^{(\alpha)}(x, y) &= 0, \quad x \in \Omega_I, \\ T(\partial x)D_1^{(\alpha)}(x, y) &= T(\partial x)D^{(\alpha)}(x, y), \quad x \in \partial S_t, \\ D_1^{(\alpha)}(x, y) &= D^{(\alpha)}(x, y), \quad x \in \partial \Omega_I \setminus \partial S_t. \end{aligned}$$

It should be noted that the boundary values  $D^{(\alpha)}(x, y)$  and  $T(\partial x)D^{(\alpha)}(x, y)$  are smooth in this case since for  $x \in \partial \Omega_I$  and  $y \in \Gamma \subset \Omega_I$ ,  $x \neq y$ , ever. Consequently, from the existence result for the interior mixed problem for the anti-plane deformation in micropolar elasticity (for the proof we refer the reader to [91]) it is possible to show that  $D_1(x, y)(\alpha)$  exists uniquely for each  $y \in \Gamma$  in the class  $C^2(\Omega_I) \cap C^1(\overline{\Omega_I} \setminus \{a, b\})$ .

Then, it is not difficult to show that  $(V\phi)_I(x)$  from (8.5) satisfies all conditions of the problem  $(8.4)_I$  provided the density  $\phi$  satisfies the following system of integral equations on  $\Gamma$  :

$$\begin{aligned} &\frac{1}{2}\phi(x) + I^{-1}(x) \int_{\Gamma} T(\partial x)D(x, y)I(y)\phi(y)ds_y + hR^*(d_x) \cdot \\ &\cdot \int_{\Gamma} I^{-1}(x)D(x, y)I(y)\phi(y)ds_y = hR(d_x) \int_{\Gamma} I^{-1}(x)D_1(x, y)I(y)\phi(y)ds_y - \\ &\quad - hR_0I^{-1}(x) \int_{\Gamma} D(x, y)I(y)\phi(y)ds_y + \\ &\quad + I^{-1}(x) \int_{\Gamma} T(\partial x)D_1(x, y)I(y)\phi(y)ds_y + g(x), \quad x \in \Gamma. \end{aligned} \quad (8.6)$$

The integrals on the left-hand side of (8.6) can be interpreted them in the sense of principal value, while the integrals on right-hand side are simply improper. Now, let

us establish the following result which will prove extremely useful later.

**Theorem 8.3.** *The trivial solution  $\phi_0 = 0$  is the only possible solution to the homogeneous system of integral equations (8.6)<sup>0</sup> (i.e. (8.6) with  $g \equiv 0$ ).*

*Proof.* Let  $\phi_0 \in C^{1,\alpha}(\Gamma)$  be a solution of (8.6)<sup>0</sup>. Then,

$$(V\phi_0)_I(x) = \int_{\Gamma} [D(x,y) - D_1(x,y)] I(y) \phi_0(y) ds_y$$

is a solution of the homogeneous interior problem (8.4)<sub>I</sub><sup>0</sup> (i.e. (8.4)<sub>I</sub> with  $g \equiv 0$ ). Moreover, by Theorem 8.1  $(V\phi_0)_I(x) = 0$ ,  $x \in S$ . Recall that  $(V\phi_0)_I(x) \in C(\bar{S})$ , so that it is continuous up to the boundary  $\partial S$ , particularly up to the reinforcement  $\Gamma$  so that  $(V\phi_0)_I(x) = 0$ ,  $x \in \Gamma$ .

Next, using the definition of the matrix  $D_1(x,y)$ , we can formulate the interior Dirichlet boundary value problem

$$\begin{aligned} L(\partial x)(V\phi_0)_I(x) &= 0, & x \in \Omega_I \setminus S, \\ (V\phi_0)_I(x) &= 0, & x \in \partial\Omega_I \setminus \partial S, \\ (V\phi_0)_I(x) &= 0, & x \in \Gamma. \end{aligned}$$

This problem has a unique solution (see [92] for the proof) and it means that  $(V\phi_0)_I(x) = 0$  in the bounded domain  $\Omega_I \setminus S$ , on the inner part of the boundary  $\Gamma$  particularly.

Summarizing, we have shown that  $(V\phi_0)_I$  vanishes on both sides of the boundary  $\Gamma$ . If we will apply the boundary operator to a single layer potential on  $\Gamma$  we will arrive at

$$(TV)_I^+(\phi_0) - (TV)_I^-(\phi_0) = \phi_0 = 0,$$

which is the desired conclusion. □

## 8.2.2 Unbounded domain

To construct the solution for the exterior boundary value problem we should take into account the behavior of the solution at the infinity and use the following matrix  $M^\infty(x) \in \mathcal{M}_{3 \times 3}$  given in terms of polar coordinates by [102]

$$M^\infty(\tilde{r}, \tilde{\theta}) = \pi[4\alpha^2(\mu + \alpha)(\gamma + \kappa)(2\gamma + \beta)]^{-1} \begin{pmatrix} 0 & 0 & \tilde{r}^{-1} \sin \tilde{\theta} \\ 0 & 0 & -\tilde{r} \sin \theta \\ 0 & 0 & 2 \ln \tilde{r} \end{pmatrix}.$$

It can be shown that  $LM^\infty = 0$  in  $\mathbb{R}^2 \setminus \{0\}$ .

We wish to find the solution of the boundary value problem (8.4)<sub>E</sub> which is of the form of the generalized single layer potential:

$$u(x) = (V\phi)_E(x) = \int_{\Gamma} [\Psi(x, y) - D_2(x, y)] I(y) \phi(y) ds_y, \quad x \in S, \quad (8.7)$$

Here  $\phi \in \mathcal{M}_{3 \times 1}$  is an unknown vector density of the Holder class  $C^{1,\alpha}(\Gamma)$ ,  $\alpha \in (0, 1)$ , defined on  $\Gamma$ ,  $\Psi \in \mathcal{M}_{3 \times 3}$  is the smooth matrix given by

$$\Psi(x, y) = D(x, y) - M^\infty(x)F^T(y)$$

and the columns  $D_2^{(\alpha)}$  of matrix  $D_2(x, y) \in \mathcal{M}_{3 \times 3}$ ,  $y = (y_1, y_2) \in \Gamma$  are constructed to satisfy the following classical mixed boundary value problem. Let  $\Omega_E$  be the multiply-connected unbounded domain with sufficiently smooth boundary  $\partial\Omega_E$  so that  $S \in \Omega_E$ ,

$\Gamma \in \Omega_E$ ,  $\partial S_u \cup \partial S_t \subseteq \partial\Omega_E$ ,  $\{0\} \notin \overline{\Omega_E}$ . Then

$$\begin{aligned} L(\partial x)D_2^{(\alpha)}(x, y) &= 0, \quad x \in \Omega_E, \\ T(\partial x)D_2^{(\alpha)}(x, y) &= T(\partial x)\Psi^{(\alpha)}(x, y), \quad x \in \partial S_t, \\ D_2^{(\alpha)}(x, y) &= \Psi^{(\alpha)}(x, y), \quad x \in \partial\Omega_E \setminus \partial S_t. \end{aligned}$$

From the existence result for the exterior mixed problem for the anti-plane deformation in micropolar elasticity (see [91] for the proof) it is possible to show that that  $D_2(x, y)(\alpha)$  exists uniquely for each  $y \in \Gamma$  in the class  $C^2(\Omega_E) \cap C^1(\overline{\Omega_E} \setminus \{a, b\}) \cap \mathcal{A}^*$ .

Also, it can be seen that  $(V\phi)_E(x)$  satisfies all conditions of the problem (8.4)<sub>E</sub> except the requirement  $(V\phi)_E \in \mathcal{A}^*$  and condition on  $\Gamma$ . The fact that  $(V\phi)_E \in \mathcal{A}^*$  can be proved as follows.

It can be stated that

$$\begin{aligned} \int_{\Gamma} \Psi(x, y)I(y)\phi(y)ds_y &= \int_{\Gamma} D(x, y)I(y)\phi(y)ds_y - M^\infty(x) \int_{\Gamma} F^T(y)I(y)\phi(y)ds_y = \\ &= u_0 \in \mathcal{A}, \\ \int_{\Gamma} D_2(x, y)I(y)\phi(y)ds_y &= \int_{\Gamma} D_2^\alpha(x, y)(I\phi)_\alpha(y)ds_y \in \mathcal{A}^*, \end{aligned}$$

the latter one is valid as  $D_2^{(\alpha)} \in \mathcal{A}^*$  for all  $y \in \Gamma$ . Therefore  $u$  given by (8.7) is of class  $\mathcal{A}^*$ .

The remaining reinforcement condition is given by a system of integral equation:

$$\begin{aligned}
& \frac{1}{2}\phi(x) + I^{-1}(x) \int_{\Gamma} T(\partial x)D(x, y)I(y)\phi(y)ds_y + \\
& \quad + hR^*(d_x) \int_{\Gamma} I^{-1}(x)D(x, y)I(y)\phi(y)ds_y = \\
& = hR(d_x) \int_{\Gamma} I^{-1}(x)[M^\infty(x)F^T(y) + D_2(x, y)]I(y)\phi(y)ds_y - \\
& \quad - hR_0I^{-1}(x) \int_{\Gamma} [D(x, y) - \Psi(x, y)]I(y)\phi(y)ds_y + \quad (8.8) \\
& + I^{-1}(x) \int_{\Gamma} T(\partial x)[M^\infty(x)F^T(y) + D_2(x, y)]I(y)\phi(y)ds_y + g(x), \quad x \in \Gamma.
\end{aligned}$$

Again, we interpret the integrals on the left-hand side of (8.8) in the sense of principal values, while the integrals on the right-hand side do not affect the solvability analysis. Now, let us establish the following result which will be needed later.

**Theorem 8.4.** *The trivial solution  $\phi_0 = 0$  is the only possible solution to the homogeneous system of integral equations (8.8)<sup>0</sup> (i.e. (8.8) with  $g \equiv 0$ ).*

*Proof.* Let  $\phi_0 \in C^{1,\alpha}(\Gamma)$  be a solution of (8.8)<sup>0</sup>. Then,

$$(V\phi_0)_E(x) = \int_{\Gamma} [\Psi(x, y) - D_2(x, y)]I(y)\phi_0(y)ds_y$$

is a solution of the homogeneous interior problem (8.4)<sub>E</sub><sup>0</sup> (i.e. (8.4)<sub>E</sub> with  $g \equiv 0$ ). We can now proceed analogously to the proof of Theorem 8.3 and show that  $(V\phi_0)_E$  vanishes on both sides of the boundary  $\Gamma$ . If we will apply the boundary operator to a

single layer potential on  $\Gamma$  we will arrive at

$$(TV)_E^+(\phi_0) - (TV)_E^-(\phi_0) = \phi_0 = 0,$$

which is the desired conclusion. □

### 8.3 Analysis of the resulting systems of singular integro-differential equations arising from the proposed model

In the previous sections we have reduced each of the boundary value problems  $(8.4)_I$  and  $(8.4)_E$  to the following system of integral equations (general form of the corresponding systems (8.6) and (8.8))

$$\begin{aligned} & \frac{1}{2}\phi(x) + I^{-1}(x) \int_{\Gamma} T(\partial x)D(x, y)I(y)\phi(y)ds_y + hR^*(d_x)\tilde{D} \cdot \\ & \cdot \int_{\Gamma} [I^{-1}(x)\ln|x-y|]I(y)\phi(y) = \int_{\Gamma} \Lambda(x, y)\phi(y)ds_y + g(x), \quad x \in \Gamma. \end{aligned} \quad (8.9)$$

For the interior boundary value problem and system (8.6)

$$\Lambda(x, y) = hR(d_x)I^{-1}(x)D_1(x, y) - hR_0I^{-1}(x)D(x, y) + I^{-1}(x)T(\partial x)D_1(x, y),$$

while for the exterior boundary value problem and system (8.8)

$$\begin{aligned}\Lambda(x, y) = & hR(d_x)I^{-1}(x)[M^\infty(x)F^T(y) + D_2(x, y)] - hR_0I^{-1}(x)[D(x, y) - \\ & - \Psi(x, y)] + I^{-1}(x)T(\partial x)[M^\infty(x)F^T(y) + D_2(x, y)].\end{aligned}$$

Now, we wish to analyze the system (8.9) by opening up every term and making a decision on the appropriate existence theory.

From the definition of matrices  $D_1(x, y)$ ,  $D_2(x, y)$ ,  $M^\infty(x)$ ,  $F^T(y)$  and properties of the matrix of fundamental solutions  $D(x, y)$  (accompanied with the coefficient matrix  $R_0$  only) it can be deduced that  $\Lambda(x, y)$  is a matrix with weak singularities, so that the integral on the right-hand side of (8.9) is improper and does not affect the existence theory.

As before, let us investigate the remaining terms on the left-hand side of (8.9) in complex form, so that again  $x = x_1 + ix_2$ ,  $y = y_1 + iy_2$ .

The first integral on the left-hand side of (8.9) was investigated in [91]:

$$I^{-1}(x) \int_{\Gamma} T(\partial x)D(x, y)\phi(y)ds_y = -p e_{\gamma\beta}E_{\gamma\beta} \int_{\Gamma} \frac{\phi(y)}{x - y} dy,$$

where

$$p = \frac{(\gamma + \kappa)(\gamma - \kappa) - \beta(2\gamma + \beta)}{2(\gamma + \kappa)(2\gamma + \beta)}, \quad e_{\gamma\beta}E_{\gamma\beta} = \begin{pmatrix} 0 & 1 & 0 \\ -1 & 0 & 0 \\ 0 & 0 & 0 \end{pmatrix}.$$

Our next objective is to evaluate the second integral on the left-hand side of (8.9) was analyzed in [59]. It can be shown that

$$\begin{aligned} \int_{\Gamma} d_x[I^{-1}(x) \ln|x-y| I(y)\phi(y)]ds_y &= \int_{\Gamma} \frac{\phi(y)}{x-y} dy + \int_{\Gamma} K_1(x,y)\phi(y)ds_y, \\ \int_{\Gamma} d_x^2[I^{-1}(x) \ln|x-y| I(y)\phi(y)]ds_y &= e^{i\theta(x)} \int_{\Gamma} \frac{\phi'(y)}{x-y} dy + \\ &+ d_x\theta(x)e_{\gamma\beta}E_{\gamma\beta} \int_{\Gamma} \frac{\phi(y)}{x-y} dy + \int_{\Gamma} K_2(x,y)\phi(y)ds_y, \end{aligned}$$

so that now (8.9) can be written as a system of singular integro-differential equations:

$$\begin{aligned} \frac{1}{2}\phi(x) + M_0(x) \int_{\Gamma} \frac{\phi(y)}{x-y} dy + M_1(x) \int_{\Gamma} \frac{\phi'(y)}{x-y} dy &= \int_{\Gamma} K(x,y)\phi(y)ds_y + \\ &+ g(x), \quad x \in \Gamma. \end{aligned} \quad (8.10)$$

Here  $K_1(x,y)$ ,  $K_2(x,y)$ ,  $K(x,y)$  are matrices with weak singularities and the matrices  $M_0(x)$ ,  $M_1(x) \in \mathcal{M}_{3 \times 3}$  associated with strongly singular terms are given by the following expressions

$$M_0(x) = -\frac{p}{2\pi} e_{\gamma\beta}E_{\gamma\beta} + h(R_1 + R_2 d_x\theta(x)e_{\gamma\beta}E_{\gamma\beta})\tilde{D}, \quad M_1(x) = e^{i\theta(x)}hR_2\tilde{D}.$$

The main difficulty in considering the system (8.10) is that it is not well adapted to the classical existence theory for singular integro-differential equations [84, 83]. The reason for that is that (8.10) has a too complicated form caused by the reinforcement boundary condition. Nevertheless, it is still possible to write it in a simpler form, for which existence can be proved. To do this, let us introduce a vector  $\rho \in \mathcal{M}_{5 \times 1}$  with

components

$$\rho_1 = \varphi_1, \quad \rho_2 = \varphi_2, \quad \rho_3 = w, \quad \rho_4 = \varphi_2', \quad \rho_5 = w'.$$

Then we can re-write (8.10) as

$$A(x)\rho(x) + \frac{1}{\pi i} \int_{\Gamma} \frac{B(x, y)\rho(y)}{y - x} = \int_{\Gamma} K^*(x, y)\rho(y)ds_y + T(x), \quad (8.11)$$

where

$$A(x) = \begin{pmatrix} \frac{1}{2} & 0 & 0 & 0 & 0 \\ 0 & \frac{1}{2} & 0 & 0 & 0 \\ 0 & 0 & \frac{1}{2} & 0 & 0 \\ 0 & 0 & 0 & 0 & 0 \\ 0 & 0 & 0 & 0 & 0 \end{pmatrix},$$

$$B(x) = -\pi i \cdot$$

$$\begin{pmatrix} 0 & -\frac{p}{2\pi} & 0 & 0 & 0 \\ \frac{p + bhd_x\theta(x)(\bar{\gamma} + \bar{\kappa})}{2\pi} & 0 & \frac{h\bar{\alpha}}{\pi(\mu + \alpha)} & 0 & 0 \\ 0 & -\frac{h\bar{\alpha}b}{\pi} & 0 & 0 & 0 \\ 0 & 0 & 0 & -\frac{he^{i\theta(x)}b(\bar{\gamma} + \bar{\kappa})}{2\pi} & 0 \\ 0 & 0 & 0 & 0 & -\frac{he^{i\theta(x)}(\bar{\mu} + \bar{\alpha})}{2\pi(\mu + \alpha)} \end{pmatrix},$$

$K^*(x, y)$  is a matrix with weak singularities and  $T(x)$  involves components of  $g(x)$ .

Clearly, the systems (8.10) and (8.11) are equivalent.

For (8.11) we can show that the index of the singular integral operator from (2.4)  $\kappa = 0$  and  $\det(A \pm B) \neq 0$  everywhere on  $\Gamma$ . This therefore by Noether's theorem makes

it legitimate to apply Fredholm's theorems to (8.11) and its corresponding adjoint equation, so that now we are in positions to establish and prove the following theorems.

**Theorem 8.5.** *If  $g \in C^{0,\alpha}(\Gamma)$ ,  $0 < \alpha < 1$ , then a density  $\phi \in C^{1,\alpha}(\Gamma)$ ,  $0 < \alpha < 1$  is the unique solution of the system of singular integro-differential equations (8.6) and a modified single-layer potential (8.5) containing this density is the unique solution of the interior boundary value problem (8.4)<sub>I</sub>.*

*Proof.* On account of the above results, the index of the corresponding singular operator from (8.11) is equal to zero. Hence, Fredholm's theorems hold for (8.11) and its adjoint system. Moreover, since systems (8.6) and (8.11) are equivalent, from Theorem 8.3 we deduce that homogeneous system (8.11)<sup>0</sup> (i.e. (8.11) with  $T(x) = 0$ ) has the only solution  $\rho^0 \in C^{0,\alpha}(\Gamma)$ ,  $0 < \alpha < 1$  and this solution is trivial. We thus can conclude from Fredholm's theorems that  $\rho \in C^{0,\alpha}(\Gamma)$ ,  $0 < \alpha < 1$  is the unique solution of (8.11), provided  $T \in C^{0,\alpha}(\Gamma)$ ,  $0 < \alpha < 1$ . It follows immediately that  $\phi \in C^{1,\alpha}(\Gamma)$ ,  $0 < \alpha < 1$  is the unique solution of (8.6), provided  $g \in C^{0,\alpha}(\Gamma)$ ,  $0 < \alpha < 1$ .

We are now in the position to establish that (8.4)<sub>I</sub> is uniquely solvable. Indeed, with  $\phi \in C^{1,\alpha}(\Gamma)$  vector-function  $u$  from (8.5) satisfies all conditions of the problem (8.4)<sub>I</sub>, including the highly non-standard reinforcement boundary condition. Therefore, by the uniqueness Theorem 8.1, it represents the only solution of the interior boundary value problem (8.4)<sub>I</sub>, which completes the proof. □

**Theorem 8.6.** *If  $g \in C^{0,\alpha}(\Gamma)$ ,  $0 < \alpha < 1$ , then a density  $\phi \in C^{1,\alpha}(\Gamma)$ ,  $0 < \alpha < 1$  is the unique solution of the system of the singular integro-differential equations (8.8) and a modified single-layer potential (8.7) containing this density is the unique solution of the exterior boundary value problem (8.4)<sub>E</sub>.*

*Proof.* The theorem may be proved in much the same way as Theorem 8.5.  $\square$

To conclude, we have considered a comprehensive model of anti-plane deformations of a solid which takes into account both the surface and microstructural effects. Despite its mathematical complexity, we could perform the model's well-posedness analysis and have demonstrated that the solution to the corresponding boundary-value problems exists uniquely. These findings provide evidence of the proposed model's reliability. Moreover, we regard these as the core results of the research. The results derived in Part I were necessary to provide an insight on how to tackle well-posedness analysis for the surface reinforcement model enhanced with micropolar mechanics.

Now, after having achieved the primary objective of the current research, we want to provide a justification of the model's effectiveness for the example of a semi-infinite crack in a micro-featured solid with surface effect. As was stated in Chapter 1, this demonstration of the surface effect contribution is difficult but can be adequately shown using the couple stress theory, particular case of the micropolar theory. Indeed, the couple stress theory is preferable for many applications since it is less complicated, easier to be verified experimentally and also reflects micro-features of real materials as well as the micropolar theory. That is why it is chosen to serve as a test theory for the demonstration of the microstructural and surface effects' contribution to fracture mechanics; this analysis is presented in the following chapter.

---

## CHAPTER 9

# The contribution of micropolar surface effect to fracture mechanics

As before, we are going to justify that the proposed model incorporating both microstructural and surface effect can be used for the description of a real-life problem. In Part I we have studied the contribution of surface effect to classical linear elastic fracture mechanics. In this chapter we will go further and examine how the effect of microstructure can enhance the model incorporating the single surface effect.

In brief, we seek to combine both surface effects via a theory of couple stress boundary reinforcement and a Cosserat material model (incorporating couple stresses) of a bulk solid together in a more comprehensive model of deformation. Our motivation comes from three sets of results: firstly, the study from [72] and Chapter 6, in which the framework of classical linear elasticity is used to show that the addition of surface mechanics significantly improves several models of deformation used in classical linear elastic fracture mechanics (for example, the elimination of the oscillatory behavior of the stress field in the vicinity of an interface crack tip in a solid subjected to plane deformations); secondly, the results established by the authors in [95, 96] for a mode-III

crack in a couple stress elastic solid, demonstrating a strong singularity in the skew-symmetric stress distributions in the vicinity of the crack tip; and, finally, we desire to provide the reader with an illustrative example supporting the model proposed and examined in Chapters 7 and 8.

To this end, let us consider a semi-infinite crack in a couple stress elastic solid subjected to anti-plane deformation in which the crack incorporates couple stress boundary elasticity via a thin reinforcing film perfectly bonded to its crack faces. Asymptotic analysis will show that, in this case, the corresponding stress distributions established in [95] are bounded in the vicinity of the crack tip.

It should be noted that some passages in this chapter have been quoted verbatim from the author's publication [101].

## 9.1 Governing equations and reinforcement boundary conditions

A state of anti-plane shear in the micropolar solid is characterized by a displacement and microrotation fields of the form

$$\begin{aligned} u_1(x_1, x_2, x_3) = u_2(x_1, x_2, x_3) = 0, \quad u_3(x_1, x_2, x_3) = w(x), \\ \varphi_1(x_1, x_2, x_3) = \varphi_1(x), \quad \varphi_2(x_1, x_2, x_3) = \varphi_2(x), \quad \varphi_3(x_1, x_2, x_3) = 0, \end{aligned}$$

where the out-of-plane displacement  $w$  and in-plane microrotations  $\varphi_1, \varphi_2$  are functions of  $x$  on a cross-section  $S$  of the cylinder.

In the couple stress theory microrotations are no longer independent of the displace-

ment field but, in fact, are aligned with the usual continuum mechanics macrorotation of the body (one half of the curl of the displacement field) through the relation:

$$\varphi_i = \frac{1}{2}\epsilon_{ijk}u_{k,j}.$$

To this end, the governing equation of equilibrium for the anti-plane shear deformations is given in the bulk solid by a simple bi-harmonic equation [9]

$$\Delta w - l^2 \Delta \Delta w = 0, \quad (9.1)$$

where  $l^2 = \frac{\alpha}{\mu}$ .

In the case of isotropic couple stress elasticity the strain energy is a quadratic function  $W$  of the strain and curvature components [108]:

$$W(\varepsilon, \kappa) = \frac{1}{2}\lambda(\varepsilon_{kk})^2 + \mu\varepsilon_{ij}\varepsilon_{ij} + 2\alpha\kappa_{ij}\kappa_{ij} + 2\beta\kappa_{ij}\kappa_{ji},$$

where  $\kappa_{ij}$  are the components of the micro-strain tensor, defined in Chapter 2.

For this particular case of anti-plane shear, the non-zero components of the reduced traction and couple-stress traction in terms of displacement  $w$  are:

$$\begin{aligned} \mu \frac{\partial w}{\partial x_2} - \frac{\partial}{\partial x_2} \left[ (2\alpha + \beta) \frac{\partial^2 w}{\partial x_1^2} + \alpha \frac{\partial^2 w}{\partial x_2^2} \right] &= \tilde{p}_3, \\ 2\alpha \frac{\partial^2 w}{\partial x_2^2} - 2\beta \frac{\partial^2 w}{\partial x_1^2} &= \tilde{q}_1. \end{aligned}$$

Here  $\tilde{p}_3$ ,  $\tilde{q}_1$  represent the prescribed stresses and couple stresses on the reinforcement.

Assume that the bulk material undergoes anti-plane deformation but that part of

Fig. 9.1: Crack in a couple-stress linear, homogeneous and isotropic elastic solid without (a) and with surface effect (b) on its tips

its boundary is coated with a thin couple-stress elastic film with thickness  $h$  perfectly bonded to the bulk and henceforth referred to as a reinforcement. Accordingly, the reinforcement is represented by a thin plate with material parameters of shear type  $\bar{\lambda}$ ,  $\bar{\mu}$ ,  $\bar{\alpha}$ ,  $\bar{\beta}$ , whose displacement field at any cross section is characterized by  $w = u_3(x_1)$

Equilibrium of the reinforcement now requires that

$$\frac{\partial \sigma_{13}}{\partial x_1} + F_3 = 0, \quad \frac{\partial m_{12}}{\partial x_1} + e_{213}\sigma_{13} + e_{231}\sigma_{31} + C_2 = 0,$$

with the body force component  $F_3$  acting in the axial direction and the body couple component  $C_2$  along the outward unit normal  $n$  to the plate. In terms of the displacement field  $w$  of the plate, we can write:

$$F_3 = -\bar{\mu} \frac{\partial^2 w}{\partial x_1^2} + \bar{\alpha} \frac{\partial^4 w}{\partial x_1^4}, \quad C_2 = 0.$$

Thus, the reinforcement transmits the following stresses to the bulk:

$$-h\bar{\mu} \frac{\partial^2 w}{\partial x_1^2} + h\bar{\alpha} \frac{\partial^4 w}{\partial x_1^4}.$$

Taking into account the force transmitted by the reinforcement to the bulk, we arrive at the following (boundary) conditions for the bulk displacement field  $w$  on the

reinforced section of its boundary:

$$\begin{aligned} \mu \frac{\partial w}{\partial x_2} - \frac{\partial}{\partial x_2} \left[ (2\alpha + \beta) \frac{\partial^2 w}{\partial x_1^2} + \alpha \frac{\partial^2 w}{\partial x_2^2} \right] &= \tilde{p}_3 - h\bar{\mu} \frac{\partial^2 w}{\partial x_1^2} + h\bar{\alpha} \frac{\partial^4 w}{\partial x_1^4}, \\ 2\alpha \frac{\partial^2 w}{\partial x_2^2} - 2\beta \frac{\partial^2 w}{\partial x_1^2} &= \tilde{q}_1. \end{aligned}$$

## 9.2 The contribution of the microstructure to the crack with the surface effect on its tips

In Part I we have studied the effect of the surface on the crack in a classical linear, homogeneous and isotropic solid. In this chapter we will continue our investigations by incorporating the effect of microstructure on the crack faces and solid in an attempt to improve the existing results.

Let us consider the case of a mode-III crack in a couple-stress elastic solid in which the faces of the crack are coated by a thin reinforcing film of separate couple-stress elastic material. We assume that a semi-infinite crack extends along the negative  $x_1$  - *axis* of a Cartesian coordinate system  $(x_1, x_2)$  (so that the crack tip is located at the origin). Our particular interest lies in the case when the crack faces (described here by  $x_2 = 0$ ,  $x_1 < 0$  or in polar coordinates by  $\tilde{\theta} = \pi$ ,  $0 < \tilde{r} < \infty$ ) are reinforced with a thin solid film whose bending rigidity is taken to be negligible. Assume that on the crack faces ( $\tilde{\theta} = \pi$ ) the reinforcement transmits traction and vanishing couple stress traction as discussed above. Therefore, we have the following problem.

Find the displacement field  $w(\tilde{r}, \tilde{\theta})$  satisfying (9.1) in the bulk solid and the bound-

ary conditions

$$w = 0, \quad \alpha \frac{\partial^2 w}{\partial x_2^2} - \beta \frac{\partial^2 w}{\partial x_1^2} = 0, \quad (9.2)$$

when  $x_1 > 0$ ,  $x_2 = 0$  ( $\tilde{\theta} = 0$ ) and

$$\begin{aligned} \mu \frac{\partial w}{\partial x_2} - \frac{\partial}{\partial x_2} \left[ (2\alpha + \beta) \frac{\partial^2 w}{\partial x_1^2} + \alpha \frac{\partial^2 w}{\partial x_2^2} \right] &= -h\mu \frac{\partial^2 w}{\partial x_1^2} + h\alpha \frac{\partial^4 w}{\partial x_1^4}, \\ \alpha \frac{\partial^2 w}{\partial x_2^2} - \beta \frac{\partial^2 w}{\partial x_1^2} &= 0, \end{aligned} \quad (9.3)$$

when  $x_1 < 0$ ,  $x_2 = 0$  ( $\tilde{\theta} = \pi$ ).

To draw conclusions regarding the contribution of the reinforcement, we make comparisons with the results presented in [95] concerning the singularity of stresses near the crack tip for the same crack problem but in the absence of any reinforcement on the crack faces. To this end, we assume a polar coordinate system  $(\tilde{r}, \tilde{\theta})$  centered at the crack tip and seek the leading order solution as  $\tilde{r} \rightarrow 0$  in the following standard form:

$$w(\tilde{r}, \tilde{\theta}) = \tilde{r}^\lambda F_\lambda(\tilde{\theta}), \quad (9.4)$$

where  $\lambda > 0$  and  $F_\lambda$  are the eigenvalues and eigenfunctions to be determined. Negative values of  $\lambda$  are excluded in order to prevent the displacement field from the singular behavior as  $\tilde{r} \rightarrow 0$ . Retaining only leading order terms as  $\tilde{r} \rightarrow 0$ , the governing equation (9.1) yields the following ordinary differential equation for the unknown function  $F_\lambda(\tilde{\theta})$  [95]

$$F_\lambda''''(\tilde{\theta}) + 2(\lambda^2 - 2\lambda + 2)F_\lambda''(\tilde{\theta}) + \lambda^2(\lambda - 2)^2 F_\lambda(\tilde{\theta}) = 0$$

while the boundary conditions (9.2) and (9.3) result in the requirements that

$$\begin{aligned}
F_\lambda(0) &= 0, \\
F_\lambda''(0) &= 0, \\
\alpha F_\lambda''(\pi) + \lambda(\alpha + \beta - \beta\lambda)F_\lambda(\pi) &= 0, \\
F_\lambda(\pi)\lambda(\lambda - 1)(\lambda - 2)(\lambda - 3) &= 0.
\end{aligned} \tag{9.5}$$

As in [95], we find that for  $\lambda \neq 1$ ,

$$F_\lambda(\tilde{\theta}) = B_1 \sin \lambda \tilde{\theta} + B_2 \cos \lambda \tilde{\theta} + B_3 \sin[(\lambda - 2)\tilde{\theta}] + B_4 \cos[(\lambda - 2)\tilde{\theta}]. \tag{9.6}$$

Here  $B_1$ ,  $B_2$ ,  $B_3$  and  $B_4$  are constants to be determined with the help of boundary conditions. The first two boundary conditions in (9.5) (at  $\tilde{\theta} = 0$ ) require that  $B_2 = B_4 = 0$  while the remaining boundary conditions (at  $\tilde{\theta} = \pi$ ) indicate that non-trivial values of  $B_1$  and  $B_3$  exist if and only if  $\lambda = k$ , where  $k$  is an integer. In [95], a consideration of the corresponding  $J$ -integral reveals that boundedness of the flux of energy toward the crack tip requires  $\lambda \geq 3/2$ . We note further that the contribution of the surface mechanics to the  $J$ -integral, in turn, requires  $\lambda \geq 2$ . Thus, in both cases the first admissible value of  $\lambda$  is  $\lambda = 2$ .

When  $\lambda = 1$ , we find, as in [95], that

$$F_1(\tilde{\theta}) = (A_1 + A_2\tilde{\theta}) \sin \tilde{\theta} + (A_3 + A_4\tilde{\theta}) \cos \tilde{\theta}.$$

The first two boundary conditions of (9.5) at  $\tilde{\theta} = 0$  again (as in [95]) result in  $A_2 = A_3 = 0$ . The remaining boundary conditions (at  $\tilde{\theta} = \pi$ ) are satisfied identically. We

thus obtain that

$$F_1(\tilde{\theta}) = A_1 \sin \tilde{\theta} + A_4 \tilde{\theta} \cos \tilde{\theta},$$

with  $A_1$  and  $A_4$  arbitrary constants. We recall that we are interested only in solutions which maintain boundedness of the flux energy toward the crack tip. Consequently, if we wish to incorporate a contribution to the leading order terms from  $\lambda = 1$  to the asymptotic expansion of the displacement we must choose  $A_4 = 0$ , otherwise the term with  $A_4 \neq 0$  does not correspond to a rigid body motion [95]. Solutions corresponding to  $\lambda = 3$  and beyond do not contribute to the leading order solution.

Consequently, from (9.4), the leading order solution takes the form:

$$w(\tilde{r}, \tilde{\theta}) = A_1 \tilde{r} \sin \tilde{\theta} + B_1 \tilde{r}^2 \sin 2\tilde{\theta}.$$

The corresponding fields of interest are then:

$$\begin{aligned} \varphi_1 &= \frac{A_1}{2} + B_1 \tilde{r} \cos \tilde{\theta}, \\ \varphi_2 &= -B_1 \tilde{r} \sin \tilde{\theta}, \\ \sigma_{13} &= \sigma_{31} = 2\mu B_1 \tilde{r} \sin \tilde{\theta}, \\ \sigma_{23} &= \sigma_{32} = \mu(A_1 + 2B_1 \tilde{r} \cos \tilde{\theta}), \\ m_{11} &= -m_{22} = 4(\alpha + \beta)B_1. \end{aligned}$$

It can be seen that the corresponding stress distributions are bounded in the vicinity of the crack tip. For the case of the crack in the absence of the reinforcement [96] (see Figure 9.1), the corresponding asymptotic fields describing couple stresses and skew-

symmetric stresses have the following order:

$$m_{11} = O\left(\frac{1}{\sqrt{\tilde{r}}}\right), \quad \text{and} \quad \sigma_{[13]} = \sigma_{[23]} = O\left(\frac{1}{\sqrt{\tilde{r}^3}}\right) \text{ as } \tilde{r} \rightarrow 0.$$

Clearly, couple stresses display the square-root singularity, while the skew-symmetric part of the stresses show an even stronger type of singularity of order  $3/2$ . On the basis of these results it can be observed that the addition of surface mechanics via boundary reinforcement eliminates completely the singularity in the stresses near the crack tip indicating a more accurate and comprehensive model of deformation can be achieved in this way.

**Remark.** *There are several limiting cases arising from this problem which are of great interest. When the surface microstructural parameter  $\bar{\alpha}$  tends to zero in (9.3), we recover exactly the singular leading order solution from the corresponding problem studied in [95]. When both bulk and surface microstructural parameters  $l^2, \bar{\alpha} \rightarrow 0$ , the corresponding problem becomes analogous to that considered in [100] where it was found that the contribution of the surface effect is to introduce the possibility of a solution with weakened singularity of the logarithmic type near the crack tip: a solution which does not appear in the classical theory.*

To summarize, the model including both effects of surface and microstructure has proven efficient in solving the problem of semi-infinite crack with surface effect under the framework of couple stress theory, a simplified version of micropolar mechanics. In this problem, the contribution of the reinforcement to the stress distributions in the vicinity of the crack tip was investigated. This example demonstrated rather strikingly that the reinforcing film perfectly bonded to the crack faces eliminates the well-known

stress-singularity in the crack tip, so that the surface effect is, undoubtedly, worth including in the corresponding models. To this end, the model proposed in Chapter 7 appears to be of both theoretical and practical importance.

---

## CHAPTER 10

# Conclusions and future works

In this work we proposed a comprehensive model of anti-plane deformation by combining both the theory of boundary reinforcement and the micropolar material model of a bulk solid. Much attention was given to the discussion of physical assumptions of the model, while our main objective was to provide a rigorous proof of the model's mathematical adequacy. Coupling the mathematical complexity of the micropolar bulk model with micropolar surface mechanics was challenging; nevertheless, the following results were obtained:

- The corresponding interior and exterior mixed boundary-value problems were formulated and shown to have unique solutions in the appropriate function space. By assuming solutions in the form of modified single-layer potentials which have been adjusted to account for non-standard boundary reinforcement, boundary integral equation methods could be employed to reduce these boundary value problems to systems of singular integro-differential equations. Thorough analysis of these systems allowed for the existence of solutions to the proposed mixed boundary-value problems to be established. Thus, the model has proven reliable and well-posed.

- To demonstrate a significant advantage of this theory, the stress distributions in the vicinity of a semi-infinite crack tip was examined for a couple stress material (particular case of micropolar material) with surface reinforcement. Our results indicate that the reinforcing layer on the crack faces eliminates the well-known nonphysical stress singularity at the crack tip and thereby demonstrates the effectiveness of implementing surface and microstructural effects in continuum models.

A supplementary classical linear elastic analogue to the proposed model was analyzed and ultimately contributed to the solidification of the final derived results. This supplementary model neglects the microstructural effects but takes into account surface effects and therefore contains a highly non-standard boundary reinforcement condition. Although challenging, its mathematical treatment was beneficial since it gave us confidence in the mathematical model as a basis to develop a more generalized version involving microstructural effects as described above. The following results have been obtained in the analogue analysis:

- For the case of a reinforced boundary which is given by a set of closed curves in the cross-section of a classical linear elastic body, we have established the corresponding interior and exterior mixed boundary-value problems. A representation of the solutions in the form of modified single-layer potentials was used to reduce these problems to singular integro-differential equations from which unique solutions were proven to exist.
- Results were extended to the case of a reinforced boundary which is represented by a set of open curves in the cross-section of the body. For this problem we

must satisfy additional end-point conditions. To avoid complicated solvability conditions with no clear physical meaning, we have modified the boundary integral equation method using an equivalent (lower-order) reinforcement condition which led to the desired solvability results for the corresponding boundary value problems.

- To demonstrate the surface effect modeled as a reinforcing film for the supplementary linear elastic model, asymptotic analysis was performed for reinforced interface cracks. In contrast to the well-known classical results predicting a square-root singularity in the point of crack tip, it was found that the addition of reinforcement provides another possible solution which is characterized by a weaker logarithmic singularity.

To reiterate, these supplementary problems were vitally important as a simplified test for our approach before proving that the general micro-featured model with the surface effect was mathematically and physically adequate. The research presented in this work can serve as a stepping stone for numerous future research projects.

First of all, the proposed methods of analysis for highly non-standard boundary value problems and usage of modified potentials can be further employed in a variety of boundary-value problems arising in different theories such as classical elasticity, micropolar elasticity, thermoelasticity, and piezoelectricity. For example, well-posedness analysis of boundary value problems describing plane stress deformations of a micropolar solid with the surface effect have not been tackled. Another interesting example would be the boundary value problem arising for the torsion of a micro-featured solid with reinforced boundaries.

Secondly, only static problems have been considered in the current work. The addition of dynamics, even the simple case of forced oscillations, would result in the emergence of more difficult boundary value problems. It would be interesting to analyze dynamic boundary value problems on well-posedness and determine if the modified boundary integral equation approaches are still valid.

Last but not least, further research is needed for problems which include multiple media. An interesting problem occurs when considering interface effects between two different materials. This model and its rigorous mathematical treatment could advance our understanding of composite materials and many biological solids.

---

# Bibliography

- [1] Voigt, W.: Theoretische Studien über die Elastizitätsverhältnisse der Kristalle, Dieterichsche Verlags-buchhandlung, Göttingen (1887)
- [2] Cosserat, E., Cosserat, F.: Théorie des corps déformables. A. Hermann et fils, Paris (1909)
- [3] Schaefer, H.: Das Cosserat kontinuum. Z. Angew. Math. Mech. **47**, 485–498 (1967)
- [4] Truesdell, C., Toupin, R.A.: The classical field theories. Encyclopedia of Physics **3(1)**, Springer, Berlin (1960)
- [5] Rajagopal, E.S.: The existence of interfacial couples in infinitesimal elasticity. Ann. der Physik **6**, 192–201 (1960)
- [6] Toupin, R.A.: Elastic materials with couple-stresses. Arch. Ration. Mech. Anal. **11**, 385–414 (1962)
- [7] Mindlin, R.D., Tiersten, H.F.: Effects of couple-stresses in linear elasticity. Arch. Ration. Mech. Anal. **11**, 415–488 (1962)
- [8] Koiter, W.T.: Couple stresses in the theory of elasticity, I and II. Proc. Ned. Akad. Wet. B. **67**, 17–44 (1964)

- [9] Hadjesfandiari, A.R., Dargush, G.F.: Couple stress theory for solids, *Int. J. Solids Struct.* **50**, 1253–1265 (2013)
- [10] Eringen, A.C.: Linear theory of micropolar elasticity. *J. Math. Mech.* **15**, 909–923 (1966)
- [11] Eringen, A.C.: Theory of Micropolar Elasticity. In: Liebowitz, H. (ed.) *Fracture* **2**, 621–729. Academic Press, New York (1968)
- [12] Nowacki, W.: *Theory of Asymmetric Elasticity*. Polish Scientific, Warsaw (1986)
- [13] Schijve, J.: Note on Couple Stresses. *J. Mech. Phys. Solids.* **14**, 113–120 (1966)
- [14] Gauthier, R.D., Jahsman, W.E.: Quest for micropolar elastic-constants. *J. Appl. Mech. Tran. ASME* **42(2)**, 369–374 (1975)
- [15] Lakes, R.S.: Dynamical study of couple stress effects in human compact bone. *J. Biomech. Eng.* **104**, 6–11 (1981)
- [16] Yang, J.F.C., Lakes, R.S.: Experimental study of micropolar and couple stress elasticity in compact bone in bending. *J. Biomech.* **15**, 91–98 (1982)
- [17] Lakes, R.S.: Size effects and micromechanics of a porous solid. *J. Mat. Sci.* **18**, 2572–2580 (1983)
- [18] Lakes R. Experimental Microelasticity of Two Porous Solids. *Int. J. Solids Struct.* **22(1)**, 55–63 (1986)
- [19] Park, H.C., Lakes, R.S.: Cosserat micromechanics of human bone: strain redistribution by a hydration sensitive constituent. *J. Biomech.* **19**, 385–397 (1986)

- [20] Lakes, R., Nakamura, S., Behiri, J., Bonfield, W.: Fracture mechanics of bone with short cracks. *J. Biomech.* **23**, 967–975 (1990)
- [21] Lakes R. Experimental Micro Mechanics Methods for Conventional and Negative Poisson’s Ratio Cellular Solids as Cosserat Continua. *J. Eng. Mater. Techn.* **113(1)**, 148–155 (1991)
- [22] Lakes, R.: Experimental methods for study of Cosserat elastic solids and other generalized elastic continua. In: Muhlhaus, H.B. (ed.) *Continuum Models for Materials with Microstructure*, 1-22. Wiley, New York (1995)
- [23] Li, L., Xie, S.: Finite element method for linear micropolar elasticity and numerical study of some scale effects phenomena in MEMS. *Int. J. Mech. Sci.* **46**, 1571–1587 (2004)
- [24] Walsh, S.D.C., Tordesillas, A.: Finite element methods for micropolar models of granular materials. *Appl. Math. Model.* **30(10)**, 1043–1055 (2006)
- [25] Gomez, J., Basaran, C.: Computational implementation of Cosserat continuum. *Int. J. Mater. Prod. Techn.* **34**, 3–36 (2009)
- [26] Chróscielewski, J., Witkowski, W.: FEM analysis of Cosserat plates and shells based on some constitutive relations. *Z. Angew. Math. Mech.* **91(5)**, 400–412 (2011)
- [27] Sargsyan, A.H., Sargsyan, S.H.: Dynamic model of micropolar elastic thin plates with independent fields of displacements and rotations. *J. Sound Vib.* **33(18)**, 4354–4375 (2014)

- [28] Freund, J., Karakoc, A., Sjolund, J.: Computational homogenization of regular cellular material according to classical elasticity. *Mech. Mater.* **78**, 56–65 (2014)
- [29] Altenbach H., Maugin G.A., Erofeev V.: *Mechanics of Generalized Continua*. Springer, Heidelberg (2011)
- [30] Eremeyev V.A., Lebedev L.P., Altenbach H.: *Foundations of Micropolar Mechanics*. Springer, Heidelberg (2013)
- [31] Ellis, R.W., Smith, C.W.: A thin-plate analysis and experimental evaluation of couple-stress effects. *Exp. Mech.* **7(9)**, 372–380 (1967)
- [32] Suiker, A.S.J., De Borst, R., Chang, C.S.: Micro-mechanical modelling of granular material. Part 1: Derivation of a second-gradient micro-polar constitutive theory. *Acta Mech.* **149**, 161–180 (2001)
- [33] Liu, Q.P., Liu X.Y., Li, X.K., Li S.H.: Micro-macro homogenization of granular materials based on the average-field theory of Cosserat continuum. *Adv. Powder Technol.* **25(1)**, 436–449 (2014)
- [34] Hill, J.M., Selvadurai, A.P.S.: *Mathematics and Mechanics of Granular Materials*. *J. Eng. Math.* **52**, 1–9 (2005)
- [35] Liu, S., Su, W.: Effective couple-stress continuum model of cellular solids and size effects analysis. *Int. J. Solid. Struct.* **46**, 2787–2799 (2009)
- [36] Arzt, E.: Size effects in materials due to microstructural and dimensional constraints: a comparative review. *Acta Mater.* **46(16)**, 5611–5626 (1998)

- [37] Mindlin, R. D.: Influence of couple-stresses on stress-concentrations. *Exp. Mech.* **3**, 1–7 (1963)
- [38] Cowin, S.C.: Singular stress concentrations in plane Cosserat elasticity. *Z. Angew. Math. Phys.* **20**, 979–982 (1969)
- [39] Ariman, T.: On the Stresses Around a Circular Hole in Micropolar Elasticity. *Acta Mech.* **3**, 216–229 (1967)
- [40] Fatemi, J., Van Keulen, F., Onck, P.R.: Generalized continuum theories: Application to stress analysis in bone. *Meccanica* **37**, 385–396 (2002)
- [41] Andrews, E.W., Gioux, G., Onck, P., Gibson, L.J.: Size effects in ductile cellular solids. II. Experimental results. *Int. J. Mech. Sci.* **43**, 701–713 (2001)
- [42] Ericksen, J.L., Truesdell, C.: Exact theory of stress and strain in rods and shells. *Arch. Rational Mech. Anal.* **1**, 295–323 (1958)
- [43] Altenbach, J., Altenbach, H., Eremeyev V.A.: On generalized Cosserat-type theories of plates and shells: a short review and bibliography. *Arch. Appl. Mech.* **80(1)**, 73–92 (2010)
- [44] Lukaszewicz, G.: *Micropolar Fluids: Theory and Applications*. Birkhauser, Boston (1999)
- [45] Gibbs, J.W.: *The Scientific Papers of J. Willard Gibbs*. In Bumstead, H.A., Van Name, R.G. (ed.) *Thermodynamics* **1**. Longmans & Co, London (1906)

- [46] Cherkaoui, M., Capolungo, L.: Atomistic and continuum modeling of nanocrystalline materials: Deformation mechanisms and scale transition. Springer, New York (2009)
- [47] Pomeau, E., Villiermaux, E.: Two Hundred Years of Capillarity Research. *Phys. Today* **59(3)**, 39–44 (2006)
- [48] Lennard-Jones, J.E., Dent, B.M.: The Change in Lattice Spacing at a Crystal Boundary. *Proc. R. Soc. London Ser. A* **121(787)**, 247–259 (1928)
- [49] Shuttleworth, R.: The surface tension of solids. *Proc. Phys. Soc. London Sect. A* **63**, 444–457 (1950)
- [50] Cammarata, R.C.: Surface and interface stress effects on interfacial and nanostructured materials. *Mater. Sci. Eng. A* **237(2)**, 180–184 (1997)
- [51] Cuenot, S., Fretigny, C., Champagne, S.D., Nysten, B.: Surface tension effect on the mechanical properties of nanomaterials measured by atomic force microscopy. *Phys. Rev. B* **69**, 165410–165414 (2006)
- [52] Zhang, W.X., Wang, T.J., Chen, X.: Effect of surface stress on the asymmetric yield strength of nanowires. *J. Appl. Phys.* **103**, 123527 (2008)
- [53] Ebnesajjad, S., Ebnesajjad, C.: *Surface Treatment of Materials for Adhesive Bonding*. William Andrew Pub., Norwich, NY (2013)
- [54] Müller, P., Saúl, A., Leroy, F.: Simple views on surface stress and surface energy concepts. *Adv. Nat. Sci.: Nanosci. Nanotechnol.* **5**, 013002 (2014)

- [55] Gurtin, M.E., Murdoch, A.: A continuum theory of elastic material surfaces. *Arch. Ration. Mech. An.* **57**, 291–323 (1975)
- [56] Gurtin, M.E., Weissmuller, J., Larche, F.: A general theory of curved deformable interface in solids at equilibrium. *Philos. Mag. A* **78**, 1093–1109 (1998)
- [57] Ru, C.Q.: Simple geometrical explanation of Gurtin-Murdoch model of surface elasticity with clarification of its related versions. *Sci. China* **53**, 536–544 (2010)
- [58] Steigmann, D.J., Ogden, R.W.: Plane deformations of elastic solids with intrinsic boundary elasticity. *Proc. R. Soc. London Sect. A* **453**, 853–877 (1997)
- [59] Schiavone, P., Ru, C.Q.: Integral Equation Methods in Plane-Strain Elasticity with Boundary Reinforcement. *Proc. R. Soc. London Sect. A* **454**, 2223–2242 (1998)
- [60] Miller, R.E., Shenoy, V.B.: Size-dependent elastic properties of nanosized structural elements. *Nanotechnology* **11(3)**, 139–147 (2000)
- [61] Altenbach, H., Morozov, N.F.: *Surface Effects in Solid Mechanics: Models, Simulations and Applications*. Springer, Berlin (2013)
- [62] Yang, F.Q.: Size-dependent effective modulus of elastic composite materials: spherical nanocavities at dilute concentrations. *J. Appl. Phys.* **95**, 3516–3520 (2004)
- [63] Chen, T., Dvorak, G.J., Yu, C.C.: Size-dependent elastic properties of unidirectional nano-composites with interface stresses. *Acta Mech.* **188**, 39–54 (2007)

- [64] Zhang, W.X., Wang, T.J.: Effect of surface energy on the yield strength of nanoporous materials. *Appl. Phys. Lett.* **90**, 063104 (2007)
- [65] Wang, J., Huang, Z.P., Karihaloo, B.L.: Size-dependent effective elastic constants of solids containing nano-inhomogeneities with interface stress. *J. Mech. Phys. Solids* **53(7)** 1574–1596 (2005)
- [66] Mi, C.W., Kouris, D.A.: Nanoparticles under the influence of surface/interface elasticity. *J. Mech. Mater. Struct.* **1**, 763–791 (2006)
- [67] Wang, G.F., Wang, T.J., Feng, X.Q.: Surface effects on the diffraction of plane compressional waves by a nanosized circular hole. *Appl. Phys. Lett.* **89**, 231923 (2006)
- [68] Fang, X.O., Zhang, L.L., Liu, J.X., Feng W.J.: Surface/Interface Effect on Dynamic Stress Around a Nanoinclusion in a Semi-Infinite Slab Under Shear Waves. *J. Vib. Acoust.* **134(6)**, 061011 (2012)
- [69] Wang, X., Schiavone, P. Role of surface effects in the finite deformation of an elastic solid with elliptical hole. *Int. J. of Nonlinear Mech.* **54**, 1–4 (2013)
- [70] Grekov, M.A., Yazovskaya, A.A.: The effect of surface elasticity and residual surface stress in an elastic body with an elliptic nanohole. *J. Appl. Math. Mech.* **78(2)**, 172–180 (2014)
- [71] Antipov, Y.A., Schiavone, P.: Integro-differential equation for a finite crack in a strip with surface effects. *Q. J. Mech. Appl. Math.* **64**, 87–106 (2011)

- [72] Kim, C.I., Ru, C.Q., Schiavone, P.: A Clarification of the Role of Crack-tip Conditions in Linear Elasticity with Surface Effects. *Math. Mech. Solids* **18**(1) 59–66 (2013)
- [73] Hosseini-Hashemi, S., Fakher, M., Nazemnezhad, R., Sotoude Haghghi, M.H.: Dynamic behavior of thin and thick cracked nanobeams incorporating surface effects. *Compos. Part B-Eng.* **61**, 66–72 (2014)
- [74] Dingreville, R., Qu, J., Cherkaoui, M.: Surface free energy and its effect on the elastic behavior of nano-sized particles, wires and films. *J. Mech. Phys. Solids* **53**, 1827–1854 (2005)
- [75] Lachut, M.J., Sader, J.E: Effect of surface stress on the stiffness of thin elastic plates and beams. *Phys. Rev. B* **85**, 085440 (2012)
- [76] Chen, H., Hu, G.K., and Huang, Z.P.: Effective moduli for micropolar composite with interface effect. *Int. J. Solids Struct.* **44**, 8106–8118 (2007)
- [77] Chen, H., Liu, X., Hu, G.: Overall plasticity of micropolar composites with interface effect. *Mech. Mater.* **40**, 721–728 (2008)
- [78] Gao, X.L. and Zhang, G.Y.: A microstructure- and surface energy-dependent third-order shear deformation beam model. *Z. Angew. Math. Phys.* (Accepted)
- [79] Shaat, M., Mahmoud, F.F., Gao, X.L., Faheem, A.F.: Size-dependent bending analysis of Kirchhoff nano-plates based on a modified couple-stress theory including surface effects. *Int. J. Mech. Sci.* **79**, 31–37 (2014)

- [80] Gao, X.L., Mahmoud, F.F.: A new Bernoulli-Euler beam model incorporating microstructure and surface energy effects. *Z. Angew. Math. Phys.* **65**, 393–404 (2014)
- [81] Salehi, S., Salehi, M.: Numerical investigation of nanoindentation size effect using micropolar theory. *Acta Mech.* **225**, 3365–3376 (2014)
- [82] Kupradze, V.D.: Potential methods in the theory of elasticity. IPST, Jerusalem (1965)
- [83] Vekua, N.P.: Systems of singular integral equations. Noordhoff, Groningen (1967)
- [84] Ishanov, R.S.: On a class of singular integro-differential equations. *Sov. Math. Dokl.* **1**, 529–532 (1960)
- [85] Gakhov, F.D.: Boundary Value Problems. Pergamon press, Oxford (1966)
- [86] Muskhelishvili, N.I.: Singular Integral Equations: Boundary Problems of Functions Theory and Their Applications to Mathematical Physics. Noordhoff, Leyden (1977)
- [87] Mikhlin, S.G., Prössdorf, S.: Singular Integral Operators. Springer, Berlin (1986)
- [88] Schiavone, P., Ru, C.Q.: The traction problem in a theory of plane strain elasticity with boundary reinforcement. *Math. Mech. S.* **5(1)**, 101–115 (2000)
- [89] Iesan, D.: Existence theorems in the theory of micropolar elasticity. *Int. J. Eng. Sci.* **8**, 777–791 (1970)
- [90] Schiavone, P.: Integral equation methods in plane asymmetric elasticity. *J. Elasticity* **43**, 31–43 (1996)

- [91] Potapenko, S., Schiavone, P., Mioduchowski, A.: On the Solution of Mixed Problems in Anti-Plane Micropolar Elasticity. *Math. Mech. Solids* **8**, 151–160 (2003)
- [92] Potapenko, S., Schiavone, P., Mioduchowski, A.: Anti-Plane Shear Deformations in a Theory of Linear Elasticity with Microstructure. *Z. Angew. Math. Phys.* **56**, 516–528 (2005)
- [93] Horgan, C.O.: Antiplane shear deformations in linear and nonlinear solid mechanics. *SIAM Rev.* **37(1)**, 53–81 (1995)
- [94] Kress, R.: *Linear integral equations*, Springer, Berlin (1989)
- [95] Radi, E.: On the effects of characteristic lengths in bending and torsion on Mode III crack in couple stress elasticity. *Int. J. Solids Struct.* **45(10)**, 3033–3058 (2008)
- [96] Piccolroaz, A., Mishuris, G., Radi, E.: Mode III interfacial crack in the presence of couple stress elastic materials. *Eng. Fract. Mech.* **80**, 60–71 (2012)
- [97] Sigaeva, T., Schiavone, P.: Solvability of the Laplace equation in a solid with boundary reinforcement. *Z. Angew. Math. Phys.* **65**, 809–815 (2014)
- [98] Sigaeva, T., Schiavone, P.: Solvability of a theory of anti-plane shear with partially coated boundaries. *Arch. Mech.* **66**, 113–125 (2014)
- [99] Sigaeva, T., Schiavone, P.: Surface effects in anti-plane deformations of a micropolar elastic solid: Integral equation methods. *Continuum Mech. Therm.* DOI:10.1007/s00161-014-0404-3 (2014)

- [100] Sigaeva, T., Schiavone, P.: The Effect of Surface Stress on an Interface Crack in Linearly Elastic Materials. *Math. Mech. Solids*, DOI:10.1177/1081286514534871 (2014)
- [101] Sigaeva, T., Schiavone, P.: Influence of Boundary Elasticity on a Couple Stress Elastic Solid with a Mode-III Crack. *Quart. J. Mech. Appl. Math.* (Accepted)
- [102] Constanda, C.: A mathematical analysis of bending of plates with transverse shear deformation. Longman Scientific & Technical, Harlow (1990)
- [103] Mandal, B.N., Chakrabarti, A. Applied Singular Integral Equations. Science Publishers, Enfield, NH; CRC Press, Boca Raton, FL(2011)
- [104] Constanda, C.: Direct and Indirect Boundary Integral Equation Methods. CRC, Boca Raton; Times Mirror, London (1999)
- [105] Radok, J.R.M.: Problems of plane elasticity for reinforced boundaries. *J. Appl. Mech.* **77**, 246–254 (1955)
- [106] Martin, P.A.: End-point behaviour of solutions to hypersingular integral equations. *Proc. R. Soc. London Sect. A* **432**, 301–320 (1991)
- [107] Günther, N.M.: Potential theory and its applications to basic problems of mathematical physics. Frederick Ungar Publishing, New York (1967)
- [108] Lubarda, V.A.: Circular Inclusions in Anti-Plane Strain Couple Stress Elasticity. *Int. J. Solids Struct.* **40**, 3827–3851 (2003)
- [109] Sun, C.T., Jin, Z.H.: Fracture mechanics. Academic Press, Waltham, MA (2012)

- [110] Kim, C.I., Ru, C.Q., Schiavone, P.: The Effect of Surface Elasticity on a Mode-III Interface Crack. *Arch. Mech.* **63(3)**, 267–286 (2011)
- [111] Wang, X.: A mode III arc shaped crack with surface elasticity. *Z. Angew. Math. Phys.* DOI: 10.1007/s00033-014-0482-x (2014)
- [112] Constanda, C.: The boundary integral equation method in plane elasticity. *Proc. Am. Math. Soc.* **123**, 3385–3396 (1995)